University of Strathclyde
Strathclyde Institute of Pharmacy and Biomedical Sciences

Development of a non-ionic surfactant vesicles formulation of gemcitabine for pulmonary delivery

By

Fatima Jalal Al-Gawhari

A thesis presented in fulfilment of the requirements for the degree of Doctor of Philosophy in Pharmacy

2013

This thesis is the result of author's original research. It has been composed by the author and has not been previously submitted for the examination which has led to the award of a degree.

Fatima Jalal Al-Gawhari

Date 14/10/2013

I would like to dedicate this thesis to the memory of my father and all the teachers who made their best efforts to improve our thinking

Acknowledgments

I would like to thank my supervisors, Dr. Katharine Carter, and Prof. Alex Mullen who greatly supported my PhD progress. I would not have done this without your support and patience. I am very grateful to the Iraqi Ministry of Higher education for the financial support that made my PhD work possible and all who may support my work on Nano-formulation in the future. I am grateful to Roy, Khulood and Damiaa and all staff at the Iraqi Embassy and Iraqi scholarship office.

I take this opportunity to thank Dr Linda Harvey for her help in HPLC analysis and Dr Valerie Ferro for her advice.

I also acknowledge Dr. Helen Dutton for the travel bursary to attend the Nano-formulation 2012 and 2013 conferences.

I would also like to thank all student members of the lab, past and present, for their friendship, advice and cooperation. Also, I would like to thank all the staff at the BPU, University of Strathclyde for their kindness all over the time.

I would also like to thank my mother, husband, son, friends and colleagues who worked with me: Peter Gardner, Basma Doro, Mireia Pug and Craig Shaw.

Abstract

Lung cancer is a major cause of death in the world. Cancer chemotherapy is limited by adverse toxicities to normal tissues. Targeted delivery of anticancer drugs to lung cancer by inhalation would help to reduce these toxicities. Lipid based delivery systems have been shown to be effective in improving the delivery of a number of drugs and the potential of using non-ionic surfactant vesicles (NIV) to improve the delivery of Gemcitabine (Gem) was studied in this project.

NIV were used to encapsulate Gem (Gem-NIV) for delivery by the pulmonary route. NIV were prepared using different concentrations of lipid (30, 60 and 150 mM) and characterised on the basis of size, drug entrapment efficiency and zeta potential. *In vitro* pulmonary delivery of Gem-NIV was compared with Gem solution using a multistage liquid impinger (MSLI). *In vivo* pulmonary delivery of Gem-NIV was also compared with Gem solution using two rodent models (Sprague-Dawley rats and BALB/c mice). The cytotoxicity of Gem formulations was assessed in *in vitro* studies using the B16-F0 luciferase melanoma cell line and in *in vivo* studies using lung cancer bearing BALB/c mice. Gem-NIV composed of 60 mM lipid exhibited the highest entrapment efficacy (80 ± 4%), nebulization efficiency (87 ± 6%) and physicochemical stability over a three-month period. Gem-NIV (60mM) were more effective at reaching the lower stages of the MSLI compared to Gem solution with significantly ($P < 0.01$) greater amounts of the drug being present in stage 1 and 2 of the MSLI, whereas Gem solution had a higher deposition in the mouth piece ($P < 0.01$). *In vivo* drug delivery studies showed that there was a greater accumulation of Gem in the lungs of rats when administered as a NIV formulation prepared with 30 or 60 mM lipid at a dose of Gem of 15 or 6 mg/kg in comparison with free drug

treatment. In lung cancer bearing mice, the Gem lung level was higher for Gem-NIV (60 mM) treated mice at dose 14 mg/ml (0.5ml) compared with the same dose of Gem solution. Gem-NIV prepared with 60 mM lipid were significantly ($P < 0.01$) more cytotoxic (IC_{50} 0.87 ± 0.01 mg/ml) than Gem solution (IC_{50} 4.45 ± 0.03 mg/ml) against the B16 F0 cell line. In this study, male mice had a significantly ($P<0.05$) higher severity of lung cancer than female mice according to lung weight data. On treatment with Gem-NIV (60 mM), a dose of 7 mg/ml was more effective in reducing the tumour burden in lungs than Gem solution in male BALB/c mice.

The results of these studies indicate that Gem-NIV show significant potential to improve delivery of Gem for the treatment of lung cancer using pulmonary administration compared with Gem solution alone.

Communications

- F.J.Al-Gawhari, K.C. Carter A.B. Mullen. The efficacy of non-ionic surfactant vesicles of gemcitabine in the treatment of lung cancer. .Abstract for poster presentation at Strathclyde University symposium.

- F.J.Al-Gawhari, K.C. Carter, and A.B. Mullen. The efficacy of non-ionic surfactant vesicles of gemcitabine in the treatment of lung cancer. Abstract for poster presentation at Nanoformulation conference in Baecelona (May 2012) and at the cell- Biology Symposium (2012).

- F.J.Al-Gawhari, K.C. Carter, and A.B. Mullen. Formulation of non-ionic surfactant vesicles as a pulmonary delivery system for gemcitabine in treatment of lung cancer. Abstract for poster presentation at Nanoformulation conference in Manchester University (2013).

Publications

- Alsaadi, M , Italia, J. L. , Mullen, A. , Kumar, M. N. V. R., Candlish, A. A., Williams, R., Shaw, C. D. , Al-Gawhari, F., Coombs, G. , Wiese, M., Thomson, A., Puig-Sellart, M. , Wallace, J. , Sharp, A., Wheeler, L., Warn, P. and Carter, K. (2012). The efficacy of aerosol treatment with non-ionic surfactant vesicles containing amphotericin B in rodent models of leishmaniasis and pulmonary aspergillosis infection. Journal of Controlled Release. 160:685-691.

- Al-Gawhari, F., Alsaadi, M.A, Puig-Sellart, M., Henriquez, S., Vass, M., Ferro, V. A., Mullen, A. B. and Carter, K. C. Pulmonary delivery using non-ionic surfactant vesicles: determination of the characteristics important in delivery of gemcitabine to the lungs (manuscript in preparation).

TABLE OF CONTENTS

LIST OF FIGURES

LIST OF TABLES

List of Abbreviations

ATP	Adenosine triphosphate
BALB/c	Albino, laboratory-bred strain
BL	Bioluminescence
CT	Computing tomography
Deox	Deoxcycytidine
DCP	Dicetyl phosphate
DMEM	Dulbecco's modified eagle medium
DNA	Deoxyribose nucleic acid
DCTP	Deoxycytidine triphosphate
EGFR	Epidermal growth factor receptor
FL	Fluorescence
Gem	Gemcitabine
HPLC	High performance liquid chromatography
Luc	Luciferase
MRI	Magnetic resonance imaging
NIV	Non-ionic surfactant vesicles
NP-HPLC	Normal phase-HPLC
NSCLC	Non-small cell lung cancer
PEG	Polyethylene glycol
PET	Positron-emission tomography
RR	Ribonucleotide reductase

RP-HPLC	Reverse phase-HPLC
rpm	Rotations per minute
RNA	Ribonucleic acid
RSD	Relative standard deviation
SCID	Severe combined immunodeficiency
SCLC	Small cell lung cancer
UV	Ultraviolet
ZP	Zeta potential

Chapter 1: Introduction

1.1 Lung cancer

Lung cancer is a major cause of death and in 2008 it was responsible for 1.38 million deaths, accounting for 18.2% of all cancer deaths in the world. There were 1.61 million new cases worldwide with the highest frequency in developed countries (Ferlay *et al*., 2010). In 2010, 34,859 people died because of lung cancer in the UK (Figure 1.1) and smoking was associated with 90% of cases in men and 80% of cases in women. Lung cancer occurs mainly in men aged 40 years and older, and women aged 60 or more (Siegel, 2012).

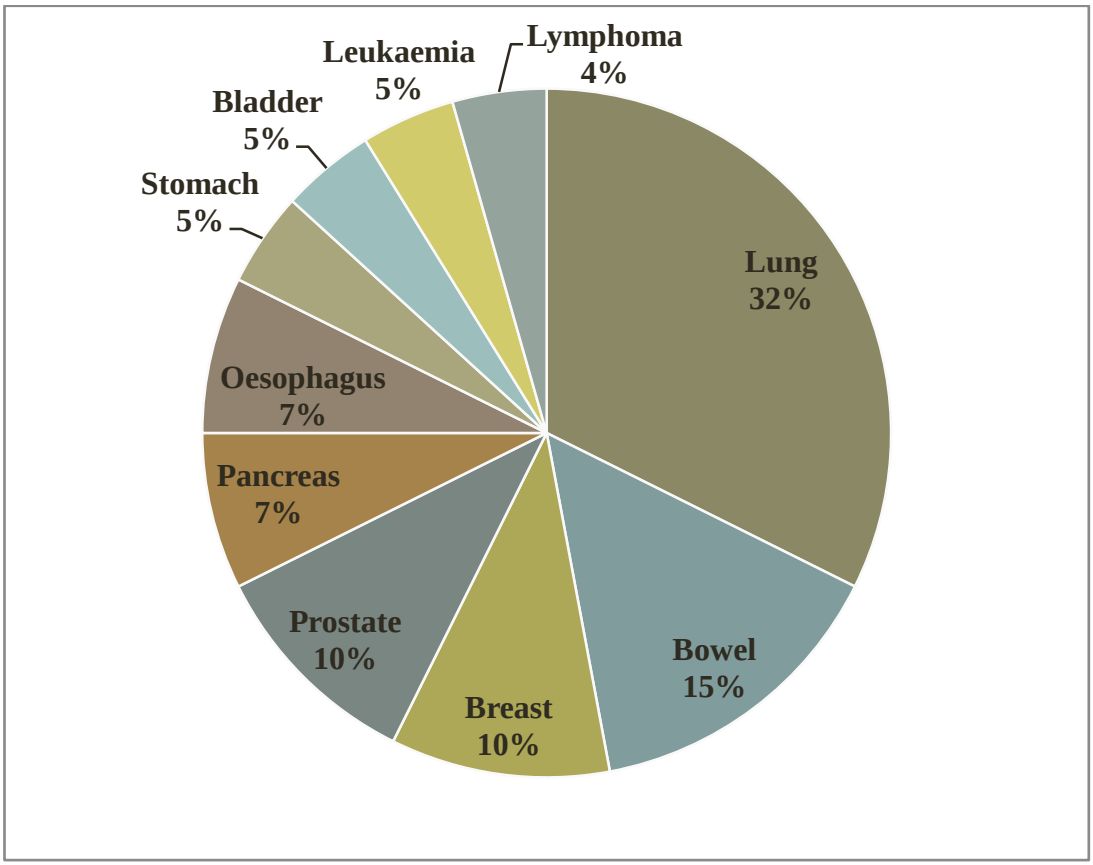

Figure 1.1 The percentage of cancer deaths in the UK accessed and reproduced from data of Cancer Research UK 2012 (http://publications.cancerresearchuk.org). Accessed November 2012.

A cancer starts as a single mutated cell. This single cell proliferates abnormally and forms a tumour mass, which can metastasize to other tissues of the body through the blood circulation or lymphatic system. A tumour mass obtains nutrients for growth by passive diffusion until it reaches a size of about 2 mm^3 (Jones, 1998). When the mass becomes larger nutrients cannot diffuse sufficiently to the centre of the tumour, leading to the formation of 3 distinct regions: an inner necrotic core (dead cells), a hypoxic region (i.e. an area of low oxygen) where cells do not proliferate, and an outer proliferating edge (Goerner, 2010; Kim, 1993).

New blood vessel formation (angiogenesis) will start to supply nutrients to the growing tumour as a result of signals from biological growth factors. The membranes of blood vessels supplying the tumour are abnormal with decreased numbers of endothelial cells (Baban and Seymour, 1998). The size of the junctions between the cancerous endothelial cells has a range from 100 to 780 nm (Hobbs, 1998; Rubin, 1966; Shubik, 1982), whereas normal endothelial junctions are naturally 5 to 10 nm in size. This subsequently leads to an increase in the permeability of the vessel wall and facilitates diffusion into the interstitium of the tumour mass.

Tumours consist of cancer cells, stromal cells, angiogenic blood vessels and the interstitium (Jain, 1994). Besides the stromal cells, there are immune cells (i.e. macrophages, lymphocytes and neutrophils) (Friedl and Alexander, 2011). Cancer and stromal cells represent the major portion of tumours, having more than 50% of the tumour mass. Angiogenic vessels represent up to 10% of the tumour mass, while the interstitium constitutes the remainder of the tumour and provides its structural

framework. Stromal cells affect the production of growth factors and vice versa (Friedl and Alexander, 2011), whereas the normal cellular microenvironment can prevent cell proliferation. In addition, the cancer microenvironment greatly stimulates and protects its own growth. For example, a tumour generates barriers that can prevent or limit chemotherapeutic agents from entering and targeting cancer cells in the tumour, thereby limiting the efficacy of treatment (Flieder, 2005; Jain, 1996). Lung cancer is classified into two main types on the basis of the microscopic appearance of the tumour cells; small cell lung cancer (SCLC) or non-small cell lung cancer (NSCLC). NSCLC is the more common form and accounts for 75-80% of lung cancers (Hoffman *et al.*, 2000) and it can be subdivided into four groups. Firstly, squamous cell carcinoma presents as obstructive lesions of the bronchi and occurs in approximately 40% of cases. Secondly, adenocarcinoma, which arises from the abnormal growth of mucus cells in the bronchial epithelium, and then extends into pleura and lymph nodes and may metastasis to the brain and bones. This type is more common in non-smokers, women and elderly people and occurs in 10% of all lung cancer cases. The third type of lung cancer is large cell carcinoma that is a less differentiated form of squamous cell and adenocarcinoma. It accounts for 25% of all lung cancer cases and metastasizes early in the disease to the brain and bones. Lastly, broncheoalveolar cell carcinoma accounts for only 1-2% of lung cancers and presents as peripheral or diffuse nodular lesions. This form is associated with the production of very large volumes of mucous sputum.

SCLC is divided into limited and extensive staging and accounts for 20-25% of all lung cancers. SCLC tumours are rapidly growing and highly malignant. Although this form of lung cancer responds well to chemotherapy, the prognosis remains poor

in most cases (Kumar *et al*., 2005). The median survival time is only 2 to 4 months for patients without treatment and with therapy patients have a two year period before relapse (Johnson, 1990). Limited SCLC is clinically restricted to one side of the chest and the main treatment for this stage is a combination of radiotherapy and chemotherapy (Johnson, 1990; Yamamoto, 2006).

Tumour size is an important prognostic factor for both NSCLC and SCLC and the stage of a cancer refers to the extent to which a cancer has spread in the body. Staging involves both an evaluation of a cancer's size as well as the presence or absence of metastasis in the lymph nodes or in other organs. Thus, cancer is classified on the basis of the "TNM staging system", which takes into account the size, and spread of the primary tumour (T), presence of tumour cells in the lymph nodes (N), and whether the tumour shows metastasis (M). For example, N2 (T > 2 cm) is twice as likely to have nodal metastasis as N1 carcinoma (T < 2 cm, Flieder, 2005, Table 1.1).

T	Primary tumour Diameter (cm)	N	Lymph node involvement	M	Presence of Metastasis
T1	Tumour ≤ 3	N0	No regional lymph node metastasis	M0	No distant metastasis
T1a	Tumour ≤ 2	N1	Ipsilateral hilar or peribronchial nodes	M1	Distant metastasis present
T1b	Tumour >2 but ≤ 3	N2	Ipsilateral mediastinal or subcarinal nodes	M1a	Separate tumour nodule(s) in a contralateral lobe or tumor with pleural nodules or malignant pleural/pericardial effusion
T2	Tumour >3 but ≤ 7	N3	Contralateral mediastinal or hilar nodes or ipsilateral/contralateral scalene or supraclavicular nodes	M1b	Distant metastases
T2a	Tumour ≤ 5				
T2b	Tumour >5 but ≤ 7				
T3	Tumour >7				
T4	Tumor invades any of mediastinum, heart, vessels, trachea, laryngeal, nerve and esophagus.				

Table 1.1 TNM classification of NSCLC lung cancer. T refers to the size of the tumour, N refers to the presence of lymph node metastasis and M refers to the presence or absence of distant metastasis (Tsim *et al.*, 2010) and National Comprehensive Cancer Network available at http://www.nccn.org. Accessed November 2012.

Surgical removal is the major treatment option for a patient in stage I NSCLC. The survival rate of stage IA has a range of 58 - 76% and in stage IB (T2N0M0) survival reaches 60% (Chang *et al.*, 2007; Ost *et al.*, 2008). In stage II NSLC the intrapulmonary lymph nodes are affected by the cancer, causing a drop in survival rates to 52%. Adjuvant chemotherapy after surgical resection in stages IB and II NSCLC is recommended and provides an increase in survival rates of approximately 5% compared to the median survival rates (Pignon, 2008). Stage III NSCLC was treated by radiotherapy alone until the mid-1990s and the median survival times were 9-11 months (Rolland *et al.*, 2007). Then treatment with chemotherapy and radiotherapy showed a significant improvement in survival rates (of about 2.6%) in stage III patients. Patients with stage IV are now treated with more cycles than stages II or III (up to 6 cycles) of chemotherapy as the first line of treatment (Pfister *et al.*, 2004).

Stage	TNM			Treatment
Stage IA	T1a/T1b	N0	M0	Surgical resection and adjuvant chemo-therapy
Stage IB	T2a	N0	M0	
Stage IIA	T1a/T1b T2a T2b	N1 N1 N0	M0 M0 M0	Surgical resection and adjuvant chemo-therapy
Stage IIB	T2b T3	N1 N0	M0 M0	
Stage III	T(any) T4	N3 N2	M0 M0	Chemo-radiotherapy
Stage IV	T(any)	N(any)	M1a/M1b	Chemotherapy

Table 1.2 Stages of lung cancer based on TNM classification, criteria of cancer and treatment (Shepherd *et al.*, 2007; Tsim *et al.*, 2010).

Chemotherapies used against lung cancer can act in a variety of targets that ultimately block cell replication or production of growth factors that stimulate cell growth (Figure 1.2). Most chemotherapy is targeted at the process of cell division; the rationale being that cancer cells are more likely to replicate than normal cells. Alkylating agents contain groups, which are capable of reacting with DNA. They can thus form bridges between a single strand and two separate strands of DNA; interfering with DNA replication. Several antibiotics such as anthracyclines (e.g. doxorubicin and daunorubicin) are used in the treatment of lung cancer. They act by intercalating DNA or inhibiting RNA synthesis. Others types of drugs used in the treatment of lung cancer act by different mechanisms. The vinca alkaloids (e.g. vinblastine, vincristine, vindersine and vinorelbine) bind to tubulin and thus interrupt cell mitosis. Taxanes (e.g. paclitaxel and docetaxel) also bind to tubulin and prevent assembly of microtubules. Enzymes in turn are responsible for the structure, metabolic activity and function of the cells. So antimetabolites, which inhibit the activity of these enzymes, are active as anticancer drugs with fewer side effects compared with other compounds (British Medical, 2011; Sweetman, 2011). Inhibitors of the epidermal growth factor receptor (EGFR) e.g. erlotonib and gefitinib, block EGFR signal transduction causing cell apoptosis (Ritter, 2008).

Erlotinib is used as a single agent to treat NSCLC that overexpress EGFR. Its adverse effects include diarrhoea, skin rash, nausea and anorexia, hepatitis, pneumonitis and decreased cardiac contractility. Erlotinib is best absorbed orally, with a mean elimination half-life of 36 hours. Therefore, it is given once daily (Ritter, 2008).

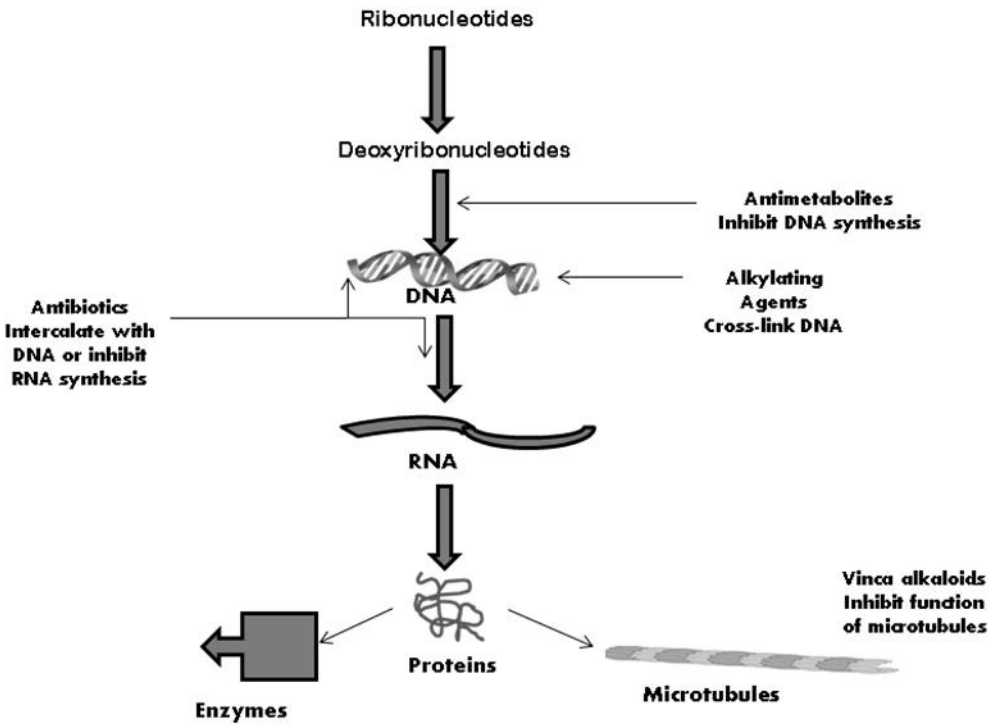

Figure 1.2 Mechanisms of action of various anticancer drugs (adapted from Sweetman, 2011).

Platinum compounds (e.g. cisplatin, carboplatin and oxaliplatin) and nitrogen mustards (e.g. cyclophoshamide), cross link DNA by forming covalent bonds with it and thus prevent DNA replication. Cisplatin is the main drug used in treating lung cancer. However, its use is associated with adverse side effects that include nephrotoxicity, peripheral nerve damage and ototoxicity. It may be possible to protect against some of these side effects. For example, antioxidants might be useful in reducing cisplatin neurotoxicity, which occurs as a result of generation of reactive oxygen species which are responsible for damage to dorsal root ganglia neurons (Carozzi *et al.*, 2010; McDonald *et al.*, 2005).

Animal studies have found that sulphur compounds such as L-N acetylcysteine and D-methionine act as otoprotectors due to their strong antioxidant activity (Korver, 2002; Thomas *et al*., 2004) and noise conditioning can be used against ototoxicity side effects (Theneshkumar *et al*., 2009). Ifosfamide, an analogue of cyclophosphamide, has also been used to treat lung cancer, but it causes nephrotoxicity due to direct tubular injury (Nissim *et al.*, 2006) and causes encephalopathy in 10-30% of treated patients (Ajithkumar *et al*., 2007; Alici-Evcimen and Breitbart, 2007).

Doxorubicin is the most widely used antibiotic in lung cancer, but it can cause acute, chronic and life threatening adverse side effects which include cardiotoxicity and bone marrow suppression; these side effects limit use of the drug. Cardiomyopathy leads to death in up to 60 % of those who develop signs of congestive heart failure (Buja *et al*., 1973; Lefrak *et al*., 1973). Agents to protect against doxorubicin-induced cardiomyopathy are being investigated. For example, certain antioxidants such as tocopherol may protect against cardiotoxicity without affecting its anticancer properties. Doxorubicin is poorly absorbed and must be administered intravenously. It does not enter the central nervous system (CNS). Unchanged doxorubicin and its active metabolites (e.g. doxorubicinol) appear in bile at a proportion of 40%. Therefore, dose reduction is recommended in patients with hepatic disease. Its elimination half-life is about 30 hours and tumour resistance to this drug can be suppressed by verapamil (Morrow *et al*., 1987; Remington and Allen, 2013).

The semi-synthetic vinca alkaloid, vinorelbine, is the most widely used drug of this group against NSCLC and it is usually used in combination with cisplatin especially in elderly patients (Pereira *et al*., 2004). Acute adverse effects of vinorelbine include nausea, vomiting and neurotoxicity. An injectable of vinorelbine is formulated and already marketed (Navelbine® injection - Pierre Fabre Médicament) for the treatment of NSCLC and advanced breast cancer. Additionally, an oral formulation of vinorelbine was developed to be administered with the same weekly schedule of intravenous administration (Marty *et al.*, 2001).

Docetaxel was established as a second line treatment for advanced lung cancer ten years ago. It is a semisynthetic taxane, a derivative of paclitaxel and administered intravenously. It causes myelosuppression and peripheral fluid retention; it also causes less cardio- and neurotoxicity than paclitaxel, so it is more tolerated than paclitaxel. Neurotoxicity and hypersensitivity reactions can be avoided by using steroids and H1 and H2 histamine antagonists prior to treatment (Nakamura and Yamamoto, 2009).

Antimetabolites (e.g. fluorouracil, gemcitabine, etoposide, irinotecan and toptecan) block one or more of the metabolic pathways involved in DNA synthesis. Etoposide is a semisynthetic derivative of podophyllotoxin extract from the Mandrake plant; is a DNA repair inhibitor and forms a complex with topoisomerase II enzyme. Etoposide is given either by intravenous injection or orally. It is metabolised by the liver into an inactive metabolite and a small amount is eliminated in the urine. Its use is associated with nausea, vomiting, chills and fever, postural hypotension, tachycardia, palpitations and bronchospasm, all of which can occur during and after

rapid intravenous infusion. Delayed toxicities of etoposide are likely to include myelosuppression (which occurs 7-10 days after treatment in 60-90% of patients), thrombocytopenia (which occurs 2-3 days after treatment in 28-41% of patients) and anaemia (which is found in approximately 33% of patients). Gastrointestinal toxicity demonstrated by nausea and vomiting, stomatitis and diarrhoea occurs in 50% of the patients and is easily managed. The frequency of gastrointestinal toxicity may be increased when it is given orally. Alopecia also occurs, but the degree of alopecia is less severe than that associated with doxorubicin and vincristine treatment. Less common side effects such as fever, chills, Steven–Johnson syndrome, hepatotoxicity and peripheral neuropathy may also be present (Jinturkar *et al*., 2012; Remington and Allen, 2013; Sengupta *et al.*, 2000; Sinkule, 1984).

Gemcitabine (Gem) is less toxic than platinum based drugs and it requires less hospitalisation compared with cisplatin or etoposide as single therapies (Gatzemeier *et al*., 1996; Guchelaar *et al*., 1996). It is one of the main drugs used to treat lung cancer. Gem is a nucleoside analogue (Figure 1.3) that requires intracellular phosphorylation to produce its active diphosphate and triphosphate metabolites.

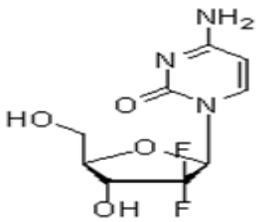

Figure 1.3 Gemcitabine structure

The triphosphate metabolite blocks DNA synthesis by inhibition of the ribonucleotide reductase (RR) enzyme. The diphosphate metabolite is incorporated onto the end of DNA strands and it competes with deoxycytidine triphosphate (DCTP) and causes chain termination and an inhibition of DNA replication (Huang *et al*., 1991).

Gem causes myelosuppression, thrombocytopenia and anaemia. It also induces vomiting and malaise, but these are usually mild and occur at a much lower incidence than that reported for cisplatin. Co-treating patients with anti-emetic agents can control the nausea and vomiting and the flu like symptoms respond well to paracetamol. Gem is rapidly deaminated by the presence of cytidine deaminase, which is present in the blood and tissues, to its inactive metabolite which is excreted in urine (Zhu *et al*., 2012).

Many approaches have been attempted to extend the half-life of Gem and improve its *in vivo* cytotoxic activity. For example, conjugation of a long fatty chain (e.g. valeroyl, heptanoyl, lauroyl, stearyl and linear acyl derivatives) on to the 4-amino group of Gem protects it from chemical catabolism in plasma (Immordino *et al*., 2004). Another way to increase the half-life of Gem is to use a suitable drug delivery system (see section 1.2), (Reddy and Couvreur, 2008a; Stella *et al.*, 2007).

Most anti-cancer drugs are given in a combination therapy as it significantly enhances efficacy compared with monotherapy and the sequence in which the drugs are administered can be important (see Tables 1.3-1.5).

Stages	Combination regimen (4 cycles)
I and II	Cisplatin 75 mg/m^2 on day 1 with gemcitabine 1250 mg/m^2 on days 1 and 8, every 21days
	Cisplatin 100 mg/m^2 on day 1 with etoposide 100 mg/m^2 on days 1-3, every 28 days
	Cisplatin 80 mg/m^2 on days 1, 22, 43, and 64 plus vinblastine 4 mg/m^2 on days 1, 8, 15, 22, and 29; then every 2 week after day 43 until completion of cisplatin every 21 days
	Cisplatin 50 /m^2 on days 1 and 8 with vinorelbine 25 mg/m^2 on days 1, 8, 15 and 22, every 28 days
	Cisplatin 75 mg/m^2 on day 1 with docetaxel 75 mg/m^2 on day 1, every 21 days

Table 1.3 Combined adjuvant regimens to treat stage I and II NSCLC (Arriagada *et al.*, 2004; Arriagada *et al.*, 2010; Douillard *et al.*, 2006; Fossella *et al.*, 2003; Pepe *et al.*, 2007; Pignon *et al.*, 2008; Winton *et al.*, 2005) and http://www.nccn.org. Accessed December 2012.

Stages	Combination regimen(4-6 cycles)
III	Cisplatin 100 mg/m^2 on day 1 with gemcitabine 1000 mg/m^2 on days 1, 8 and 15, every 28 days
	Cisplatin 50 mg/m^2 on days 1, 8, 29, and 36 with etoposide 50 mg/m^2 on days 1-5 and days 29-33
IV	Cisplatin 75 mg/m^2 on day 1 with paclitaxel 175 mg/m^2 on day 1, every 21 days
	Cisplatin 100 mg/m^2 on days 1 and 29 with vinblastine 5 mg/m^2 weekly for 5 weeks
	Cisplatin 60 mg/m^2 on day 1 with gemcitabine 1000 mg/m^2 on days 1 and 8, every 21 days
	Cisplatin 75 mg/m^2 on day 1 with docetaxel 75 mg/m^2 on day 1, every 21 days

Table 1.4 First line combined regimens to treat stage III or IV NSCLC (Albain *et al.*, 2002; Gandara *et al.*, 2003; Hanna et al., 2007; Hanna *et al.*, 2008; Rusch *et al.*, 2007; Park *et al.*, 2007; Schiller *et al.*, 2002; Brodowicz and Zwitter, 2006; Gridelli et al., 2007) and http://www.nccn.org. Accessed December 2012.

Stages	Combination regimen
Limited	Cisplatin 60-80 mg/m^2 on day 1 with etoposide 80-120 mg/m2 IV on days 1-3, every 21-28 days
	Cisplatin 80 mg/m^2 on day 1 with etoposide 100 mg/m^2 on days 1-3 every 28 days
Extensive	Cisplatin 60-80 mg/m^2 on day 1 with etoposide 80-120 mg/m^2 on days 1-3, every 21-28 days
	Cyclophosphamide 800-1000 mg/m^2 on day 1 with doxorubicin 40-50 mg/m^2 on day 1 and vincristine 1-1.4 mg/m^2 on day 1, every 21-28 days
	Cisplatin 60 mg/m^2 on day 1 plus irinotecan 60 mg/m^2 on days 1, 8, and 15, every 28 days
	Cisplatin 30 mg/m^2 on days 1 and 8 or 80 mg/m^2 on day 1 with irinotecan 65 mg/m^2 on days 1 and 8, every 21 days

Table 1.5 Combination of chemotherapy (4 cycles) with radiation to treat limited SCLC and first line chemotherapy (4-6) for extensive stage (Eckardt, 2006; Hermes, 2008; Lara, 2009; Takada, 2002; Turrisi, 1999; von Pawel, 1999). Accessed December 2012.

1.2 Drug delivery systems

Researchers have been investigating new systems to deliver drugs directly to the target to improve the therapeutic efficiency and reduce systemic side effects of these drugs. In these systems, it is possible to modify the pharmacokinetics and bio-distribution of drugs, which have poor solubility, poor stability, short half-life and undesirable toxicity (Allen and Cullis, 2004; Yoo *et al*., 2011; Martinho, 2011). Delivery systems are administered by oral, pulmonary, transdermal, transmucosal, ocular and parenteral routes. The materials used to prepare the delivery systems include inorganic materials (e.g. gold), biologics (e.g. albumin), lipids (e.g. phospholipid and cholesterol) and polymers (e.g. chitosan and alginate). Alternatively, lactic-glycolic acid copolymers have been used to design and modify delivery systems (Letchford and Burt, 2007). Drugs may be incorporated into the delivery system using various mechanisms, such as surface adsorption, aqueous inclusion, solid-phase immobilization and complexation of aggregates (Sung *et al*., 2007).

Delivery systems have various structures (e.g. nanocapsules, micelles, liposomes, non-ionic surfactant vesicles, solid nanoparticles and microparticles, see Table 1.6). The advantages of nanoscale delivery systems are their potential applications in pulmonary and cancer treatments because of their ability to penetrate tumour microvasculature, which is leaky and contains pores ranging from 100 to 780 nm in diameter (Orive *et al*, 2003b; Panyam and Labhasetwar, 2003; Birnbaum and Brannon-Peppas, 2004).

Delivery system	Drugs	Type
Gelatin nanoparticles	Cisplatin	*In vivo and in vitro*
Liposome	Cisplatin	*In vivo*
Liposome	Doxorubicin	Licensed for use in USA
Liposome	Docetaxel	*In vitro*
Immunoliposome	Vincristine	*In vivo*
Liposome	Vinorelbine	*In vivo*
Immunoliposome	Gemcitabine	*In vivo*
PLGA micropaticles	Doxorubicin	*In vitro*
Nanocapsules	Paclitaxel	*In vitro*
Micelles	Paclitaxel	Clinical study
Nanocapsules	Etoposide	*In vivo*
Cyclodextrin nanocapsules	Paclitaxel	*In vitro*
Nonionic surfactant vesicles	Cisplatin	*In vivo*

Table 1.6 The types of delivery systems used in lung cancer studies (Tseng *et al*., 2009; Mylonakis *et al*., 2009; Poveda *et al*., 2005; Jinturkar *et al*., 2012; Noble *et al*., 2009; Chang *et al*., 2009; Kim *et al*., 2009; Yang *et al*., 2009; Zhou *et al*., 2013; Mastsumura, 2008;Tang *et al*., 2010 ;Bilensoy *et al*., 2008; Gude *et al*.,2002).

1.2.1 Nanocapsules

Nanocapsules have a size range of 100-200nm, consist of an oily core within which the hydrophobic drugs are surrounded by a polymeric or lipid membrane. In polymeric nanocapsules, the drug to polymer ratio can be as high as 5:1, which is a lower polymer ratio in comparison with nanospheres (1:10, Letchford and Burt, 2007). Lipid nanocapsules (LNCs) can be used to overcome the problem of low encapsulation efficiency of cisplatin. The low solubility of cisplatin in water, resulting in low encapsulation efficiencies in liposomes, thus low encapsulation efficiency has disadvantaged the development of an effective lipid formulation of cisplatin. The encapsulation of cisplatin in LNCs provides advantage of the limited solubility of cisplatin in water and produces cisplatin nanocapsules, bean-shaped nanoprecipitates of cisplatin coated by a lipid bilayer (Velinova *et al.*, 2004).

Additional benefit of LNCs is their suitability for pulmonary administration. For example, paclitaxel LCNs can be administered by the pulmonary route more efficiently in contrast to Taxol® (paclitaxel being the marketed intravenous formulation) which contains a highly viscous solubilizing agent (Cremophor®EL; polyoxyl 35 castor oil) making it unsuitable for direct delivery into the lungs by inhalation (Hureaux *et al*., 2009).

1.2.2 Micelles

Micelles have a size range of 10-100nm and the structure is spherical. This structure is formed by the self-association of amphiphilic surfactants or polymers in an aqueous solution. Hydrophobic drugs can be incorporated into the core of the micelle (Letchford and Burt, 2007).

Micelles have been used to increase the solubility and stability of cytotoxic drugs and enhance their anticancer effects. For example, micelles improve solubilisation efficiency, *in vitro* release and blood circulation of docetaxel as a result of encapsulation into the inner micelle core. In addition, *in vitro* and *in vivo* antitumor efficiency of docetaxel micelles against A549 (human lung adenocarcinoma cell line) or A549 cells xenografted in nude mice were higher than Taxotere® injections (Chen *et al*., 2012). Studies using micelles containing doxorubicin also showed that A549 cells treated with a micellar formulation had an IC_{50} of 0.21 µg /ml, which was a third of that estimated for treatment with doxorubicin solution. This ability of micelles to lower the dose of doxorubicin required is an important achievement as the drug can have significant systemic toxicity (Wang *et al.*, 2009).

1.2.3 Polymeric nanoparticles

Microparticles have a size range of 0.1-500 µm and are prepared from naturally or synthetic polymers. For example, doxorubicin microparticles formulated using PLGA (Poly d, l-lactic-co-glycolic acid) polymer has a sustained release (over 2 weeks) after pulmonary administration in a lung cancer model. Additionally, doxorubicin released from PLGA microparticles eradicated 81.6% of B16 F10 cells after 6 hours *in vitro*. The same cell line was implanted into mice in an *in vivo* study. Mice treated with doxorubicin microparticles had reduced numbers and a smaller mass of tumours compared with mice treated with doxorubicin solution (Kim *et al*., 2012)

1.2.4 Biological vesicles

Biological vesicles (50-150 nm), released by non-pathogenic eukaryotic Amoeba, were evaluated in *vitro* as a carrier for hypericin, a polycyclic anthraquinone which is usually used for photodynamic therapy of cancer. Hypericin, which is delivered by biological vesicles, has an intracellular localization tendency, resulting in the death of cancer cells. However, the problem of immune responses to the Amoeba can limit their *in vivo* application (Lavialle *et al*., 2009).

1.2.5 Lipid based delivery systems – liposomes and nonionic surfactant vesicles (NIV)

Liposomes usually consist of phospholipids (e.g. phosphatidylcholine) and a sterol (e.g. cholesterol) which when added to solution can form bilayered vesicles that can encapsulate a hydrophilic drug in their aqueous core or a lipophilic drug in their lipid bilayer.

Liposomal size ultimately depends upon the method of manufacture and lipids used. Multilamellar liposomes range in size from 0.1–5.0 µm; small unilamellar liposomes' size range is 0.02–0.05 µm, and the large unilamellar liposomes' size range varies from 0.06 µm and greater (Chrai, 2001). The surface charge on a liposome is determined by inclusion of different lipids. For example, a long-chain amine provides a positive charge, whilst dicetyl phosphate (DCP) provides negatively charged liposomes (Ugwu *et al.,* 2005). Liposomal design can be undertaken to improve drug delivery and decrease drug toxicity and this has been achieved through many approaches including pegylation or immune-conjugation. Pegylated liposomes are prepared by coating with polyethylene glycol to avoid the

uptake by the reticuloendothelial system, thus improving drug delivery. Non-pegylated doxorubicin liposomes (Myocet®) had a shorter half-life than Doxil® or Caelyx® which are pegylated liposomes (Immordino *et al*., 2006).

In immunoliposomes, antibodies are conjugated onto liposomal surfaces in order to direct therapy against specific antigens on a cancer cell surface. For example, vincristine anti-HER2 liposomes have been evaluated to target vincristine into the HER2-over-expressing human mammary carcinoma cell lines SKBR-3 and BT474. Treatment with immune-conjugated liposomes increased their cytotoxicity compared with non-immunoliposomes by 63- and 253-fold for BT474 and SKBR3 cells, respectively (Noble, 2009).

Nebulizers have been usually used for the delivery of liposomes (Schreier *et al.*, 1993). However, problems of drug leakage have been observed to arise when liposomes are delivered as liquids (Taylor *et al.*, 1990a). Liposomal dry powder formulations have been examined in clinical trials in order to overcome such problems (Joshi and Misra, 2001;Shah and Misra, 2004; Taylor *et al.*, 1990b; White *et al.*, 2005).

There are other types of lipid-based vesicles called non-ionic surfactant vesicles (NIV). NIV are preferred over liposomes in nebulized formulations. NIV have the same structures as liposomes, but are formulated using non-ionic surfactants instead of phospholipids that have poor stability. Therefore, NIV have been widely studied as an alternative formulation to liposomes. Surfactant forming NIV are biodegradable, non-immunogenic and biocompatible. Incorporating anticancer drugs (e.g. bleomycin) into NIV enhances the efficacy and bioavailability of drugs in

comparison with the free form. NIV also have osmotic activity, as they increase the stability of the entrapped drug during storage or nebulization. Drug release from NIV is influenced by vesicle size, outer bilayer composition and surface charge and this can improve the ability of the formulation to act as a depot at the targeted area (Kaur, 2012). The particle size and surface charge of NIV are very important because they influence the *in vivo* and *in vitro* activity of NIV. Particle size affects the therapeutic activity and cytotoxicity of NIV, influencing their phagocytic uptake, targeting and stability (Verma *et al*., 2003: Šentjurc *et al*., 2000; Szoka *et al*., 1987; Shi *et al.*, 2006; Nagayasu *et al*., 1994).

The quantity of cholesterol used affects the size of NIV; increasing linearly with rising cholesterol content (McIntosh, 1978; Fang *et al.*, 2001; Lopez-Pinto *et al*., 2005; Lee *et al.*, 2005). Furthermore, the addition of dicetyl phosphate (DCP) and stearylamine (SA) increases the vesicle size by increasing the volume of aqueous core as a result of repulsion in charge between DCP or SA and the polar group of the surfactant (Fang *et al.*, 2001; Van Hal *et al.*, 1996). In addition to the lipid composition, the formulation processing (e.g. homogenization and sonication) affects the vesicles' size (Essa, 2010; Wagner and Karola, 2011). The production of NIV requires an input of energy such as agitation or heat. NIV can be prepared by ether injection, handshaking, and reverse phase evaporation or by trans-membrane pH gradient approaches (Khandare *et al*., 1994; Parthasarathi *et al*., 1994; Baillie *et al.* 1985; Martin, 1990; Mayer, 1985). Like liposomes, an antibody can be conjugated onto NIV which can be used to target specific cells (Hood, 2007). Pegylated NIV can be produced by the inclusion of polyethylene glycol in their formulation, in order to increase the residence time of the NIV in the blood to prevent NIV clearance by

phagocytosis. Studies have shown that coupling transferrin (TF) to the terminal group of PEG allows interaction with TF receptors which are over expressed in cancer cells and improves targeting and delivery to those cells (Hong, 2009).

Among the various drug delivery systems including liposomes, nanocapsules and micelles, NIV have been widely applied as a drug delivery of anticancer drugs (Venkatesh, 2010). NIV increases the half-life of methotrexate, bleomycin and daunorubicin in the blood circulation and allows sustained release of these drugs (Udupa, 1993; Raja Naresh, 1996; Balasubramaniam,2002). Adriamycin NIV inhibited cancer in mice with fewer adverse cardiac effect when compared with adriamycin solution (Kerr,1988). The anticancer activity of cytarabine NIV was greater than that for free cytarabine in mice (Kerr, 1988). Doxorubicin NIV had a longer half-life than free doxorubicin (Rogerson, 1988) and had a slightly lower IC_{50} against ovarian cancer cells when compared with traditional doxorubicin (Uchegbu, 1996). Another study related to doxorubicin, doxorubicin-NIV reported a 6-fold increase in the bioavailability of doxorubicin when compared with the solution form in solid tumour bearing mice (Uchegbu, 1995). The adverse side effects of anticancer drugs (e.g vincristine) are decreased using NIV which delivers drug at the tumour site (Parthasarathi, 1994; Agarwal, 2001).

1.3 Pulmonary drug delivery

Another way to improve drug treatment of lung cancer is to choose a mode of administration that improves delivery to the lung. Drug delivery systems can be used to improve drug activity, but treatment by inhalation can be used to improve targeting to the lungs.

Generally, intravenous administration of drugs to treat lung cancer results in systemic distribution and oral treatment is also not ideal for lung cancer because it exposes the drugs to first pass metabolism (Gagnadoux *et al*., 2008; Forbes, 2000). Pulmonary administration is ideal as the lung provides a large surface area (~100 m^2) and has a high number of phagocytic cells, which can provide a depot for drug release. Inhaled drug particles must generally be smaller than 5µm in order to reach the alveolar space. Particles that are smaller than 0.5 µm in diameter can penetrate the lung deeply, but also have a high tendency to be exhaled without deposition (Islam and Rahman, 2008). The use of mucoadhesive agents (e.g. chitosan) can be exploited to improve the effectiveness of pulmonary or nasal delivery. In 2001, Lim *et al*. examined the *in vivo* (using rabbits) and *in vitro* (using impinger and epithelial cells) features of microparticles formulated from hyaluronan or chitosan or a combination of both. The *in vivo* bioavailability of gentamicin formulated using the above mentioned microparticles were enhanced compared with an intranasal solution of gentamicin (Lim *et al*., 2001). Therefore, chitosan has been used as a coating agent in pulmonary liposomes (Zaru *et al.*, 2009). For example, rifampicin was formulated into liposomes and these were then coated with chitosan and xanthan gum to improve pulmonary delivery to lungs (Manca *et al*., 2012b).

Drugs for pulmonary administration can be formulated in solution, suspension, emulsions or micronized dry powder forms. Lipid based vesicles (liposomes and NIV) are one of the most broadly investigated systems for the controlled delivery of drug to the lung (Zeng *et al.*, 1995). They are particularly suitable for drug delivery to the lung, since the vesicles can be formulated from compounds which are

endogenous to the lungs, such as lung surfactant, and these properties make vesicles attractive candidates as pulmonary drug delivery systems (Kellaway, 1990).

Different types of delivery devices, such as nebulisers, pressurised metered dose inhalers (PMDI) and dry powder inhalers (DPI) can be used in pulmonary administration (Groneberg *et al.*, 2003). DPI and PMDI have been widely used in the treatment of asthma and chronic obstructive pulmonary disease (COPD). With the PMDI type, a micronised drug is dissolved or suspended with a surfactant in propellant under pressure, to be aerosolised as a spray, foam or semisolid by exposure to pressure after activation of the device's valve. Surfactant is often added to prevent any clumping of the drug.

A lubricant is also added to facilitate the valve's actuation. A PMDI is a commonly used inhalation device because it has a small size; however, it also has several disadvantages. These include extensive oropharyngeal deposition, difficulty in use even after careful training, bronchoconstriction due to propellants or surfactants and restrictions on the use of some propellants such as chlorofluorocarbon (CFC) due to their effect on ozone depletion (Ehtezazi *et al.*, 2010; Hickey, 2003; Smyth, 2003; Tan *et al.*, 2012). In a PDI, drugs are used as powdered particles with a size diameter range of 0.5-5 µm and usually have particles which are monodispersed and spherical in shape. The formulated drug is blended with a large sized carrier molecule such as lactose to improve flow properties and the monodispersion of the dose. The advantages of DPI over PMDI are the stability of the drug; they are free from propellants and patient compliance. Patient compliance is important to the success of an inhalation product. The compliance is a frequent difficulty for inhalation device

users, with inappropriate technique common among patients. Their disadvantages include that they are inspiratory flow rate dose-dependent; an aggregation of powder due to humidity can occur and a dose loss due to accidental exhalation into the DPI is also possible (Chougule *et al.*, 2007; Islam and Rahman, 2008).

Nebulisers have been used for many years to treat respiratory diseases. Three types of nebulisers are available on the market, namely, pneumatic or (air jet), ultrasonic and vibrating mesh nebulisers. The jet nebulizer acts when the drug solution drawn up from the fluid reservoir is dispersed into droplets in the gas stream as a response of a low level of pressure presents at the outlet of the adjacent solution. Ultrasonic nebulisers use a high frequency ultrasound to convert the drug solution into a fine droplet mist. The method therefore does not require compressed air. In vibrating nebulisers, a rapidly vibrating membrane is used to nebulise a drug solution (Boe *et al.*, 2001;Gupta and Hickey, 1991; Hess, 2008).

In preclinical studies of lung cancers, many anticancer drugs were assessed by administering them to the airways using nebulisers, intra-tracheal instillation and intranasal administration (Karhale Ashish *et al.*, 2012). Nebulisers are principally used in a rodent experimental model and less frequently for those involving larger animals (e.g. dogs). Passive inhalation studies are more representative of drug delivery to the human lungs than intra-tracheal or intranasal instillation of large volumes of liquids because animals are awake and allowed to breathe normally. The evaluation of formulations which, delivered by passive nebulisation to the lungs, are conducted using the head only, the nose only and a chamber for whole body exposure systems. Animals can be placed in a sealed box that is connected to a

nebuliser or a generator of a dry powder aerosol for whole body aerosol exposure system. The disadvantages of this system in comparison with the head only or nose only exposure systems are that there is absorption of the drug across the skin after deposition on the animal' fur or the nasal mucosa and the gastrointestinal tract. Direct intra-tracheal instillation using a simple micro-syringe enables potential administration to the lung and to the highest bioavailability. The main advantage of intra-tracheal administration is the avoidance of drug loss in the device or other regions within the respiratory tract. For example, in Sprague Dawley rats, Gem was administered by intravenous injection, intra-tracheal instillation via tracheotomy (i.t.t.), and intra-tracheal instillation via orotrachea (i.t.o.) or intragastric (i.g.) routes. Gem was quickly absorbed after i.t.t. or i.t.o. administration and the concentration of Gem in blood after i.t.t. and i.t.o. administration was 91% and 65% , respectively (Min *et al.*, 2008). Intranasal administration can also be used for intrapulmonary drug administration in mice using a micropipette. The solution is deposited on a nostril and aspirated in respiratory airways during breathing. Use of a small volume limits intranasal administration of the drug. To assess pulmonary delivery of anticancer drugs *in vitro*, impingers or impactors have been used in many experiments (Karhale Ashish *et al.*, 2012).

1.4 Project Aims

The overall aim of this study was to determine if NIV could be used as a delivery system for Gem in a lung cancer treatment administered via the pulmonary route. Gem is a promising agent with documented clinical activity in lung cancer. It is similar to the normal substance (pyrimidine nucleotide) within the cells and a less

toxic agent than platinum compounds and requires a shorter period of hospital care than cisplatin or etoposide as single therapies.

Specific objectives included:

- To quantify Gem levels present in serum, tissues and Gem-NIV formulations, HPLC method development was carried out.

- To determine changes in the amount of lipids (surfactant, cholesterol and dicetyl phosphate), HPLC method evaluation was carried out which was required to show the stability of the NIV formulations and to determine the effectiveness of Gem entrapment inside the NIV. It is important to determine lipid content as changes in their chemical properties may affect NIV stability (see Chapter 3).

- To determine the effects of altering vesicle composition on the characteristics of the Gem-NIV (size, ZP and entrapment efficiency, see Chapter 4).

- To investigate the capability of NIV to improve the pulmonary delivery of Gem by inhalation was determined using the MSLI as an *in vitro* model and rodents as an *in vivo* model. Furthermore, a metabolism study was conducted to determine whether or not incorporation of the Gem into NIV protected it from deactivation by the enzymes that are present in tissues (liver and spleen, see Chapter 5).

- To determine the cytotoxicity of various Gem-NIV formulations against the B16 F0 Luc murine melanoma cell line in comparison with Gem solution.

  Specific steps required:

  - To determine cell proliferation using two methods, fluorescence and bioluminescence.
  - To establish the incubation time and cell concentrations.
  - To assess the effects of vesicle size, vesicle composition and lipid concentration on the activity of Gem-NIV in order to facilitate optimal formulation for *in vivo* studies (see Chapter 6).

- To establish the most appropriate model for *in vivo* drug studies by evaluating the effects of mouse strain and gender on the development and progression of lung cancer.

- To determine whether or not using Gem-NIV improved the outcome of treatment in comparison to the Gem solution using IVIS® bioluminescence imaging and lung weights (Chapter 7).

- To investigate the stability of the lead Gem-NIV formulation over three months by measuring drug entrapment, vesicle size, zeta potential, lipid content and viscosity (Chapter 8).

Chapter 2: Materials and Methods

2.1 Materials

The materials required for this research were sourced as follows:

- Tetra-ethylene glycol mono n-hexadecyl ether (surfactant VIII) was obtained from Nikko Chemicals Co., Ltd. through Jan Dekker UK Ltd. (Hampshire, UK). Cholesterol was obtained from Croda Chemicals Ltd. (East Yorkshire, UK).
- Dicetyl phosphate (DCP), deoxycytidine (2-deoxycytidine > 99%), sodium acetate, Penicillin-Streptomycin and Trypan blue were obtained from Sigma-Aldrich Inc. (Poole, UK).
- Gemcitabine (Gem) was obtained from Sequoia Research Products Ltd, Pangbourne, UK.
- The B16 F0 cell line was obtained from the American Type Culture Collection (ATCC) (Uxhridge, Middlesex, UK). Resazurin tablets were purchased from BDH (Londonderry, Northern Ireland, UK).
- Dulbecco's Modified Eagle Medium (DMEM) and TrypLE™ Express were obtained from Invitrogen (Paisley, UK).
- L-Glutamine was obtained from Lonza Wokingham Ltd. (Wokingham, Berkshire, UK).
- Foetal bovine serum was obtained from Biosera Ltd. (Biosera, East Sussex, UK).

- Acetonitrile and propan-2-ol, isohexane, ethyl acetate and glacial acetic acid were obtained from Fisher Scientific (Loughborough, Leicestershire, UK).
- Luciferin was obtained from Caliper Life Sciences Ltd. (Runcorn, UK).
- Isofluo® was obtained from Abbott Labs. Maidenhead, UK.
- Euthatal® was obtained from Merial Animal Health Ltd. (Harlow, Essex, UK).
- Hypnorm® was obtained from Veta Pharma Ltd (Leeds, UK).
- Hypnovel® was obtained from Roche Pharmaceuticals (Nutley, USA).

2.2 Animals

Male and female inbred BALB/c and C57BL6 mice, 8-10 weeks old, weighing 20-25g were obtained from the colonies at Strathclyde University or purchased from Harlan Olac (Bicester, UK). Male, nude BALB/c mice (BALB/c OlaHsd-Fox1nu) were obtained from Harlan Olac. Male Sprague-Dawley rats weighing 200-260g bred in-house were used for tissue analysis studies. All animal experiments had University of Strathclyde ethical approval and were carried out under a UK Home project licence.

2.3 Methods

2.3.1 Formulation of NIV suspensions

Mono-n-hexadecyl ether tetraethylene glycol, cholesterol and dicetyl phosphate were weighed out using a 3:3:1 molar ratio respectively, to prepare 30, 60 and 150

mM/NIV. The lipids were melted by heating them in an oil bath at 130ºC for 5 minutes and the resultant mixture was cooled to 70ºC, and hydrated with 5 ml of preheated (70ºC) distilled water or Gem solution (3.5, 7 or 14mg/ml) to form empty-NIV or Gem-NIV suspensions, respectively. The suspensions were homogenised at 8000 ± 100 rpm for 15 minutes at 70ºC using a Silverson mixer (Model L4R SU, Silverson Machines, UK), and fitted with a five-eighth of an inch tubular work head (Chesham, Buckinghamshire, UK). In some cases, empty-NIV were aliquoted into 1ml volumes and frozen at -80°C for at least two hours. The samples were lyophilised for at least nine hours using a Modulyo freeze-drier (Crawley, England) and were stored at -20°C until used.

2.3.2 Cell Culture

A cryotube containing an aliquot of frozen B16 F0 luciferase cells (Oxbridge, Middlesex, UK) was allowed to defrost and the contents were then added to 5ml of incomplete DMEM (containing 5,000U penicillin and 5mg streptomycin/ml). The resulting cell suspension was centrifuged at 1500 rpm for 5min using a Haraeus Multifuge 3 S-R (DJB Labcare Ltd., Newport Pagnell, and Buckinghamshire, UK). The supernatant was discarded and the pellet resuspended in 5 ml fresh incomplete medium and the washing step was repeated. The pellet was then resuspended in 15ml complete medium which consists of incomplete DMEM plus 10% v/v heat inactivated foetal bovine serum and the cell suspension was added to a 25 cm^2 sterile tissue culture flask. The cells were incubated at 37°C in the presence of humidified 5% CO_2/95% air. The cells were then harvested when 70 % confluent by discarding the medium and incubating cells with 5 ml TrypLE™ for 5 min to detach them. The

resulting cell suspension was centrifuged at 1500 rpm for 5 min to pellet the cells and they were resuspended in 5 ml complete DMEM. An aliquot (15µl) of the cell suspension was mixed at a ratio of 1:1 with Trypan blue and the number of cells/ml were counted under the microscope (× 200 magnification) using a haemocytometer. Cells were passaged by adding 1 × 10^6cells/30 mls complete DMEM to a 75 cm^2 sterile flask if cultured for two days before harvest or 1 × 10^6cells/10 mls complete DMEM to a 25 cm^2 sterile flask if cultured for one day before harvest. The cells were used when in a log phase of growth.

2.3.3 Cytotoxicity assay

In initial studies, the number of cells used/ml in cytotoxicity assays was determined. 100 µl Gem solutions serially diluted (1:1) with complete DMEM medium (n = 6). B16 F0 luciferase cells (50 µl, 1 x 10^5 cell /ml) were added to the appropriate wells of a 96 well tissue culture plate. Twenty µl resazurin solution (10% v/v) was added to the appropriate wells. A negative control was also present on the plate, which contained medium (100 µl/well complete DMEM medium) and resazurin solution (20µl/well). The volume of each well was made up to 200 µl by adding the appropriate volume of complete DMEM. The cells were incubated at 37ºC for 24 hours and then the absorbance of the wells was determined at 570 and 600 nm, using a spectrophotometer. The percentage reduction of resazurin was calculated using the equation from the Alamar Blue® Technical Datasheet provided:

$$\text{Percentage reduction of resazurin} = \frac{(O2 \times A1) - (O1 \times A2)}{(R1 \times N2) - (R2 \times N1)} \times 100$$

- Where: O1 = molar extinction coefficient (E) of oxidized resazurin (Blue) at 570nm which is equal to 80586.
- O2= E of oxidized resazurin at 600nm which is equal to 117216.
- R1 = E of reduced resazurin (Red) at 570nm which is equal to 155677.
- R2= E of reduced resazurin at 600nm which is equal to 14652.
- A1 = absorbance of test wells at 570nm.
- A2 = absorbance of test wells at 600nm.
- N1 = absorbance of negative control well (media plus resazurin) at 570nm.
- N2 = absorbance of negative control well (media plus resazurin) at 600nm.

The percentage difference in resazurin reduction between treated and the control cells in cytotoxicity assays were calculated using the following equation:

$$\text{The difference between treated and control cells} = \frac{(O2 \times A1) - (O1 \times A2)}{(O2 \times P1) - (O1 \times P2)}$$

- Where O1 = molar extinction coefficient (E) of oxidized resazurin (Blue) at 570nm which is equal to 80586.
- O2= E of oxidized resazurin at 600nm which is equal to 117216.
- A1 = absorbance of test wells at 570nm.
- A2 = absorbance of test wells at 600nm.
- P1 = absorbance of positive control well (cells plus resazurin) at 570nm.
- P2 = absorbance of negative control well (cells plus resazurin) at 600nm.

In addition, in some experiments, excitation at 560 nm and emission at 590 nm instead of absorbance was determined. In this case, the values for wells containing cells and resazurin were subtracted directly from negative control wells in order to obtain the levels of fluorescence emitted by the viable cells. The number of cells present/well can also be determined by assessing the amount of luminescence released by the cells in the presence of a luciferin solution. B16 F0 luciferase cells

(50 µl, 1 x 10^6 cells/ml) were incubated with serially diluted Gem solution for 24 hours at 37°C in a humidified atmosphere of 5% carbon dioxide: 95% air (n = 6). The volume was made up to 200 µl by adding 100 µl complete medium to the cells. Negative controls contained 200 µl medium alone (n = 6).

The contents of the wells were then removed and replaced with 100 µl luciferin solution (150 µg/ml complete medium). The total flux/well of samples (photons/sec [p/s]) was measured using the Xenogen IVIS200 (Caliper Life Sciences, Manchester, UK) imaging system.

The suppression in cell proliferation was determined from absorbance, fluorescence or bioluminescence values for a particular treatment by subtracting the treated well values from the values of the untreated control wells and then dividing the resultant value by the mean control value. The suppression data was used to determine the IC_{50} for a particular formulation using a PROBIT analysis excel sheet.

2.3.4. Entrapment efficiency of Gem-NIV formulations

NIV suspensions were characterised on the basis of drug entrapment efficacy. The Gem-NIV formulation was pelleted by ultracentrifuging a diluted suspension (1:5 dilution with distilled water) at 60000 rpm for an hour using an XL-90 ultracentrifuge (Beckman Optima, Greenbelt, Maryland, USA). Pellets were disrupted by addition of 1ml isopropanol. The resultant solution was diluted 1:500 with the mobile phase. Samples were analysed for their entrapment efficiency by HPLC. Entrapment efficiency was calculated using the following equation:

$$\% \text{ Entrapment } = \frac{\text{Gem in pellets (mg)}}{\text{Initial Gem (mg)}} \times 100$$

2.3.5 Size and zeta potential (ZP) of NIV formulations

The size and zeta potential of NIV suspensions was determined using a Nano ZS® (Malvern, UK) at 25°C. Three drops of the NIV were suspended in 2.5 ml of distilled water. The suspension was added to a cuvette of capillary cells (Malvern, Worcestershire, UK) to measure size and ZP. The measurements were taken on the same day that entrapment efficiency was determined for the samples.

2.3.6 Rheological properties

The flow properties of NIV formulations were performed at 25ºC using a Carri-Med CSL2-100 Rheometer T.A. Instruments (Leatherhead, Surrey, UK). The diameter of the stainless steel geometer was 6 cm and the gap between the geometer and lower stationary plate of rheometer was 1mm. Samples were applied to the plate and allowed to equilibrate for 2 min prior to analysis. Rheograms were formed under stress by regularly increasing the shearing rates from a zero value to a 1000(1/s) value in 60 seconds, and were then returned from the 1000 (1/s) rate to the zero rate in another 60 seconds. In each of the studies, three rheograms were performed.

2.3.7 Pharmacokinetic studies

Rats used in the study were anaesthetized by subcutaneous injection at a dose of 0.27 ml of anaesthetic/100g animal body weight (prepared when required using

Hypnorm® and Hypnovel®, diluted 1:1 with distilled water). The rats were treated by inhalation with a Gem formulation given directly to the animal and the end of the nebuliser was connected to an 8cm acetate cylinder, which enclosed the nose and mouth area to the nebuliser head. At various times post-treatment (5, 30, 60 or 120 min) rats were sacrificed and lung lavages collected by inflating their lungs with 0.8 ml PBS pH 7.4 twice, and combining both washes together. Blood was collected into a microfuge tube and allowed to clot by leaving it at 4°C for approximately 2 hours. The blood was then centrifuged at 13000rpm for 15 min at 4°C and the resulting serum was then transferred to a fresh microfuge tube and stored at -20°C until required. The lungs, heart, liver, spleen and both upper part of the right kidneys were removed from the rat, weighed and stored at -20°C until required. For the Gem analysis, the organs were allowed to defrost and a sample removed/organ (0.15- 0.5 g/sample), spiked with 0.25 ml deoxycytidine (25 μg /ml saline, internal standard) and then homogenised using IKA® T10 basic homogeniser (Ultra-turrax®, Staufen, Germany) for 5 min at 30,000 rpm. The homogenized sample, defrosted serum sample or lung lavage sample was ultrafiltered at 4000 rpm for 60 min using Amicon® Ultra-4 centrifugal filter devices (30,000 MWCO, Millipore, Watford, UK). The filtrate obtained was analysed for Gem content by HPLC.

2.3.8 Gem analysis

Gem concentration in the samples was determined using an HPLC method. The HPLC system consisted of a Gynkotek® HPLC pump series P580 and auto sampler model GINA 50 (Macclesfield, Cheshire, UK) operated by Chromeleon™ software

version 6.30 SP3 Build 594 Dionex (Leatherhead, Surrey, UK). Separation was carried out on a column consisting of a Sphereclone column ODS (150 × 4.60 mm, 5µm, 100Å, Phenomenex®, Macclesfield, Cheshire, UK) connected to a UV detector operated at dual wavelengths of 282 and 269 nm. A mobile phase consisting of acetate buffer and acetonitrile (95:5 % v/v, respectively) at a pH of 5.5 was pumped through the system at a flow rate of 0.7 ml /min. Solvents were measured separately, mixed and degassed by vacuum filtration using a Millipore vacuum filtration kit from Millipore Ltd (Watford, UK) and Phenomenex® 0.22 µm membrane filters. A calibration curve was established from Gem standards ranging from 0.78-50 µg/ml were prepared in serial dilutions from a freshly prepared stock solution of 1 mg/ml Gem in the mobile phase. Deoxycytidine was added to the standard solutions in a constant concentration (25µg/ml) as the internal standard. The area under the curve (AUC) ratio was plotted against the concentration of Gem. The AUC was calculated by dividing the AUC of the detected Gem by the AUC of the deoxycytidine (Deox). From each unknown sample, 0.5 ml of acetonitrile was added to a microfuge and mixed vigorously using a vortex for 30 seconds. The tubes were centrifuged at 3500 rpm for 10 min at 4°C and the resulting supernatant transferred to a fresh tube. A further 0.5 ml of the acetonitrile was added to the pellet, mixed on the vortexer, and centrifuged under the same conditions. The supernatants were combined and the sample was evaporated using an RC 10.22 evaporator for 40 mins. The dry residue was redissolved in 0.25 ml of mobile phase and centrifuged at 3000 rpm for 10 minutes and 50 µl of the sample was loaded onto the HPLC instrument.

2.3.9 Lipid analysis

A stock solution of each lipid (1 mg/ml of chloroform) was prepared and mixed to prepare known concentrations ranging from 0.025-0.5 mg/ml for lipid analysis. The calibration curves for each lipid were plotted separately by fitting the AUC ratio versus the known concentration of the analysed lipid. The AUC ratio was estimated by dividing the AUC of each lipid by the AUC of the internal standard. The internal standard, prednisolone (2 mg/ml of methanol) and 40 µl were added to each 1 ml of standard solution. A blank sample made from 40 µl of internal standard added to 1 ml of chloroform. 100 µl of the relevant sample was centrifugally evaporated at 35ºC under normal atmospheric pressure using a SpeedVac™ (Thermo Scientific, Québec, Canada) for approximately 40 mins /sample. The resultant dry sample was dissolved in 100 µl chloroform and 20 µl was injected onto the HPLC consisting of the pump and autosampler, as mentioned in section 2.3.8, and which was used with a gradient normal phase method. An YMC-PVA Silica column (100 × 3.0 mm i.d. and 5 µm particle size, Hichrom Limited, Reading, Berkshire**,** UK) attached to a guard column packed with PVA-Sil (10 × 3.0 mm i.d. and 5 µm particle sizes, Hichrom Limited) was used for studies. This method was developed by Prof Alex Mullen and Dr M. Alsaadi (University of Strathclyde). Detection was generated using an evaporative light scattering detector model 500 (Alltech, Nottingham, UK) supplied with 5 L of nebulisation gas by a compressor and optimised at 80°C with a gas flow rate of 2.90 standard litres per minute (SLPM). The organic solvents used for the separation were as follows: Solvent A- isohexane; solvent B- ethyl acetate and solvent C- 60% propan-2-ol, 30% acetonitrile, 10% methanol, 142 µl /100 ml glacial acetic acid and

378 µl/100 ml triethylamine. The gradient elution was continued for 15 min at a flow rate of 1 ml/min.

2.3.10 Stability of Gem-NIV formulations

A 0.5L batch of Gem-NIV was prepared under aseptic conditions, where all procedures were performed in a class II safety cabinet except for weighing and melting lipid components. All equipment, including glassware, apparatus, vials, stopper and homogeniser head were sterilised by autoclaving at 121ºC.

Material	Theoretical weight in 5ml	Theoretical weight in 500ml
Surfactant VIII	53.76 mg	5.38 gm.
Cholesterol	49.76 mg	4.98 gm.
DCP	22.64 mg	2.27 gm.

Table 2.1 The amount of lipids used to prepare 500 ml of Gem-NIV.

Lipids were weighed and transferred to a sterile 0.5 L bottle, melted at 130ºC and then cooled to 70ºC. Gem solution (14 mg/ml) water was sterile filtered through a 0.2µm membrane and added to a sterile 0.5 L bottle. The solution was preheated to 70ºC and added to the lipid mixture in the Class II safety cabinet. The formulation was homogenised for 5 min at 8000 ± 100 rpm at 70ºC using an Ultraturrax T25 homogenizer fitted with an S25N-25G dispersing tool (IKAWerke GmbH, Staufen, Germany). A sample (approximately 1 ml) was withdrawn and the vesicle size and ZP were determined, as the aim was to produce a suspension with similar characteristics to the NIV used in small batch production studies. The homogenisation was continued for up to 15 min and the size and ZP checked at various points until the vesicles were the same size as that used in small batch

studies. Gem-NIV suspension (3 ml aliquots) was added to a sterile bijou and stored at 4, 25 or 37ºC. In addition, freeze-dried samples were prepared using 1.5 ml suspension/sample and store at-20ºC until required. Three samples/time points were used to determine the Gem concentration, lipid content, particle size and zeta potential at 0, 1, 2, 4, 8 and 12 weeks post-manufacture.

2.3.11 Metabolism of Gem in liver and spleen

The liver and spleen was removed from a euthanized rat, transferred to 20 ml universal tubes and kept on ice. The Gem solution and Gem-NIV (0.5 mg/ml) were freshly prepared and used to spike 1 g of tissues with 20 or 50 µg Gem. The samples were homogenised for 5 mins in an ice bath and then incubated at 37°C. One hundred µl was withdrawn at 0, 15, 30 and 60 min (n = 3/treatment) and the amount of Gem present/ml was determined by HPLC (Immordino *et al*., 2004).

2.3.12 Multi-stage liquid impinge studies

A sample of each formulation (0.5 ml, Gem-NIV or GEM solution) was nebulised into the MSLI as described above using a flow rate of 60 ± 5 L/min. Each stage of the MSLI was loaded with 20 ml of distilled water. The nebuliser device was inserted onto the mouthpiece of the MSLI and formulations were nebulised until the entire sample was used. The mouthpiece and the filter were rinsed with 20 ml of water to collect deposited formulations. The water at the different stages of the MSLI was used to rinse the surfaces of the stage and was then collected. The vesicle

size and ZP (Gem-NIV only) and the Gem/ml for samples taken from different parts of the MSLI were determined by HPLC.

2.3.13 *In vivo* cancer studies

Mice were injected with B16 F0 luciferase cells (5 x 10^5/0.2 ml complete RPMI medium using a 25G needle attached to a 1 ml syringe via a tail vein. Bioluminescence (BL) imaging was used to monitor tumour progression. Ten minutes prior to imaging, the mice were injected intraperitoneally with a luciferin solution (0.2 ml PBS pH 7.4, 150 mg/kg). The mice were then anaesthetized using 2% isoflurane® in oxygen flowing at 150 ml/min and were then transferred to the Xenogen IVIS 200 system and connected to nose tubes. Images were acquired at two mins using the cooled CCD camera and the animals were then replaced in their cages and allowed to recover. The mice were treated on different days after being given B16 F0 luciferase cells with PBS pH 7.4 (control), empty-NIV (30 or 60 mM), Gem solution (3 or 6 or 15 mg/kg, 0.5ml) or Gem-NIV (30, 60 or 150 mM) by the pulmonary route using an Aeroneb® Lab nebuliser (Aerogen® Inc., Galway, Ireland) and a Buxco® 10 nebuliser system (Wilmington, USA). The Aeroneb® Lab nebuliser was connected to a Volumatic™ Spacer (Allen and Hanbury, Middlesex, UK) containing 2-4 mice. Nebulisation was continued for 5 minutes and the animals were imaged at various points in the time during the experiment. When an experiment was terminated, the lungs and livers of animals were removed, weighed and the *ex vivo* bioluminescence of samples was determined after immersing the organs in a luciferin solution (150 µg/ml DMEM) for 2-5 minutes. The samples were transferred to a Petridish and imaged using the automatic setting.

2.3.14 Statistical analysis of data

The effect of drug treatment on cell proliferation in *in vitro* pharmacokinetic data, tumour inhibition (total flux and weights), systemic toxicity (body weights) and NIV characteristics (size and ZP) studies were analysed using the Statview® version 5.0.1 software package (SAS Institute Inc., Abacus Concept, Inc., Berkeley, USA). A Kruskal Wallis test was used to compare three or more treatments and if a significant difference was obtained then a Dunn post-hoc test was used to determine significant differences between treatments. A Mann Whitney U test was used to compare two treatments. Treatments were considered significantly different at $p < 0.05$.

Chapter 3: Analytical HPLC method development and validation

3.1 Introduction

A sensitive method to determine Gem concentrations in biological fluids (serum and lung lavages), tissues and prepared NIV was required for this project. In addition the three lipid components, i.e. surfactant, cholesterol and DCP (which form the NIV), needed to be determined to examine stability during storage. Previously, an enzyme-linked immune sorbent assay (ELISA) and a high performance liquid chromatography (HPLC) have been used to determine Gem in plasma (Abbruzzese *et al*., 1991). HPLC is a known highly sensitive analytic method that can be used to separate drugs that have been dissolved in test samples and so it was chosen for development. The method involves a small volume of sample being injected onto a HPLC column using an automated injector. The column is packed with porous particles of the stationary phase and separation is achieved using solvents, known as the mobile phase, which are pumped down the column. During the sample moving along the stationary phase, components are separated based on their relative affinity to the stationary or mobile phase. Consequently, if the sample has a higher affinity for the stationary phase than the mobile phase then its elution from the column is slower (see Figure 3.1).

The separated compounds (i.e. drugs and lipid) are detected using a detector as they leave the stationary phase and the resultant electrical signal from the detector is converted to a chromatogram which corresponds to a concentration of the compound present in the sample (Ahuja, 2007).

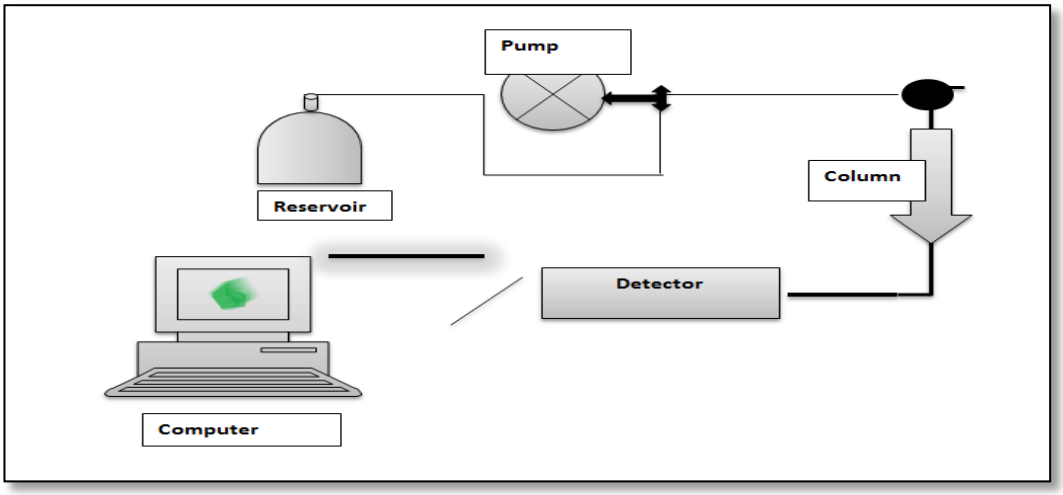

Figure 3.1 A schematic diagram of a HPLC instrument. HPLC instruments consist of a reservoir of mobile phase, a pump, an injector, a separation column, and a detector.

The samples are separated by HPLC using different techniques (e.g. normal phase or reverse-phase) depending on the polarity of the stationary phase. When, the polarity of the stationary phase is higher than the mobile phase, then polar compounds are retained longer than non-polar ones and, thus, the non-polar compounds are eluted first. This process is known as normal phase liquid chromatography (NP-HPLC). In reverse-phase liquid chromatography (RP-HPLC) an opposite system is used, whereby the stationary phase has a lower polarity than the mobile phase. Although NP-HPLC was initially used (Freeman *et al*. 1995), RP-HPLC is used by most researchers (Buszewski and Noga, 2012).

Two basic elution types are used in HPLC, namely isocratic or gradient. In an isocratic elution, the mobile phase composition remains unchanged during the run whereas in gradient elution the mobile phase composition changes throughout the separation. In addition, in a gradient elution, the elution strength of the mobile phase increases during the run so that the samples retained on the stationary phase are eluted; this is a more complicated technique than isocratic HPLC (Schellinger and Carr, 2006).

Different types of detectors are used in HPLC, and these include ultraviolet, fluorescence, refractive index, evaporative light scattering, mass spectroscopy and nuclear magnetic resonance (Dong, 2006). HPLC with mass spectroscopy (MS) has been used determine Gem and its metabolite (2, 2-difluorodeoxyuridine) in human urine (Sottani *et al.,* 2004). Liquid Chromatography/Mass Spectrometry (LC-MS) was developed to quantify Gem and its metabolites (2, 2-difluorodeoxyuridine and Gem triphosphate) in tumour tissues (Bapiro *et al.*, 2011). However, HPLC assays with ultraviolet detection to measure Gem in plasma have been widely described in the literature (Lin *et al.,* 2004; Wang *et al*., 2003; Keith *et al.,* 2003).

Proteins can be removed from biological samples so that analytes can be assessed by precipitation using acid (Wang *et al.,* 2003) or by water-miscible organic solvents including isopropanol, methanol, acetonitrile, and a mixture of acetonitrile and methanol (9:1 v/v). The solvents do not cause hydrolysis of Gem that occurs when acid is used (Lin *et al.,* 2004).

Compounds such as fluorouracil, aracytidine, deoxycytidine, floxuridine, difluorodeoxyuridine, and tegafur can be used as internal standards because of their

similar chemical structures to Gem. The internal standard is required to correct for drug loss during sample preparation (Skoog *et al.*, 1998). Deoxycytidine (Deox) is most commonly used as an internal standard for Gem studies (Decosterd *et al.* 1999; Kerr *et al*., 2001) and precipitation of proteins is achieved using a mixture of acetonitrile and methanol (9:1). Detection of Gem is performed using a wavelength of 282 nm and a mobile phase mixture of acetate buffer pH 5.0 and acetonitrile [97.5: 2.5 (v/v)] (Parshina *et al*., 2008). In RP-HPLC separation, two factors should be considered for good separation of compound - flow rate, and the percentage of organic solvent in the mobile phase. Reducing the flow rate leads to increases the retention time of the analyte(s) whereas, increasing the percentage of organic solvent in the mobile phase reduces the retention time. However, excessively high levels of organic solvent result in increased band overlap and low quality separation of analytes (Snyder *et al.*, 1997). To measure the quality of separation, the Resolution Factor, R_s of two bands can be calculated using the following equation :

$$R_s = \frac{2(t2-t1)}{W1+W2}$$

Where t_1 and t_2 are the retention times of the two bands (peaks) and W_1 and W_2 are their base line peak widths. To measure the reproducibility of the developed analytical method, Precision (RSD) can be determined using the following equation:

$$\left(\text{RSD } \% = \frac{\text{SD} \times 100\%}{\text{mean}}\right).$$

For good separation the Precision value should not exceed 15% according to Guidance for industry bio-analytical method validation (Bapiro *et al*., 2011). Thus, the level of precision is the relative standard deviation to the means (AUC) or heights recorded in the chromatogram after detection of the analytic samples.

The lowest concentration in a sample that can be detected, but cannot be well quantified is called the 'Low Limit of Detection' (LLD) under the stated experimental conditions. The LLD is important for analysis of samples containing low drug levels and it is generally recognised as the concentration yielding a signal with high noise. The concentration that gives the lowest noise signal is called 'Low Limit of Quantification' (LLQ) (Dong *et al*., 1990).

However, HPLC has previously been used as the analytical tool to determine cytotoxic drug concentrations in biological fluid, lungs and other tissues (Zhou *et al*., 2012). In particular, HPLC has been used to investigate the pharmacokinetic features of GEMRAZ® (gemcitabine solution), as opposed to Gem liposomes (Paolino *et al*., 2010). For this reason, the HPLC method was chosen in the present study and developed to determine Gem concentrations in lungs, biological fluids (serum and lung lavages) and other tissues.

3.2 Results

In initial studies it was important to show that the HPLC assay produced a linear relationship between the concentration of the analyte (i.e. Gem, surfactant, and cholesterol and dicetyl phosphate) and the AUC of the chromatogram. By plotting concentration versus AUC, it was possible to assess the linearity of the HPLC method, and an example of the data obtained for Gem and Deox is shown in Figure 3.2. A linear regression analysis showed that the Correlation Coefficient (r^2) was 0.997 for Gem and 0.993 for Deox. The best results (concentrations µg/ml) were obtained if Gem concentrations were within the range of 0.78-50 µg/ml. The

retention time of Deox was ≤ 3 min and the retention time of Gem was ≥ 4 when analysed by the method conditions set out in Table 3.1, showing that the assay gave good separation of the two compounds.

Instrument	The HPLC system consisted of a Gynkotek® HPLC pump series P580 and autosampler model GINA 50 (Macclesfield,UK) operated by Chromeleon™ software version 6.30 SP3 Build 594, Dionex (Surrey, UK).
Column	SphereClone™
Mobile phase	Acetate buffer: acetonitrile (95 : 5)
Flow rate	0.7 ml/min.
Wave length	Gem (282nm) and Deox (269 nm)
Sample size	50 µl
Retention time	5 minutes

Table 3.1 Chromatographic conditions of the evaluated HPLC method. Conditions include type of instrument and column, constituent of mobile phase, flow rate, wave lengths, size of injected sample and retention time.

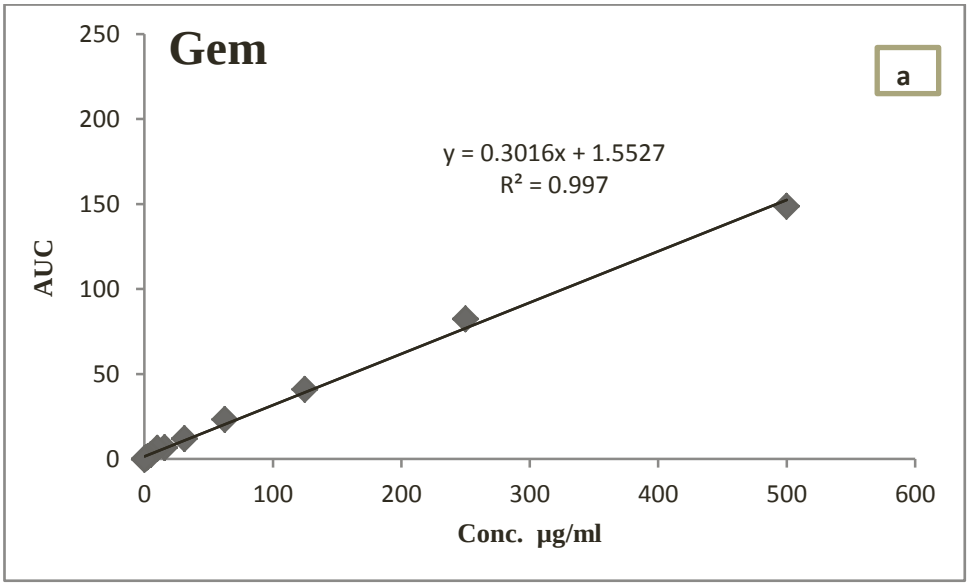

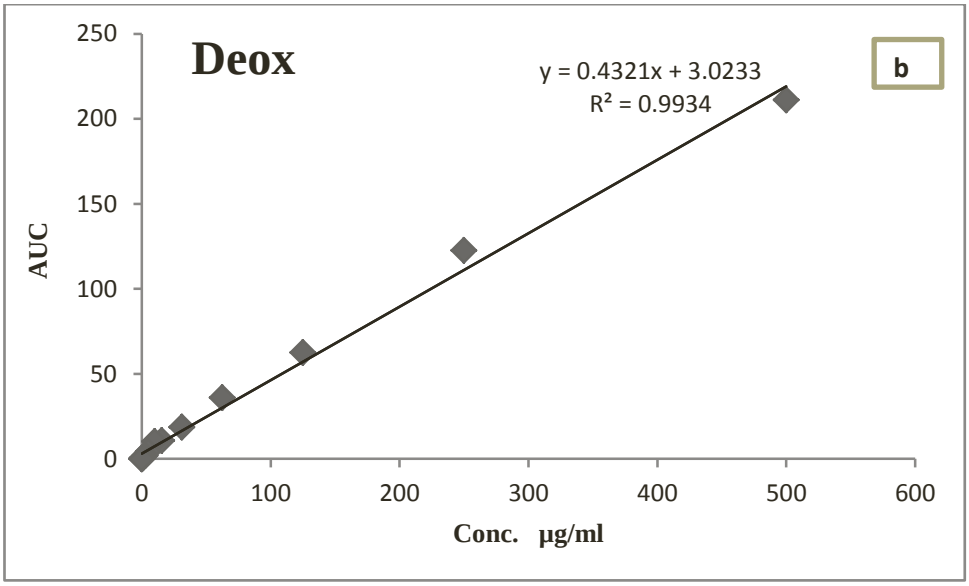

Figure 3.2 Calibration curve for Gem (a) and Deox (b), run separately using conditions of the evaluated method (Table 1.3). Gem or Deox standards ranging from 0.039-500 µg/ml were prepared in serial dilutions from a freshly prepared stock solution of 1 mg/ml Gem or Deox in the mobile phase.

The compounds were then mixed and the analysis was repeated to show that the presence of both compounds did not affect the separation. An example of the standard curve for both compounds i.e. a plot of concentration versus the ratio of AUC of Gem /AUC of Deox is shown in Figure 3.3. Linear regression analysis showed an r^2 value of > 0.99 for both compounds.

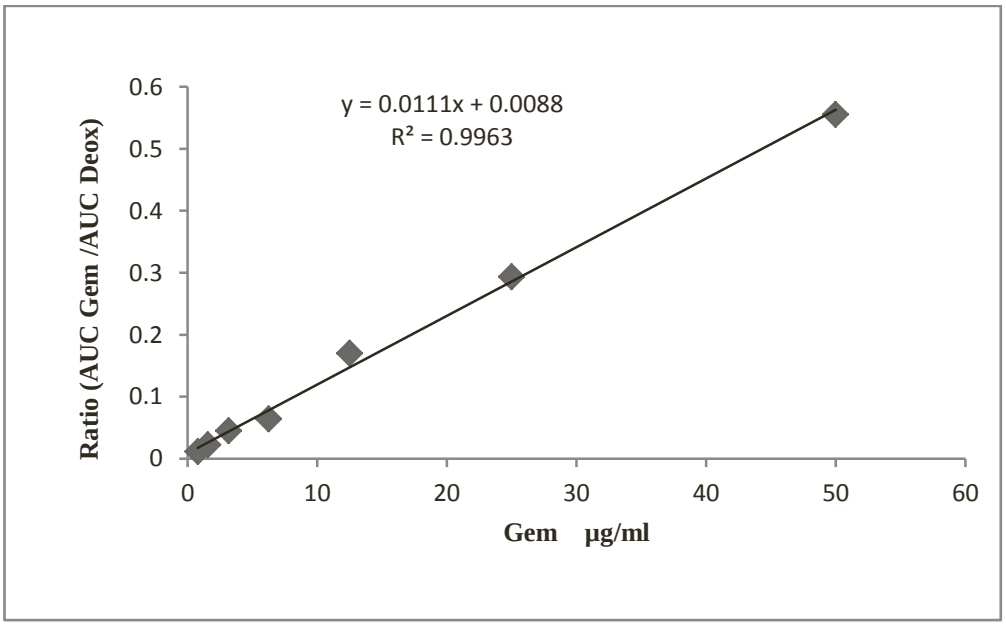

Figure 3.3 Calibration for Gem with Deox mixed before HPLC analysis. Deox was added to the standard solutions at a constant concentration (25µg/ml) as the internal standard. Gem standards ranging from 0.78-50 µg/ml were prepared in serial dilutions from a freshly prepared stock solution of 1 mg/ml Gem in the mobile phase.

The chromatogram shown in Figure 3.4 shows that there was still good separation of the Gem and Deox peaks when both compounds were present and that there was no overlap between them (R_s > 1.97).

Over the course of the study, the ratio of AUC of Gem to Deox standards were used to validate the inter-day and intra-day precision of the developed method (Table 3.2). The results showed that satisfactory relative standard deviation (% RSD) values were obtained for both inter and intra-day analysis.

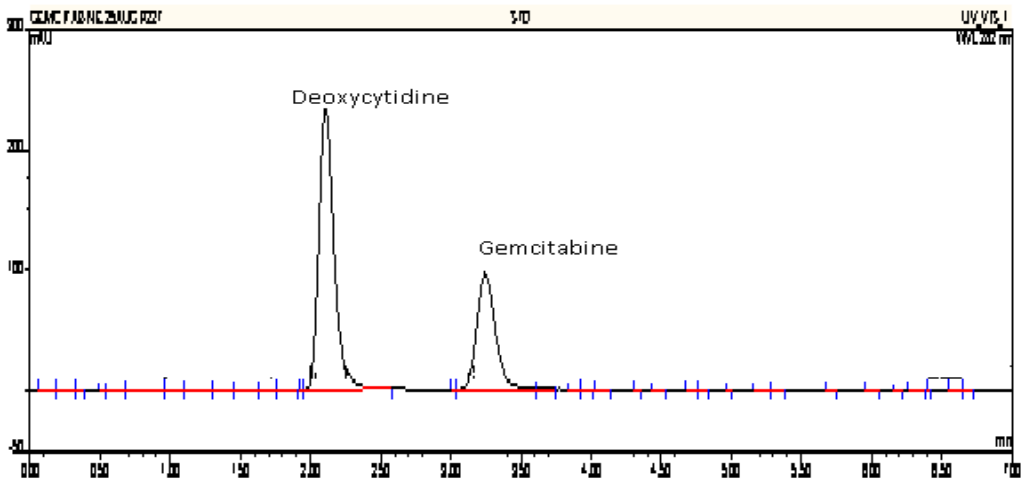

Figure 3.4 A chromatogram illustrating the separation of Gem and Deox at the lower concentration of Gem (0.78 µg /ml) used in the preparation of calibration curve standards. Deox was added to the standard solution at a constant concentration (25µg/ml) as the internal standard. Chromatographic conditions used are described in Table 3.1.

Concentration (µg/ml)	Inter-day precision (%RSD)	Intra-day precision (%RSD)
50	6.5	7
12.5	6	5.1
6.25	4.4	7
3.12	3.04	4.2
1.56	0.96	1.1
0.78	0.81	1.01

Table 3.2 The inter-day and intra-day precision levels of the developed Gem HPLC assay. Values are representative of % RSD = (SD ×100%)/mean (n=3).

The “Low limits of quantification” (LLQ) was 0.31 µg/ml and the “Low limits of detection” (LLD) for Gem was 0.039 µg/ml (see Figure 3.5).

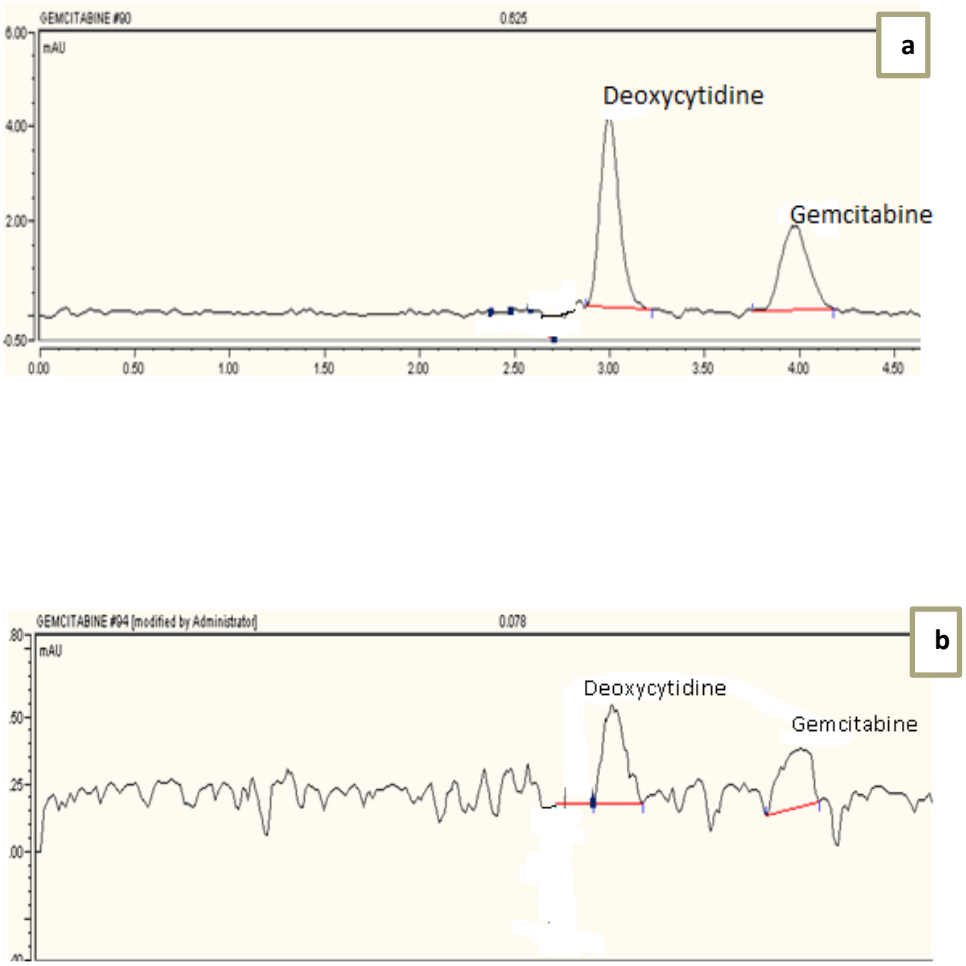

Figure 3.5 Differences in Gem and Deox Signal at LLQ and LLD. (a) Signals of Gem and Deox at LLQ where 0.31 µg Gem and Deox /ml was used (signal to noise was 10:1). (b) Signal of Gem and Deox at LLD to show the noise in the HPLC system at a concentration of 0.039 µg Gem and Deox /ml (signal to noise was 3:1).

An assessment of the recovery % of Gem from the serum or lungs using the developed method for seven concentrations and three repeat measurements at each showed that an acceptable recovery (> 97 %); the standard deviation was not greater than 3% (Table 3.3).

Gem Concentration (µg/ml)	**Serum Gem recovery %** ± SD (n=3)	**Gem Concentration (µg/gm)**	**Lung Gem recovery %** ± SD (n=3)
50	97.52±0.64	50	98.30±2.23
25	99.72±2.38	25	98.20±0.23
12.5	97.02±0.37	12.5	98.28±2.2
6.25	97.68±0.90	6.25	98.94±2.63
3.15	98.50±2.1	3.15	97.23±2.06
1.56	99.0.5±2.29	1.56	98.52±1.32
0.78	97±1.14	0.78	98.05±0.75

Table 3.3 Recovery of Gem from spiked serum and lung samples. Gem (50, 25, 12.5, 6.25, 3.15, 1.56 or 0.78 µg/ml) was added to 0.5ml serum or homogenized tissues along with the internal standard Deox (25 µg /ml). The amount of Gem present in each spiked sample was analysed by HPLC.

Similar types of studies were carried out for surfactant, cholesterol and dicetyl phosphate. The lipid had clear separation (see Figure 3.6) and a linear relationship for all three lipids in the concentration range 0.015-0.5mg/ml, when assayed alone (data not shown) or in combination (Figures 3.7 to 3.9). The intra-day and inter-day precision for cholesterol, surfactant VIII and DCP was ≤ 10 (Tables 3.4-3.6).

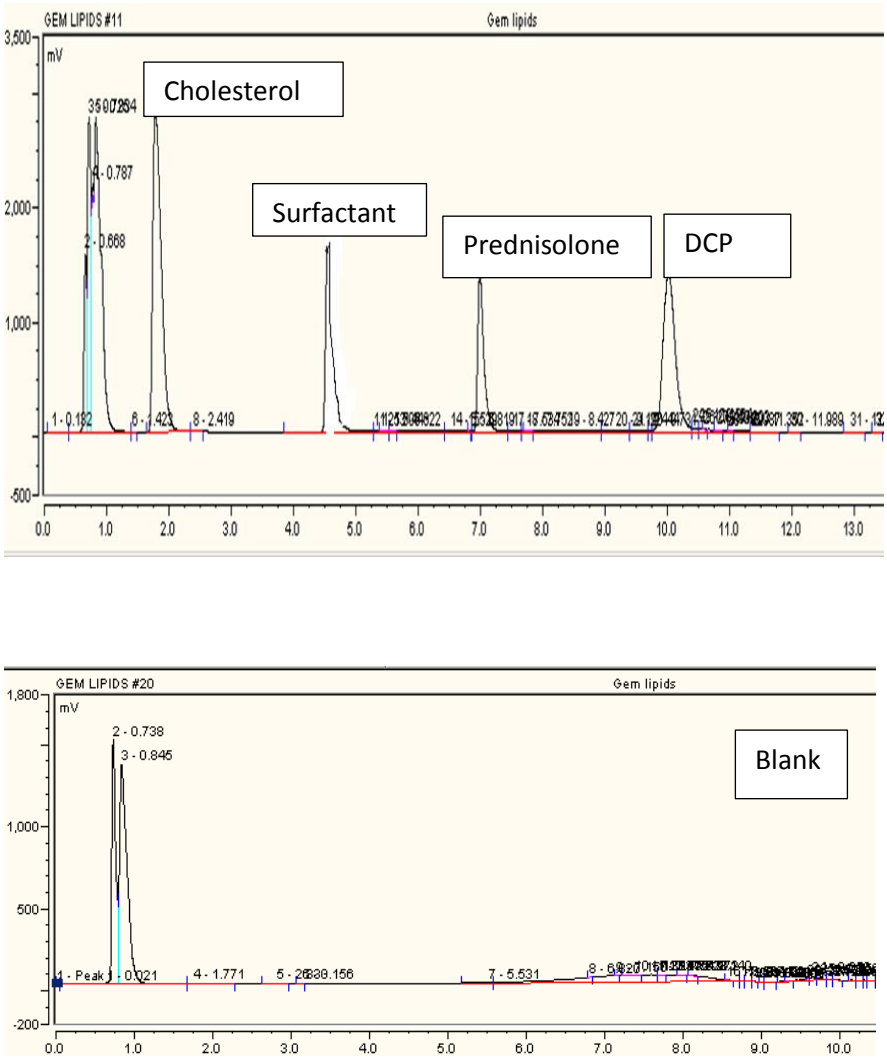

Figure 3.6 A chromatogram illustrating the separation and elution of cholesterol, surfactant and prednisolone and DCP at 2, 5, 7 and 10 min. Blank shows the inert effect of the solvent used.

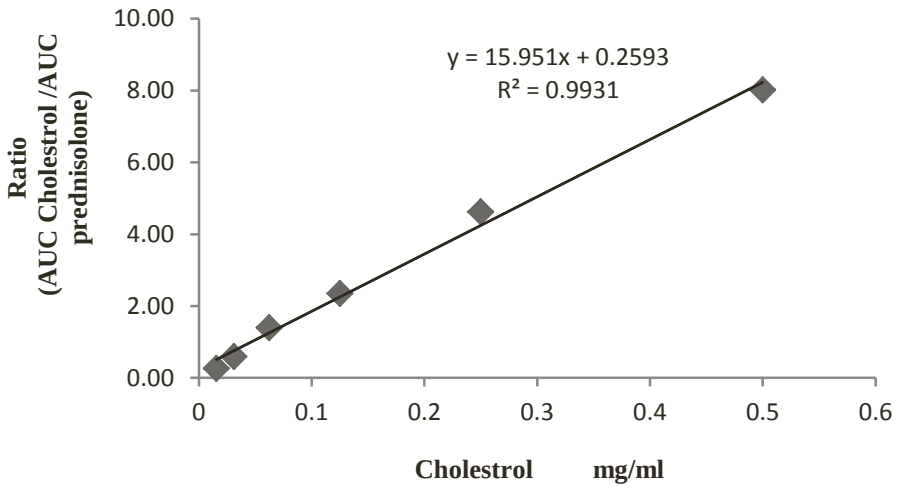

Figure 3.7 A typical HPLC calibration curve for cholesterol. A stock solution of each lipid (1 mg/ml of chloroform; cholesterol, VIII and DCP) was prepared and mixed to prepare known concentrations ranging from 0.025-0.5 mg/ml. The AUC ratio was estimated by dividing the AUC of cholesterol by the AUC of the internal standard. The internal standard, prednisolone (40µl: 2 mg/ml of methanol) was added to each 1 ml of standard solution.

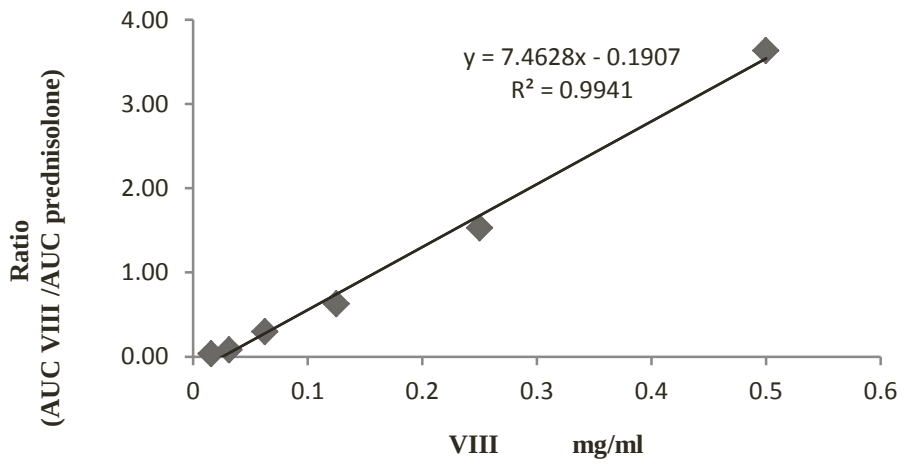

Figure 3.8 A typical HPLC calibration curve for surfactant VIII. A stock solution of each lipid (1 mg/ml of chloroform; cholesterol, VIII and DCP) was prepared and mixed to prepare known concentrations ranging from 0.025-0.5 mg/ml. The AUC ratio was estimated by dividing the AUC of VIII by the AUC of the internal standard. The internal standard, prednisolone (40µl: 2 mg/ml of methanol) was added to each 1 ml of standard solution.

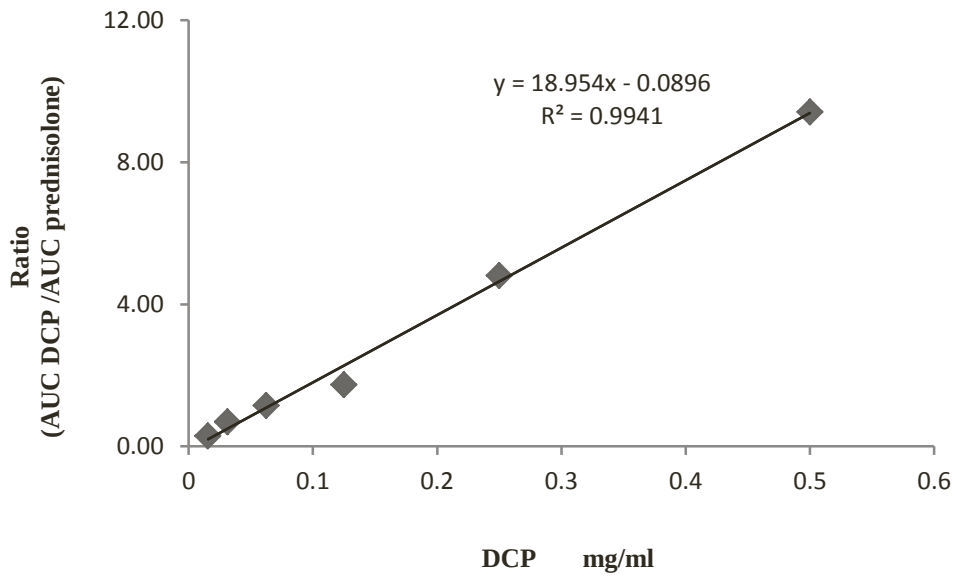

Figure 3.9 A typical HPLC calibration curve for DCP. A stock solution of each lipid (1 mg/ml of chloroform; cholesterol, VIII and DCP) was prepared and mixed to prepare known concentrations ranging from 0.025-0.5 mg/ml. The AUC ratio was estimated by dividing the AUC of DCP by the AUC of the internal standard. The internal standard, prednisolone (40µl: 2 mg/ml of methanol) was added to each 1 ml of standard solution.

Cholesterol concentration (mg/ml)	Inter-day precision (%RSD)	Intra-day precision (%RSD)
0.5	3.1	6
0.25	4	4
0.125	5.5	4
0.062	3	3
0.0312	5	6
0.015	6.9	8

Table 3.4 The intra-day and inter-day precision levels in the analysis of cholesterol standard concentrations. Values are representative of % RSD = (SD ×100%)/mean (n=3).

VIII concentration (mg/ml)	Inter-day precision (%RSD)	Intra-day precision (%RSD)
0.5	4	7
0.25	5	8
0.125	7	8
0.062	4	5
0.0312	5	5
0.015	9.2	9.5

Table 3.5 The intra-day and inter-day precision levels in the analysis of surfactant VIII standard concentrations. Values are representative of % RSD = (SD ×100%)/mean (n=3).

DCP concentration (mg/ml)	Inter-day precision (%RSD)	Intra-day precision (%RSD)
0.5	4	3
0.25	4	3
0.125	3	3
0.062	2	2.5
0.0312	4	5
0.015	7	6

Table 3.6 The intra-day and inter-day precision levels in the analysis of DCP standard concentrations. Values are representative of % RSD = (SD ×100%)/mean (n=3).

3.3 Discussion

A sensitive method was required to measure Gem in serum and tissues. The developed assay had advantages over a published assay by Parshina *et al.* (2008) because it was more sensitive. Its LLQ was better (0.31 µg/ml) than the published method (1 µg/ml). In addition, validation of the precision showed that % RSD was ≤ 7 % whereas for the published method it was ≤ 10%. The inter-day and intra-day reproducibility of the evaluated method ranged from 0.81-6.5% and 1.01- 7%, respectively. The intra-day data was less reproducible than the inter-day variation because of the increase of pressure in the HPLC system within day and lower concentrations were more precise due to the accuracy of the pipettes used to measure small volumes (Zhang *et al*., 2012).

The increase in percentage of the added acetonitrile to mobile phase from 2.5% in the published method to 5% in the developed method led to a shortened retention time and to rapid detection and quantification of Gem in samples. In the Parshina *et al*. (2008) study, acids were used in extraction steps of Gem whereas in the present study the use of acids was avoided to prevent degradation of Gem, which affects the detection of Gem and its internal standard in the tested samples (Lin *et al*., 2004).

In the analysis of Gem in the tissues, the use of acetonitrile alone was found to be effective in isolation and in the precipitation of proteins as pellets, and allowed faster evaporation (40 mins) of tested samples. In contrast, the time of evaporation was longer (60 mins) in the case of using other solvents such as isopropanol and ethylacetate as prescribed in the published assay (Freeman *et al*., 1995; Parshina *et*

al., 2008). In the published assay, heating at 42ºC was used to accelerate the time of evaporation to 20 min, but in the developed method any heating was avoided in order to keep the Gem stable.

The recovery of Gem from serum and tissues was > 97%, an acceptable recovery percentage, and one which was in agreement with the percentage published by Freeman and Parshina which averaged 96.9% and 97% recovery of Gem from plasma, respectively (Freeman *et al.*, 1995; Parshina *et al*., 2008).

The lipid method was based on one developed in this lab (Alsaadi, 2011) From the validation results the present lipid analysis method provided a simple and reliable method in the determining of the lipid content. This method was used in the analysis of the lipid content in order to study stability of the NIV (see Chapter 8). The intra-day and inter-day precision levels for cholesterol and surfactant VIII exceeded 10 for the lowest concentration (0.025mg/ml) according to Alsaadi (2011), whereas in the current lipid analysis the precision for cholesterol, surfactant VIII and DCP did not exceed 10% for the lowest concentration (0.015 mg/ml).

Chapter 3: Analytical HPLC method development and validation

4.1 Introduction

NIV are prepared by the hydration of a non-ionic surfactant, such as polyoxyethylene alkyl ethers, sorbitan monoesters or polyoxyethlene sorbitan monoesters in an aqueous medium to form a closed bilayer structure (see Figure 4.1) (Cosco *et al*., 2009; Junyaprasert, 2008; Paolino *et al.*, 2007). The addition of other lipids can influence the structure and characteristics of the vesicles that are formed. For example, cholesterol can impact on membrane permeability and entrapment efficiency. An increase in the cholesterol concentration of the NIV bilayers results in a decrease in membrane permeability and release rate of the entrapped drug, as a result of an increase in the rigidity of the resulting bilayers (Vyas and Khar 2004).

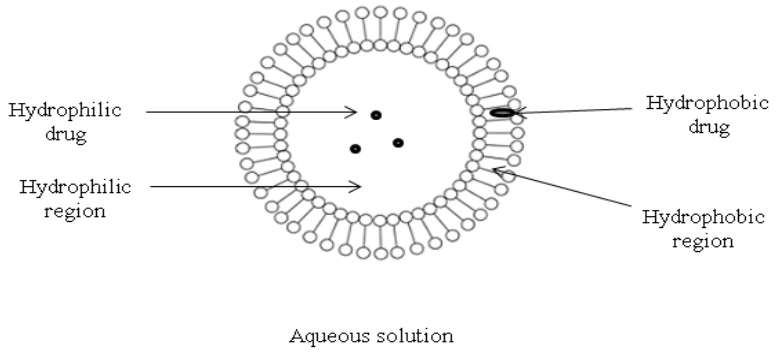

Figure 4.1 NIV structure

NIV can be stabilized by the addition of a charged molecule (i.e. an electrolyte) to the bilayer, such as DCP or phosphatidic acid which gives a negative charge to the vesicles and thus prevents their aggregation (Uchegbu and Vyas, 1998). The addition of SA or cetylpyridinium chloride has a similar effec,t but they give the vesicles a net positive charge instead (Uchegbu and Vyas, 1998). Generally, the charged electrolye is added to a NIV formulation at a concentration of 2.5–5 % because using a high concentration of charged electrolytes can prevent NIV formation (Junyaprasert *et al.*, 2008).

The amount of lipid can influence viscosity and this can in turn impact on its efficiency to be nebulised (Bridges *et al.*, 2000; Niven and Schreier, 1990; Taylor *et al*., 1990). Highly viscous fluids (over 6 cp) may have difficulties in output from the nebuliser due to the effect of viscosity on fluid flow rates because highly viscous fluids produce high resistance, thereby producing large droplets and low outputs from the nebuliser (Mc Callion and Patel, 1996; McCallion *et al.*, 1995; Newman *et al*., 1985).

In addition the site of deposition in the lungs, vesicle uptake and drug delivery can be influenced by variations in vesicle size, surface charge, and drug entrapment. The *in vivo* pulmonary uptake of liposomes increased with increasing size in the range of 100–2000 nm (Chono *et al*., 2006; 2008) and *in vitro* uptake of liposomes increased with an increase in size in the range of 100–1000 nm, and became constant at over 1000 nm. The size of lipid formulations can be adjusted by homogenisation (Bragagni *et al*., 2012; Yamaguchi *et al*., 2009; Ahlin *et al*., 1998) so the speed and

length of homogenisation needs to be optimised to produce NIV of the required mean diameter (Krause and Müller, 2001). Additional steps in the manufacturing process can also influence the *in vivo* delivery of NIV. For example, lyophilisation, which is often used to enhance the stability (shelf-life) of vesicular formulations, can have a significant effect on the final size of vesicle suspensions, as the rehydration of freeze-dried vesicles often results in an increase in vesicle size (Zhang *et al.*, 1997a). Therefore, if vesicles of a particular size are required then it is important to identify a manufacturing method that will provide vesicles with the required mean size at the point of use. Small unilamellar amphotericin B liposomes (AmBisome®) can reduce the toxicity of amphotericin B. For example, Anfogen® has the same chemical composition as Ambisome® but they are manufactured differently to produce a median particle size of 77.8 nm for AmBisome® and one of 111.5 nm for Anfogen®. AmBisome® was shown to be 10-fold less toxic than Anfogen® for uninfected mice. Furthermore, AmBisome® was less toxic at doses of 7.5 and 15 mg/kg and more efficacious than Anfogen® (Olson *et al*., 2008).

4.3 Results

The effect of lipid concentration on vesicle size and ZP was determined for NIV after manufacture and after the rehydration of lyophilised empty-NIV and Gem-NIV. Increasing the lipid concentration used to prepare empty NIV or Gem-NIV resulted in a corresponding increase in vesicle size, with the NIV prepared using 30 mM lipid having the smallest and those prepared using 150 mM lipid having the largest vesicle diameters (Table 4.1). NIV prepared using 60 or 150 mM lipid had similar ZP to empty NIV or Gem-NIV. However at 30 mM, the empty NIV had a significantly

lower ZP than that of Gem-NIV and empty NIV prepared at the higher lipid concentration (Table 4.1). The lyophilisation of empty NIV and its reconstitution with water or a Gem solution resulted in an increase in vesicle size, but there was no change in their ZP compared with the recorded values before lyophilisation. However, the ZP of Gem-NIV prepared from lyophilised empty-NIV at a 30 mM lipid concentration was much lower than that reported for freshly prepared Gem-NIV (Table 4.1). Indeed the ZP of the drug loaded NIV was similar to that of empty-NIV for the lyophilised formulation (Table 4.1).

	Empty NIV		Fresh Gem-NIV	
Lipids (mM)	Particle Size (nm) ± SD	Zeta Potential (mV) ± SD	Particle size (nm) ± SD	Zeta potential (mV) ± SD
30	277 ± 2.8	-50 ± 1	301± 15	-96 ± 1[a]
60	523 ± 37*	-78 ± 1*	582 ± 45*	-78 ± 3
150	770 ± 55*	- 75 ± 5*	870 ± 55*	-66 ± 4
	Lyophilized empty NIV		Lyophilized empty NIV hydrated with Gem solution	
30	804 ± 35[b]	-60 ± 5	832 ± 15[b]	-51 ± 2[b]
60	1049 ± 62[b]	-60 ± 8	1259± 6.2[b]	-65 ± 4
150	1720 ± 354[b]	-70 ± 1	1543± 133[b]	-61 ± 3

Table 4.1 The effect of lipid concentration, Gem incorporation and lyophilisation on the physicochemical properties of NIV. The measurements of the size and zeta potential of prepared samples was performed using a Zeta Sizer (Malvern, UK). [*]$P < 0.05$ compared the increased lipid concentration of fresh empty or Gem NIV to the initial concentration (30 mM) of fresh NIV. [a]$P < 0.05$ compared freshly prepared Gem-NIV to empty NIV. [b]$P < 0.05$ compared lyophilised NIV with freshly prepared NIV.

Lipid concentration had a significant effect ($p < 0.05$) on the percentage of Gem entrapped in NIV, with 30 mM lipid concentration having the lowest entrapment (Table 4.2). However, no significant difference ($p > 0.05$) was observed in entrapped efficiency between Gem-NIV prepared using 60 or 150 mM lipid concentration.

Entrapment efficiency ± SD		
Lipids (mM)	Fresh Gem NIV	Lyophilized empty NIV hydrated with Gem solution
30	49% ± 1	45 % ± 0.5
60	80% ± 4*	75% ± 9*
150	70% ± 6*	66 % ± 3*

Table 4.2 The effect of lipid concentration on entrapment efficiency. Freshly made Gem-NIV and Gem-NIV, prepared by hydration of lyophilised empty NIV with Gem solution were diluted 1:5 with distilled water. The resultant dispersions were ultra-centrifuged at 60000 rpm for an hour using a XL-90 ultracentrifuge (Beckman Optima, California, and U.S.A.). Pellets were disrupted by re-suspending in up to 1ml isopropanol and suitable dilutions within the range of the calibration curve were prepared using a solution of acetate buffer and acetonitrile (95:5). Samples were analysed for their entrapment efficiency by HPLC. $^{*}P < 0.05$ compared the increased lipid concentration of fresh Gem-NIV and lyophilized empty NIV (hydrated) with Gem solution to the initial concentration (30 mM) of NIV ($n = 6$).

The effect of lyophilisation on Gem-NIV was determined for vesicles prepared using 60 mM lipid only, as this gave a higher level of entrapment than 30 mM lipid samples. The size, ZP and entrapment efficiency measured was consistent with previous results (as can be seen from a comparison of Tables 4.1, 4.2 and 4.3). Lyophilisation had no significant effect ($P > 0.05$) on ZP and entrapment efficiency, but there was a significant increase ($p < 0.05$) in vesicle size (Table 4.3).

	Fresh Gem-NIV	Lyophilized Gem-NIV Rehydrated with water
Mean vesicle size (nm ± SD)	567 ± 14	801 ± 46*
Mean zeta potential (mV ± SD)	-73 ± 1	-63 ± 9
Mean entrapment efficiency (% ± SD)	82 ± 4	85 ± 4

Table 4.3 The effect of lyophilisation on physicochemical properties of Gem-NIV. Gem-NIV prepared with 60 mM lipid concentration (Fresh), then lyophilised. The measurement of size and zeta potential of prepared samples was performed using a Nano ZS (Malvern, UK), whereas the entrapment efficiency was analysed by HPLC. $^{*}P < 0.05$ compared the features of Gem-NIV before and after lyophilisation ($n = 6$).

None of the sizes and entrapment efficiency measurements was significantly different ($p > 0.05$) when SA was used (Table 4.4), which means that the surface charge had a negligible effect on size and entrapment efficiency. The effect of the surface charge on the cytotoxicity of Gem-NIV is studied in Chapter 6.

	Gem-NIV prepared using DCP	Gem-NIV prepared using SA
Mean vesicle size (nm ± SD)	567 ± 14	528 ± 26
Mean zeta potential (mV ± SD)	-73 ± 1	+65 ± 6
Mean entrapment efficiency (% ± SD)	82 ± 4	76 ± 7

Table 4.4 The effect of charged agents on physicochemical properties of Gem-NIV. Gem-NIV was prepared with 60 mM lipid concentration (Fresh). The measurement of size and zeta potential of prepared samples was performed using a Nano ZS (Malvern, UK), whereas entrapment efficiency was analysed by HPLC.

Increasing the amount of lipid is known to increase the viscosity of vesicle samples (30 mM; 1.1cp, 60 mM; 4.4 cp and 150 mM; 13.1 cp) at a constant shear rate of 500/ second and results from this study showed that increasing the lipid content by 5 fold resulted in a significant decrease in the amount of sample nebulised (Table 4.5).

Nebulization efficiency		
Lipids (mM)	Fresh empty NIV % ± SD	Fresh Gem NIV % ± SD
30	95 ± 3.7	91 ± 5.5
60	87 ± 5.6	85 ± 9.1
150	10 ± 2.5*	6 ± 4.5*

Table 4.5 The effect of lipid concentration on nebulisation efficiency. Empty NIV and Gem-NIV of 30, 60 and 150mM lipids were nebulised through an Aeroneb® Lab nebuliser (Aerogen® Inc., Ireland) operated by a Buxco® nebulisation system. The Aeroneb® Lab nebuliser was connected to a tube, where 2 ml of the intended formulation was nebulised for 5 min. After nebulisation, the nebulised NIV formulations were collected from the connected tube in order to measure nebulized volumes. *$P < 0.05$ compared the nebulisation efficiency of fresh empty and Gem-NIV of 150 mM lipids and lower lipid concentrations (30 and 60 mM) (n = 6).

In order to produce NIV of a particular size, it is important to know the effect of changing the homogenisation conditions on vesicle characteristics. Increasing the homogenisation time or the homogenisation speed was seen to result in smaller vesicles, but did not affect zeta potential (Table 4.6). Increasing the speed used was more effective than increasing homogenisation time on size reduction.

Conditions	Mean particle size ± SD (nm)	Mean zeta potential ± SD (mV)
Pre-homogenization	582 ± 44.6	-77.6 ± 3.1
5min, 20k	450 ± 11.1	-74.9 ± 0.7
10min, 20k	400 ± 3.1	-70.5 ± 0.4
15min, 20k	261 ± 2.6*	-76.3 ± 0.02
10min, 5k	314 ±6.1*	-70.6 ± 2.4
10min, 10k	259 ± 0.2*	-71.5 ± 0.7
10min, 15k	255 ± 2.1*	-70 ± 0.4

Table 4.6 The effect of homogenization time and speed on the size and zeta potential of freshly prepared Gem-NIV using the conditions of 5, 10 and 15 minutes at a 20k speed setting and 5, 10 and 15k at 10 minutes, respectively. The Gem-NIV was prepared using 60 mM lipid and divided into 2 ml aliquots in Bijou tubes to be ready to carry out homogenisation. The homogeniser used was IKA T25 digitals ULTRA-TURAX®. A polydispersity index (PDI) of Gem-NIV between 0.05 and 0.2 was used, which is a narrow size distribution for a drug particle providing a homogenous formulation. *P <0.05 compared the homogenised Gem-NIV to pre-homogenisation (n = 6).

4.4 Discussion

In these studies, the effect of altering lipid concentration and manufacture method (lyophilisation, homogenisation conditions) on vesicle characteristics was determined for empty-NIV and Gem-NIV. Increasing lipid concentration affected the entrapment efficiency of Gem-NIV. When lipid concentrations were increased from 30 to 60 mM, an increase in the entrapment efficiency of Gem-NIV resulted. However, an increase in the lipid concentrations up to 150 mM showed no extra increase in entrapment efficiency due to the fact that Gem was incorporated into an aqueous core rather than the lipid compartment of NIV. Therefore, increasing the lipid content in a ratio higher than that of an aqueous core will not further enhance the entrapment efficiency of Gem. This result is in agreement with the results of a previous study in which the entrapment efficiency was 74% for Gem-liposomes which had been prepared with Gem: dipalmitoyl phosphocholine: cholesterol: pegylated phospholipid (10: 30: 250: 25) and which had a mean vesicle size of 244 nm ± 1.7. Increasing the phospholipid concentration caused an increase in the size of the vesicles (321nmn ± 4.8) with no significant change in entrapment efficiency (Pitrubhakta *et al.*, 2012).

The inclusion of negative (DCP) or positively (SA) components was conducted to prepare two batches of Gem-NIV. The entrapment efficiency was not affected by change in the charge and this finding agreed with a previous study in which pilocarpine liposomes were prepared with DCP or SA and the encapsulation efficiency of positively or negatively charged liposomes were found to be same for both liposomes (Rathod and Deshpande, 2010). A published study showed that

positively charged liposomes had the highest loading efficiency, exceeding that of neutral ones, followed by negatively charged liposomes, using the same molar ratio of lipids. This effect of charge and loading efficiency is not associated with all drugs (Hathout *et al*., 2007). This order of entrapment efficiency of charged liposomes occurs in cases of weak acid drugs such as acetazolamide, so an attraction occurs between the anionic drug and the positively charged SA where such an interaction would not occur in neutral drugs (such as Gem hydrochloride used in the present study). In this study there was no effect of the charged agent on the entrapment efficiency of Gem-NIV. Therefore, the increase in entrapment efficiency was associated with increasing lipid concentration from 30 to 60 mM, resulting in higher drug retention.

Generally, lyophilisation affords pharmaceutical products a long shelf life when they are stored at room temperature. It also increases the solubility of products, allowing for their rapid reconstitution when required. Heat- and moisture-sensitive drugs retain their stability after lyophilisation. The disadvantage of lyophilisation is a fusion of vesicles after rehydration (Chen *et al*., 2010b). To manufacture Gem-NIV, homogenization is important to gain the desired size; by adjusting homogenisation time and speed, different Gem-NIV sizes can be obtained for use *in vivo* studies. For example, doxorubicin liposomes were serially extruded through a combination of filters of 1 μm, 0.8 μm, 0.6 μm, 0.4 μm and 0.2 μm to achieve the desired particle size with good distribution. However, extrusion requires a longer processing time and higher pressures in comparison with homogenisation. Therefore, homogenisation is commonly used in large scale production of lipid based vesicles

due to faster manufacturing times required to reach the desired size (Mohan Kale, 2012). In this study, the presence of Gem had no effect on the size of NIV. This can be explained by the fact that Gem, a hydrophilic drug, does not interact with the NIV membrane because it is incorporated into the aqueous core of NIV in contrast to lipophilic drug molecules (e.g. rifampicin) (Zaru *et al*., 2007).

The negative charge seen in the ZP arose from ionization of the acidic group of DCP, which interacts with surfactant head groups inducing repulsion between non-ionic bilayers of NIV (Essa, 2010). The ZP may be enhanced after incorporation of the drug, influenced by the feature of membrane. Therefore, the only prospective explanation for the increase in ZP after incorporation of Gem into NIV prepared with 30mM lipid is that Gem causes significant change in the orientation of non-ionic surfactant head groups on the surface of NIV which have a thin membrane, but this phenomenon is limited when Gem is incorporated into NIV with higher lipid content (60 and 150 mM) which have a thick membrane (Fatouros and Antimisiaris, 2002).

Nebulisation efficiency (NE %) is affected by the viscosity of the vesicular dispersion that is subjected to nebulisation. For example, in the case of liposomes, the dispersion viscosity is related to vesicle size and lipid concentrations. Liposomes prepared with 50 mol % of lipids had significantly lower NE% in comparison with the same liposomes with 33 mol % lipids (Zaru *et al*., 2007). In this study, the lipid concentration (150 mM) caused the formation of highly viscous NIV compared with the 30 and 60 mM concentration.

Chapter 5: Gem-NIV and Gem solution: Prediction of *in vitro* lung delivery and *in vivo* measurement of tissue distribution.

5.1 Introduction

The efficiency of NIV delivery of Gem into lungs can be modelled *in vitro* using a variety of impactors or impingers that act as an *in vitro* model for assessment of likely lung delivery (Sadler *et al*., 2011). This is commonplace and used prior to testing *in vivo* using an appropriate animal model (Chimote and Banerjee, 2010; Fauvel *et al*., 2012). Both devices consist of an inhaler induction port or mouthpiece (MP), a series of collection stages, filter systems, a flow control valve with a pressure transducer, two-way solenoid valves, a timer and a vacuum pump. The induction port aids simulation of the mouth and throat of a patient. The vacuum pump generates airflow to simulate inspiration (Guo *et al*., 2008; Menzies *et al.*, 2007; Roberts and Romay, 2005).

The nebulised formulation is carried by the airflow inside the device and particles impact on a flat collecting plate in each section. The orifice diameter of each stage, and the distance from the collecting plate are constant. Particles with a high inertial force collide with the first stages of the impactor and are captured, whereas smaller particles have the ability to reach lower stages (Mitclell *et al*., 2007).

Different types of devices are available, including the twin stage impinger, the Andersen Cascade Impactor (ACI), the Marple-Miller impactor, the Multi Stage Liquid Impinger (MSLI) and the Next Generation Impactor (NGI). In this study, a MSLI was used. It is suitable for use at a flow rate of 30-100 L/min, but the nominal

flow is designed to be 60 L/min. MSLI stages 1, 2, 3 and 4 have cut-off aerodynamic diameters of 13, 6.8, 3.1 and 1.7µm respectively, as described in the European Pharmacopeia (2011) and The United States Pharmacopeia (2010). The final part of the impinger is a filter or micro orifice collector (MOC), which collects the non-impacted particles from the airflow. Particles of less than 1µm follow a Brownian motion, where particles flow from a region of higher concentration to a region of lower concentration (Colombo *et al.*, 2013). The structure of the MSLI used is shown in Figure 5.1.

The deposition of inhaled drug delivery systems in the different regions of the respiratory system depends on breathing rate, mouth and nose breathing, lung volume and respiration volume. Deposition mechanisms of pulmonary inhalation depend on particle size, airflow, and particle location in the respiratory tract. The principal mechanisms of particle deposition into the lungs after inhalation include impaction, sedimentation, interception and diffusion (Forbes, 2000). Impaction happens most frequently in the case of large particles onto large bronchial airway walls. In the smaller bronchioles and alveoli, where air flow is slower and higher humidity exists, hygroscopic particles tend to grow in size and settle out by sedimentation. Interception most commonly occurs with fibrous material, which can reach the smaller airways due to their shape and small aerodynamic diameters relative to their size. Particles with diameters of less than 1µm are deposited by diffusion, which is controlled by Brownian motion.

In Brownian motion, as has been mentioned above, particles move from a region of high concentration to a region of lower concentration and, specifically, diffusion occurs mostly in the alveolar region of the lung (Smola *et al.*, 2008). The systemic absorption of particles in the upper airways is less efficient than that in the alveoli.

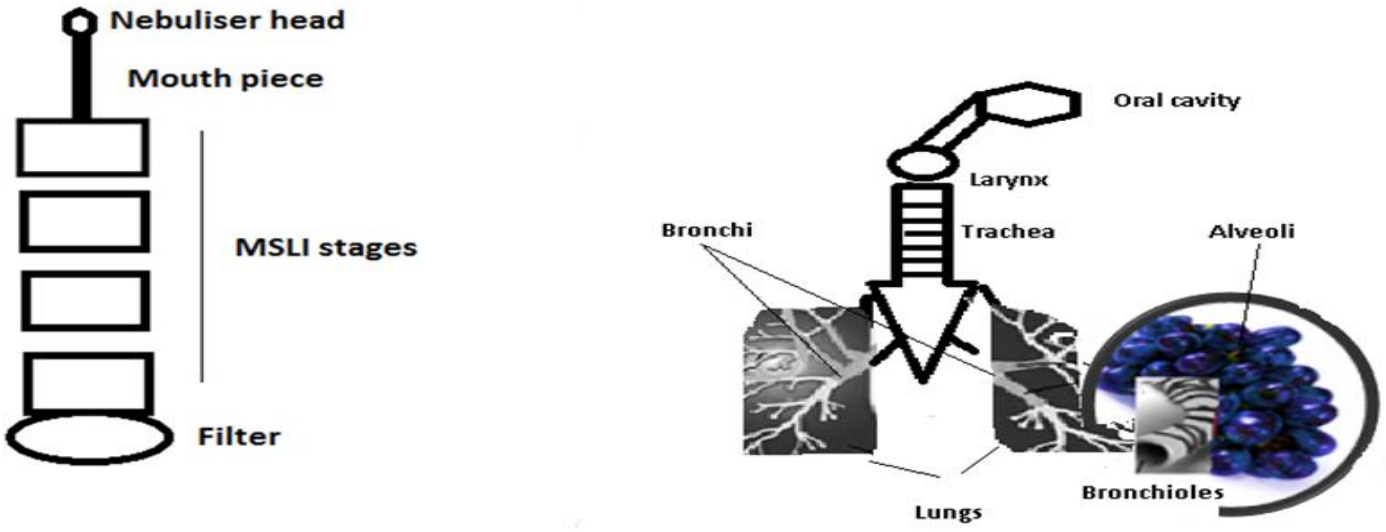

Figure 5.1 A simulation of the respiratory tract and MSLI. The mouthpiece part simulates the mouth and throat. Trachea, bronchi and bronchioles are simulated by the MSLI stages. The final part of MSLI (a filter or micro orifice collector) simulates delivery to the alveoli within lungs (Guo *et al*., 2008; Menzies *et al.*, 2007; Roberts and Romay, 2005).

Particles larger than 10μm will impact on the pharynx and not be absorbed whereas particles ≤ 3μm have 80% deposition in the lower airways of lungs and 50-60% deposition in the alveoli. Studies using gamma scintigraphy and metered dose inhalers showed that there was a correlation coefficient of 0.81 between the percentage of lung deposition and percentage of particles < 3μm (Newman and Chan, 2008).

The deposited drugs after inhalation are either cleared through mucociliary clearance, absorbed into the blood or lymphatic system, or are locally metabolised. The absorption of drugs occurs to a lower extent through a thick epithelium of 50–60 μm of the trachea compared to the thinner epithelium (0.2 μm) of the alveoli (Patton, 1996; Patton *et al.*, 2004). The thin barrier may act as sieve by allowing the diffusion of small solutes and by restricting the entrance of macromolecules through barrier pores of varying radial size, 1.3, 40 and 400 nm. The aforementioned small, medium and large sized pores in the barrier are distributed in the proportion of 68, 30 and 2% respectively across the barrier (Conhaim *et al.*, 1988).

Drugs deposited in the alveoli may be phagocytised by alveolar macrophages which number 5 to 7 alveolar macrophages per alveolus in the lungs and act as a part of the reticuloendothelial system (RES) (Stone *et al.*, 1992). Therefore, many cytotoxic drugs such as doxorubicin can be formulated to deliver specifically into the reticuloendothelial organs of the spleen, liver and lungs by exploiting phagocytosis (Goje *et al.*, 2011; Forbes, 2000).

Enzymes are present in the lung at much lower levels than in the gastrointestinal tract (Brown and Schanker, 1983; Colthorpe *et al.*, 1995; Colthorpe *et al.*, 1992; Niven *et al.*, 1995a; Niven *et al.*, 1995b). Thus, treatment by inhalation could be used to improve the efficacy of drugs that are metabolised into an inactive form such as Gem. Gem is rapidly metabolised by cytidine deaminase into a difluorouridine inactive metabolite, and is then eliminated by the kidneys after intravenous adminstration. This rapid inactivation is partly responsible for the short half-life of Gem (8–17 min) (Beumer *et al.*, 2008). Therefore, the repeated administration of Gem is required, but this also increases the risk of adverse side effects such as myelosuppression, mild and transient neutropenia, thrombocytopenia, and anemia (Reddy and Couvreur, 2008a). Lipid vesicles have been shown to facilitate its intracellular delivery to alveolar macrophages, thus reducing local and systemic toxicity (Schreier *et al.*, 1993).

Delivery to the lungs can be determined in different ways such as gamma scintigraphy and HPLC. Gamma scintigraphy, utilising radioisotopes such as technetium, provides images of pulmonary disposition (desired) or pharyngeal deposition (undesired) of the formulation. It does not directly provide information on the amounts of drug that have been deposited in the lung or in other tissues (Chrystyn, 2000; el-Araud *et al*., 1998; Newman *et al*., 1999; Forbes *et al*., 2011).

5.2 Results

A MSLI was used to study the *in vitro* deposition of Gem-NIV and Gem solution into the lung. Fresh Gem-NIV was prepared with 60 mM lipid containing 14 mg/ml of Gem. Gem solution was also prepared containing 14 mg/ml of Gem in water. Gem-NIV was recovered primarily from stages 1 and 2 whereas significantly ($P < 0.01$) higher amounts of Gem solution were recovered primarily from the MP and filter (Fig. 5.2). The results indicate that using NIV would improve the delivery of the Gem to the stages of the MSLI when compared to a Gem solution.

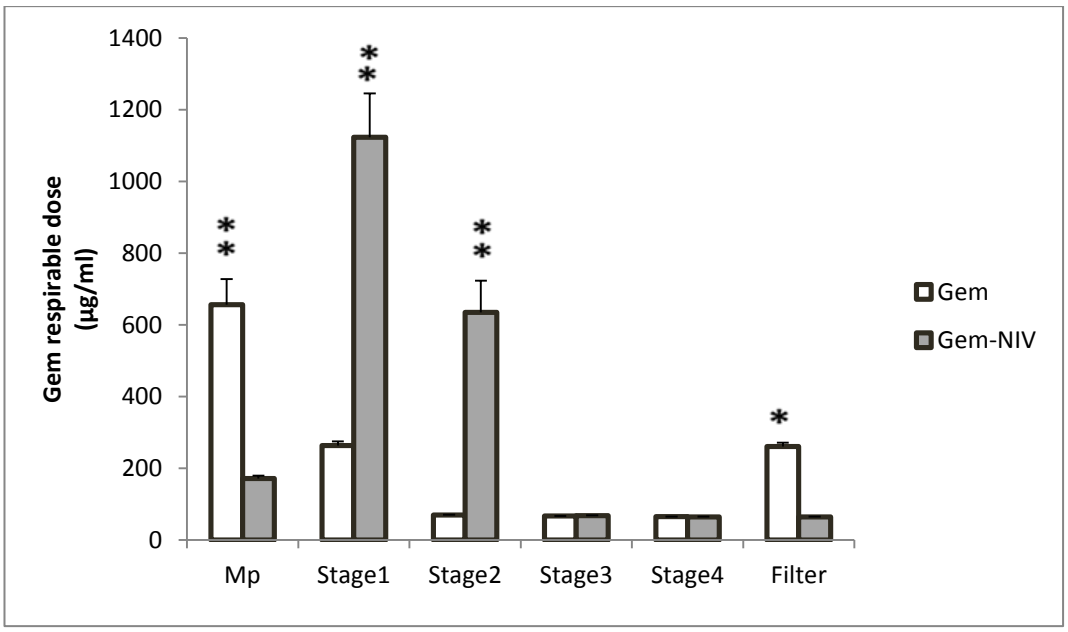

Figure 5.2 *In vitro* pulmonary deposition patterns of Gem NIV and Gem solution. The nebulization efficiency of the two formulations was evaluated using a MSLI. 0.5ml of the relevant formulation (Gem solution, 14mg/ml and Gem-NIV prepared by using 14 mg/ml Gem incorporated into NIV consisting of 60 mM lipids) was nebulised into the MSLI set at a flow rate 60 L/min and each stage contained 20 ml of a mixture of acetate buffer and acetonitrile (95:5). The Gem doses recovered from the device, the MP, stages 1–4 and the filter of the MSLI deposition are expressed as a respiration dose. Gem content was analysed by HPLC. $^{*}P < 0.05$, $^{**}p < 0.01$ compared to the respective solution value (n = 4).

The results show that nebulisation did not significantly affect the ZP of Gem-NIV (60 mM), but during the nebulisation smaller Gem-NIV (~ 250 nm) were formed, reduced from the original NIV size (Figure 5.3).

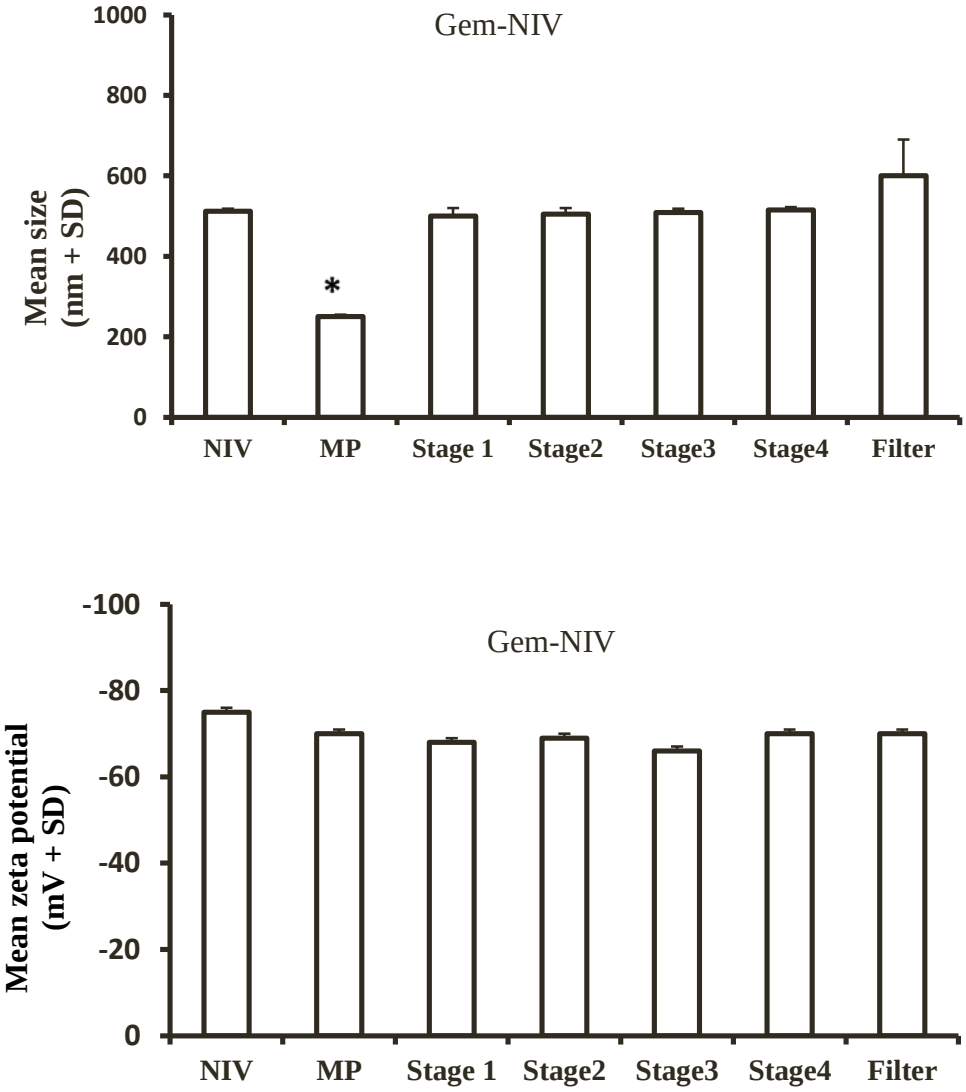

Figure 5.3 Size and zeta potential distribution of Gem-NIV. 0.5ml of the formulation prepared by using Gem (14 mg/ml) incorporated into NIV consisting of 60 mM lipids and nebulised into the MSLI set at a flow rate 60 L/min and each stage of MSLI contained 20 ml of water. The particle size and zeta potential values were measured using a Nano ZS (Malvern, UK). $^{*}p < 0.05$ compared to the respective original measurements (n = 4).

In vivo lung and tissue distribution studies were carried out on rats and mice using Gem solution and Gem-NIV prepared with different lipid concentrations of 30 or 60 mM. To ensure Gem-NIV uniformity, Gem-NIV formulations with a polydispersity (PDI) of between 0.05 and 0.2 were used, which is a narrow size distribution for a drug particle providing a homogenous formulation (Chimote and Banerjee, 2010).

Initial studies showed that a similar Gem concentration was present in the right and left lung lobes of rats treated with the Gem solution or with Gem-NIV. Therefore, only the right lung was used in subsequent studies. Pulmonary delivery resulted in significantly higher lung levels for rats given any of the Gem formulations when compared to serum levels (Table 5.1). Treatment with Gem-NIV (30 mM) at 15 mg/kg gave significantly higher lung levels when compared with treatment with a similar dose of Gem solution. The lung Gem level after the administration of the Gem solution was not significantly different from the level of fifth diluting 30 mM Gem-NIV (at a lower dose – 3 mg/kg) in the lung. Gem concentrations in serum were similar for rats given a Gem solution or Gem-NIV (30 mM) at the same drug dose (15 mg/kg), but the concentration in lung lavage was lower for rats given Gem-NIV (30 mM) (Table 5.1).

Formulations	Gemcitabine concentration ± SD			
	Serum (µg/ml)	Lungs (µg/gm.)		Lavage (µg/ml)
		A	B	
Gem solution 15 mg/kg	135.8 ± 42	365.49 ± 18[a]	312.4±13.9[a]	182.3 ± 10.1
Gem-NIV 15 mg/kg	175.1 ± 3.9	1675.7±11.8*[aa]	1640 ± 43.7*[aa]	22.2 ± 2.8*
Gem-NIV 3 mg/kg	23.6 ± 1.5	339.1 ± 21.4 [aa]	322.1±23.7[aa]	32.9± 10.7

Table 5.1 The concentration of Gem in tissues of rats administered Gem solution or Gem-NIV and diluted Gem NIV (5 fold before use) by inhalation. Rats (n = 12 /treatment) were treated using a nebulizer with Gem solution (15 mg/kg) or Gem-NIV (15 mg/kg, 30 mM lipid) and sacrificed 30 mins after treatment. The lungs were divided into A and B samples to predict the uniform distribution of Gem treatment through lungs. The amount of drug present in the tissues was determined by HPLC. $^{*}P < 0.05$ lungs or lavage concentrations of Gem-NIV compared to lungs or lavage concentrations of Gem solution. $^{a}P < 0.05$ or $^{aa}P < 0.01$ lung concentrations compared with the corresponding Gem value in serum.

Tissue pharmacokinetic data for rats treated by means of inhalation of the Gem solution (6 mg/kg) or Gem-NIV (Gem, 6 mg/kg incorporated into 30 mM lipid) at 5, 30 and 120 mins post-dosing are shown in Table 5.2. The maximum Gem concentration was found in the lung after 30 min for rats given Gem-NIV (30 mM) and the concentration then declined by 120 mins. In contrast, treatment with the Gem solution resulted in a maximum lung concentration at 5 mins, which had declined after 30 mins and was not detected after 120 mins dosing. Therefore, there is significant difference ($P < 0.05$) in the pharmacokinetic profiles, with NIV (30 mM) which was found to give a significantly higher delivery than solution.

In blood circulation (based on serum levels), Gem solution treatment gave significantly higher serum levels compared to Gem-NIV (30 mM) at 5 mins post-dosing. The Gem concentration declined to approximately half, 30 mins after inhalation, and was undetectable at 120 mins. Gem concentrations were lower for Gem-NIV (30 mM) treated rats compared to Gem solution treated rats at 5 mins in serum, but the drug did not decline to half, over 30 mins of treatment as in the case of Gem solution; however, by 120 mins the drug was also undetectable. In the kidney, Gem was not detected 5 mins after dosing with Gem-NIV (30 mM) inhalation, but low detectable levels were present at 30 and 120 mins. Treatment with Gem solution was higher in the kidney levels at 5 and 30 mins after dosing compared to Gem-NIV. The concentration of Gem in spleen showed higher levels than kidney and liver after 5 and 30 min after administration of Gem solution and had declined by 120 mins. In case of Gem-NIV (30 mM), the level of Gem in the spleen was higher than the kidney and liver levels over 120 mins after administration.

Treatments	Times post dosing (min)	Gemcitabine concentration (µg/gm of organs or ml of serum) ± SD				
		Serum	Lungs	Kidney	liver	Spleen
Gem	5	37.8 ± 3.9	292.2 ± 49.8	15.6 ± 1.2	15.3 ± 4	42.3 ± 4
	30	15.94 ± 4.5	149.82 ± 11.1	8.15 ± 1.32	8.7 ± 0.2	27 ± 5.4
	120	0.0	0.0	5.3 ± 0.4	1.21 ± 0.3	3.6 ± 0.4
Gem NIV	5	9.49± 1.77*	375.2 ± 14.7	0.0*	11.03 ± 3	18 ± 1.4
	30	10.24 ± 1.2	548.6 ± 83.2*	4.61 ± 1.1*	4.6 ± 0.8*	24 ± 2
	120	0.0	35.7 ± 7.3*	4.8 ± 1.6	1.4± 0.5	32 ± 2.9*

Table 5.2 The concentration of Gem in the tissues of rats administered Gem solution or Gem-NIV by inhalation. Rats (n = 4 /treatment) were treated using a nebulizer with the Gem solution (6mg/kg) or Gem-NIV (6mg/kg, 30mM lipid: Vesicle size, 302 ± 5.7 nm; Zeta potential, -40.3 ± 5.1 and entrapment efficiency, 49.03% ±1.03) and were sacrificed at 5, 30 or 120 mins after treatment. The amount of Gem present in the tissues was determined by HPLC. *$P < 0.05$: Gem-NIV concentration compared with the Gem solution concentration in tissues.

Gem NIV, with a higher lipid concentration (60 mM lipids) showed a higher localisation in the lung and spleen, but a lower accumulation in serum, kidney, liver, and heart than that of lower lipid Gem-NIV (30 mM, Table 5.3). To investigate the effects of reducing the dose in the lung and tissue distribution of the Gem solution and Gem-NIV prepared with a high lipid concentration (60 mM), the rats were treated with 6, 3 and 1.5 mg/ kg doses of Gem solution and Gem-NIV. The levels of Gem after the administration of treatments decreased with decreasing dose, indicating a linear dose response (Table 5.4).

The lung and tissue distribution of Gem was studied in mice. The level of Gem in the serum and lungs in mice given Gem-NIV (60 mM) was higher than for Gem solution, whereas the level of Gem in the kidney was lower in mice given Gem-NIV (60 mM) than in mice given Gem solution (Table 5.5).

In mice bearing lung tumours, the Gem level was higher in the lung in comparison with normal mice for Gem-NIV treated mice. This increase in lung level was accompanied by a decrease of Gem level in the serum and kidney after treatment with Gem-NIV. The accumulation of Gem in the liver and heart after treatment with Gem solution was higher than that observed in Gem-NIV (60 mM) treated animals. However, 60 mM Gem NIV tended to accumulate in the spleen more than free Gem as shown in Table 5.6.

The results of the metabolism study showed that significantly higher amounts of Gem were detected in spleen and liver samples spiked with Gem-NIV (60 mM) at 30 and 60 min post-incubation at both drug doses, compared to the samples spiked with Gem solution (Figure 5.4).

Gem NIV	Gemcitabine concentration (µg/gm or ml) ± SD					
	Serum	Lung	Kidney	Liver	Spleen	Heart
30 mM	10 ± 0.7	192.3 ±39.95	9.3 ± 0.8	4.87 ± 1.1	25 ± 4.9	11.87± 4.9
60 mM	1.7 ± 0.3*	477.87±25.9*	1.9 ± 1.0*	1.75 ± 0.1*	40 ± 3.9*	5.9 ± 0.3*

Table 5.3 The concentration of Gem in the tissues of rats administered Gem-NIV by inhalation. Rats (n = 4 /treatment) were treated using a nebulizer with Gem-NIV (6 mg/kg, 30mM lipid Gem-NIV; Vesicle size, 255.3 ± 1.2 nm; Zeta potential, -43.3 ± 4.2 and entrapment efficiency, 55.8% ±2.09 or 60 mM lipid Gem-NIV; Vesicle size, 545.1 ± 2.8 nm; Zeta potential, -70.2 mV ± 9.4 and entrapment efficiency, 80.05% ±4.8) and were sacrificed at 30 mins after treatment. The amount of Gem present in the tissues was determined by HPLC. $^{*}P < 0.05$: Gem-NIV (60 mM) concentration compared with Gem-NIV (30 mM).

Treatments	Doses mg/kg	Gemcitabine concentration (µg/gm or ml) ± SD					
		Serum	Lungs	Kidney	Liver	Spleen	Heart
Gem	6	20.94 ± 3.9	160.4 ± 2.1	9.9 ± 0.8	6.8 ± 1.1	21.7 ± 1.4	9.22 ± 0.8
	3	14.9± 2.0	82.97 ± 4.8	5.09 ± 0.9	4.1 ± 0.2	14.63 ± 0.5	5.17± 0.3
	1.5	5.6± 1.0	34.46 ± 2.2	1.75± 0.1	2.21 ± 0.3	6.96 ± 0.2	1.96 ± 0.1
Gem NIV	6	2.1± 0.5*	456.7± 43.7*	2.05 ± 0.08*	2.1 ± 0.4*	40.38 ± 1.9*	5.32 ± 0.2*
	3	1.1 ± 0.09*	263 ± 19.6*	1.3 ± 0.1*	0.75 ± 0.1*	22.31 ± 0.8*	3.35± 0.2*
	1.5	0.0	161.8 ± 4.3*	0.0*	0.35 ± 0.01*	9.99± 0.2*	0.91 ± 0.1*

Table 5.4 The concentration of Gem in the tissues of rats administered Gem solution or Gem-NIV, by inhalation. Rats (n = 4 /treatment) were treated using a nebulizer with Gem solution (6, 3 and 1.5 mg/kg) or Gem-NIV (6, 3 and 1.5 mg/kg: 60 mM lipid, vesicle size, 558.1 ±1.8 nm; zeta potential, -65.2mV ± 4.9 and entrapment efficiency, 77.05% ±4.5) and were sacrificed at 30 mins after treatment. The amount of drug present in the tissues shown was determined by HPLC. *$P < 0.05$: Gem NIV concentration compared with the Gem concentration in tissues.

Treatments	Gemcitabine concentration (µg/gm or ml) ± SD		
	Serum	**Lung**	**Kidney**
Gem	180.8 ± 17.1	47.5 ± 14.4	76.7 ± 18.7
Gem NIV	355 ± 24.4*	71.3 ± 17.2*	42.8 ± 1.5*

Table 5.5 The concentration of Gem in the tissues of normal mice which were given Gem solution or Gem-NIV, by inhalation. Mice (n = 5 /treatment) were treated using a nebulizer for with Gem solution or Gem NIV (60mM lipid: Vesicle size, 502 ± 6.7 nm; zeta potential, -67.3 ± 5.1 and entrapment efficiency, 79.0% ± 2.0) for 5 min (0.5 ml, 14 mg/ml) and were sacrificed 30 mins after treatment. The amount of drug present in the tissues shown was determined by HPLC. $^{*}P < 0.05$: Gem-NIV concentration compared with the Gem solution concentration in tissues.

Treatments	Gemcitabine concentration (µg/gm or ml) ± SD					
	Serum	**Lung**	**Kidney**	**Liver**	**Spleen**	**Heart**
Gem	157.2 ± 13.2	45.5 ± 10.2	42.4 ± 6.1	15± 3.1	66.7 ± 13.1	39± 2.5
Gem-NIV	212.2 ± 4.9*	124.6 ± 5.6*	14.05 ± 2.8*	4.8 ± 1.2*	80.4± 14.2*	0.0*

Table 5.6 The concentration of Gem in the tissues of cancer bearing mice administered Gem solution or Gem-NIV, by inhalation. Mice (n = 5 /treatment) were treated using a nebulizer with Gem solution or Gem NIV (60mM lipid: Vesicle size, 511 ± 7.3 nm; zeta potential, -68.3 ± 7.1 and entrapment efficiency, 75.0% ± 4.1) for 5 min (0.5 ml, 14 mg/ml) and were sacrificed 30 mins after treatment. The amount of drug present in the tissues shown was determined by HPLC. * $P < 0.05$: Gem NIV concentration compared with the Gem concentration in tissues.

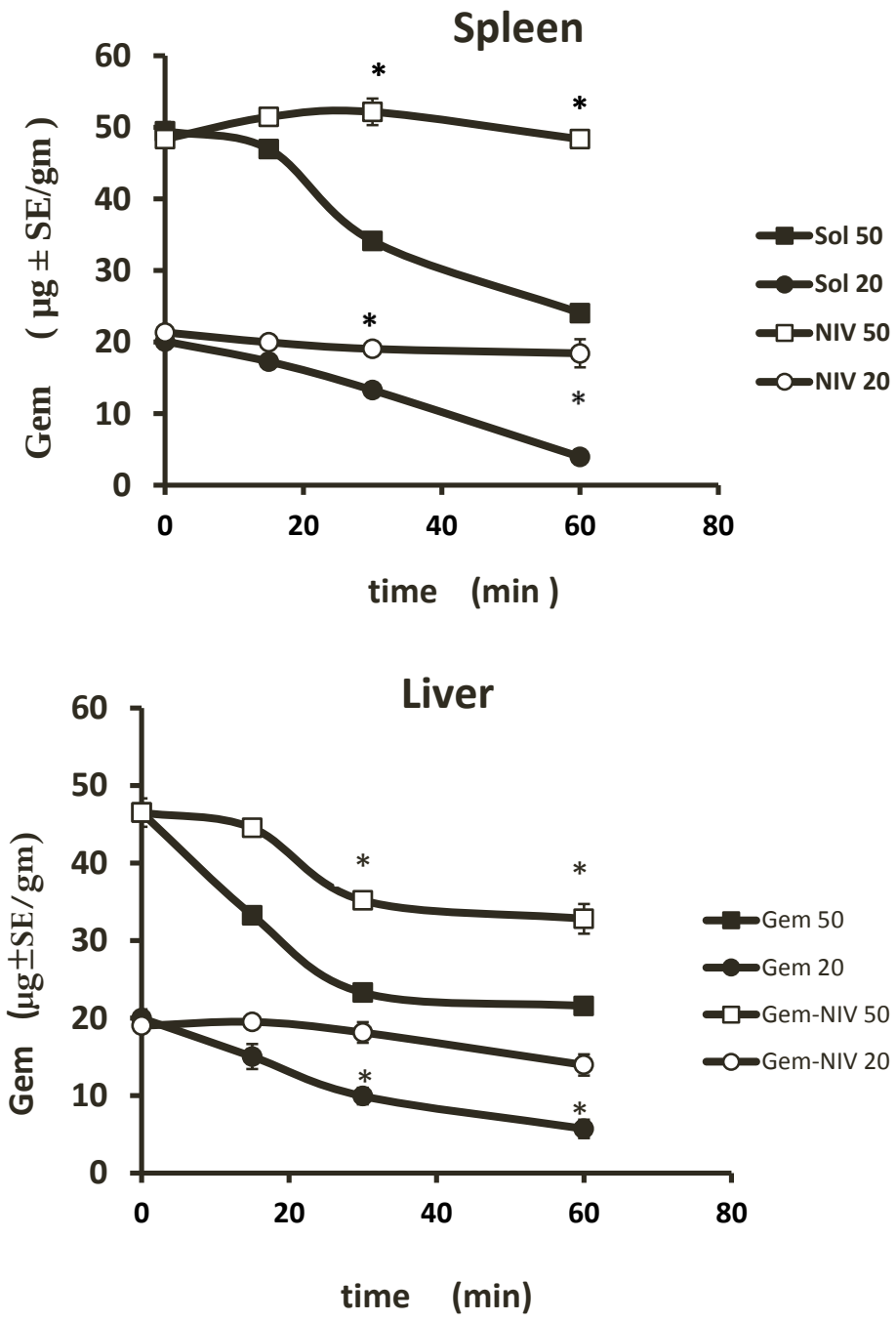

Figure 5.4 Metabolism of Gem and Gem NIV concentrations (20 and 50 µg/gm) in the spleen and liver at 37 ºC (n=3).

5.3 Discussion

Gem solution had a poor deposition in MSLI and was mostly deposited onto the MP. Theoretically, output of a Gem solution is affected by its surface tension, which is responsible for the adhesion of nebulised liquids onto the nebuliser and the MP of MSLI surfaces; or formation of spherical drops which are dispersed in airflow and penetrate the stages of MSLI.

Previous studies have investigated the physicochemical factors that influence nebulised solution and one important factor highlighted is the solubility of the drug in the delivery vehicle during nebulisation. In the nebulization process of the Gem solution into MSLI, the air-flow may dry out aqueous particles of free Gem, leading to a concentration of the nebulized solution on the MP of MSLI (O'Callaghan and Barry, 1997). Another factor that affects the deposition of a nebulised solution is the size of the nebulised droplets. If they are too large, most of the nebulised solution could be deposited and lost on the MP of MSLI (Davis, 1978). However the size of the droplets formed from Gem solution could not be determined by any of the methodologies that could be accessed within the University.

In a previous study with isoniazid, solution was also not deposited into the lower chambers of a twin impinger in contrast to 25-27% of isoniazid liposomes that reached the lower chambers of an impinger (Chimote, 2010). Also, Gem-NIV (60 mM) exhibited better deposition than Gem solution in this study. The presence of DCP and non-ionic surfactant in the NIV formulation certainly has a role in reducing the inertial impaction between NIV and enhancing the nebulisation efficiency. For

example, dipalmitoylphosphatidylcholine (DPPC), the surfactant lipid, has been combined with isoniazid, rifampicin, and ethambutol and *in vitro* deposition efficiency of the prepared formulations was assessed using the twin impinger. The results were 12.06% ± 1.87% of isoniazid, 43.30% ± 0.87% of rifampicin, and 22.07% ± 2.02% of ethambutol deposited in the deep chamber of impinger upon nebulization because these formulations had a quicker ability to reduce the surface tension at the air-aqueous interface, causing better spread of NIV into the impinger rather than adherence on the MP surface (Chimote and Banerjee, 2009).

Additionally, a previous study related to another type of delivery system also showed that the presence of a surfactant (Na glycocholate) is necessary to get easy dispersion of tobramycin nanosuspension into stage 4 and the filter regions (deep parts) of a MSLI with a decrease in deposition in the MP (Pilcer *et al.*, 2009).

The size and ZP of the droplets formed from Gem-NIV were determined using a Zeta sizer in this study. The results indicate that nebulisation did not significantly affect the ZP of Gem-NIV (60 mM), but during nebulisation smaller Gem-NIV (~ 250 nm) were formed, reduced from the original NIV size (~ 500 nm) and this finding is in agreement with a previous study which showed that the nebulisation process was associated with a significant ($P<0.05$) change in mean vesicle size of liposomes from 5.4 µm to 2.7 µm (Taylor *et al.*, 1990a). This reduction was explained by the probability of vesicle size reduction due to shear forces during their delivery by nebulisation. Vesicles with a size > 500 nm remained airborne to

penetrate the MSLI stages and establish deposition on its plates (O'Callaghan and Barry, 1997).

In vivo studies were conducted using rats and mice. Current i*n vivo* investigations showed that direct administration of Gem treatments (both Gem and Gem-NIV) to rats by inhalation resulted in high lung concentrations of Gem. This route of administration was widely used by researchers to avoid Gem metabolism associated with other routes such as intravenous and oral routes (Min *et al.*, 2008). In particular, lungs have shown a remarkably lower level of metabolism in comparison with other sites in the body (Brown and Schanker, 1983; Colthorpe *et al*., 1995; Colthorpe *et al*., 1992; Niven *et al*., 1995a; Niven *et al*., 1995b; Ruge *et al*., 2012).

The deposition of Gem is superior when delivered in NIV to the lungs of rats compared to Gem solution. Vesicular delivery systems, such as liposomes and NIV, have been reported to improve the therapeutic index by modifying Gem pharmacokinetics and increase the localization of Gem in the target organ (Bouffard *et al.*, 1993; Heinemann *et al.*, 1992; Matsuda and Sasaki, 2004). Gem-NIV levels at 30 min were higher than at 5min in lungs due to the accumulation of treatment in the lung. However, Gem lung concentrations declined rapidly following administration as a solution with a half-life of approximately 30 minutes and undetectable lung levels were present after 2 hours. These results confirmed that the concentration of free Gem was poor and transient in the lung in comparison to Gem-NIV.

Low lung lavage Gem levels after the administration of Gem-NIV suggests efficient tissue uptake. This agrees with a previous study in which Gem solution (Gewmzar®) was not detected after two hours post intravenous administration whereas liposomal Gem was found up to 24 hours after treatment (Paolino *et al.*, 2010a).

In the current study, the greatest Gem concentration was found in the spleen after inhalation of Gem solution and Gem-NIV (6 mg/kg) at 2 hours post-dosing. A previous study reported a maximum concentration of Gem in the kidney after intravenous administration of Gem solution at a dose of 10 mg/kg. This observation possibly occurred due to the differences in the route of administration and/or the strain of rat used Sprague-Dawley versus Fischer 344 (Shipley *et al.*, 1992). However, Gem NIV had a higher level in the spleen at 120 mins than Gem solution, indicating the tendency of accumulation of Gem-NIV in this highly vascularized organ (Allen and Chonn, 1987; Graeser *et al*., 2009).

Published studies have investigated the factors which influence *in vivo* deposition of lipid based vesicles (liposomes and NIV). Increasing vesicle size leads to a more rapid uptake by the macrophages in the lung, and these vesicles can act as a drug depot in the lungs after pulmonary administration whereas if the vesicles are taken up from the blood circulation after intravenous administration then they will be concentrated in the liver and spleen (Abra and Hunt, 1981; Senior, 1987). For example, liposomes with a vesicle size of 400 nm cleared from blood 7.5 times more quickly than those with a size of 200nm (Moghimi *et al.*, 2001; Senior *et al.*, 1985). In the present study, Gem-NIV (60 mM lipid and 545 nm size) delivered Gem in

high concentrations in the lung and had lower concentrations in the kidneys, liver and heart indicating lung uptake occurred after pulmonary administration.

Lipid dose also affects the bioavailability of vesicular delivery systems. Bioavailability in systemic circulation typically increases as a function of increasing lipid content due to saturation of the phagocytic capacity of macrophages (Senior *et al.*, 1985). Alternatively increases in the bioavailability can occur due to the depletion in serum proteins (Harashima *et al.*, 1993; Oja *et al.*, 1996). This means that extra increases in lipid concentration of more than 60 mM may lead to a decrease in the uptake of NIV by macrophages in systemic circulation.

Vesicle charge can also influence phagocytosis, with anionic vesicles being rapidly cleared from the blood in comparison to cationic and neutral charge vesicles after intravenous injection (Gabizon and Papahadjopoulos, 1988; Moghimi and Patel, 2002). The liver was the main organ responsible for the clearance of anionic vesicles from the blood (Moghimi and Patel, 2002). In this study, the main organ of Gem-NIV clearance seemed to be the spleen rather than the liver after pulmonary administration. Therefore, Gem-NIV, which escape from the lung, will be cleared by macrophages of RES after pulmonary administration, primarily by macrophages of the spleen and to a lesser extent via the liver.

In normal mice, free Gem and Gem-NIV show high levels of Gem in serum in comparison with their levels in lung, but the localization of Gem-NIV in cancerous lungs are higher than in normal lungs due to the tendency of Gem-NIV to

accumulate in tumours which are characterised by vasculature (Paolino *et al.*, 2010b). Gem-NIV were not detected in the hearts of cancer bearing mice. These results are similar to those described for radiolabelled free Gem in B16C3F1 mice, where the highest drug concentration was present in the spleen after 30 min of intravenous administration of 20 mg/kg (Shipley *et al.*, 1992).

Chapter 6: *In vitro* evaluation of Gem-NIV against B16 F0 luciferase cell line using resazurin and luciferin bioassays

6.1 Introduction

Vesicular delivery systems can modify the *in vitro* cytotoxic activity of Gem against cells through improved delivery of the entrapped drug (Cosco *et al*., 2012). For example, the cytotoxic effects of a Gem liposome formulation has been compared with that of Gem solution against the Caco-2 colon carcinoma cell line (Calvagno *et al.*, 2007). Caco-2 and A549 cells are widely used to evaluate drug delivery as described in published literature (Forbes, 2000). The greater cytotoxic effect of the Gem liposomal formulation was a consequence of its ability to penetrate the cell membrane by fusion or endocytotic mechanisms and deliver entrapped Gem (Vono *et al.*, 2010). In contrast, Gem in solution enters cells using nucleosides-transporters (hENT and hCNT, Ueno *et al.*, 2007). The uptake of Gem as free solution is mediated by hENT1, hENT2, hCNT1 and hCNT3. The hENT1 is the major agent for Gem transportation into cells (Mackey *et al*., 1998; Achiwa *et al*., 2004).

The ability of Gem to kill cells can be measured in different ways, for example resazurin (7-hydroxy-3H-phenoxazin-3-one10-oxide) dye has been commonly used as an indicator of cell viability for *in vitro* studies evaluating anticancer drug activities. Cell lines are cultured with anticancer drug solution and after a variable period of time, the proliferation or cytotoxicity can be measured. The reduction of resazurin to resorufin is directly proportional to the number of live cells. Mitochondrial enzymes such as NADPH dehydrogenase perform this reduction, resulting in the transfer of electrons from NADPH to resazurin to form resorufin.

The degree of reduction can be measured spectrophotometrically since resazurin shows an absorption peak at 600 nm and resorufin shows a peak at 570 nm (Borra *et al.,* 2009).

Various commercially produced resazurin-based products are available, e.g. Alamar Blue™, however resazurin alone is a cheaper solution which can be prepared in the laboratory without compromising rapidity, reliability, sensitivity or safety of the assay (Anoopkumar-Dukie *et al*., 2005; Hamid *et al*., 2004; Nakayama *et al*., 2009). Various cell lines have been used for lung cancer studies, but the most commonly utilised is the B16 cell line, which was introduced in 1970 by Dr. Isaiah Fidler. B16 cells were labelled with ^{125}I-5-iodo-2-deoxyuridine and injected intravenously into mice where they formed tumour nodules in the lung after 14 days (Gheorgheosu *et al*., 2011).

Various B16 variant sub-lines with a high level of potential to colonise lung tissues have been selected by prior studies, such as B16 F0 cells (Poste *et al*., 1980). Mice injected with B16 F0 cells rapidly form tumours in different organs including skin, lung, liver and spleen, but the lungs are the first organs affected by metastasis. More recently, B16 cells have been transfected with the luciferase gene (B16 Luc cells) so that they exhibit biophotonic activity without inhibition in growth. The luciferase gene was obtained from fireflies, bioluminescent insects that can emit light with wavelengths varying from yellow-green (560 nm) to red (620 nm). B16 F0 Luc cells allow high throughput *in vitro* cytotoxicity assays to be performed (Meroni, 2009) and also allow the determination of cancer progression in the same animals over the

course of *in vivo* studies (Tiffen *et al.*, 2010). In order to emit bioluminescence, luciferase cells need the presence of luciferin (S)-2-(6′-hydroxy-2′-benzothiazolyl) thiazoline-4-carboxylic acid, the substrate of the luciferase enzyme.

Results

The effects of the incubation period (4 or 24 hours) and cell concentration on the proliferation of B16 F0 Luc cells were evaluated using absorbance data obtained from the resazurin assay. The results, as shown in Figure 6.1, indicated that a 24 hour incubation period provided better cellular proliferation (demonstrated by % reduction in resazurin) than a 4 hour incubation period. Another important finding was that a 50% cellular proliferation was achieved at a cell seeding concentration of 1×10^5 cells/ml (Figure 6.1).

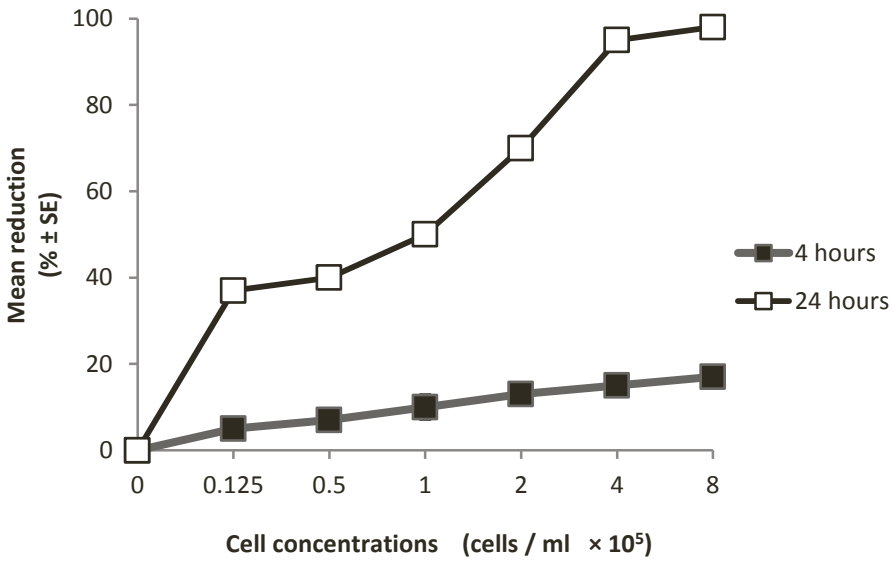

Figure 6.1 The effects of the incubation period and cell concentration on the proliferation of B16 F0 Luc cells. Cells were incubated with the medium for 4 or 24 hours at the starting concentration shown and the absorbance of the wells (n = 6/treatment) was determined at 570 and 600 nm. The mean reduction in resazurin was calculated using the equation supplied.

Further investigations into proliferation were carried out using fluorescence data, which was obtained from resazurin using an incubation time of 24 hours. The fluorescence results confirmed the previous absorbance results. Maximum fluorescence was achieved using a cell concentration of 4×10^5 cells/ml and half of the maximum fluorescence was achieved in a cell concentration of 1×10^5 cells/ml (Figure 6.2).

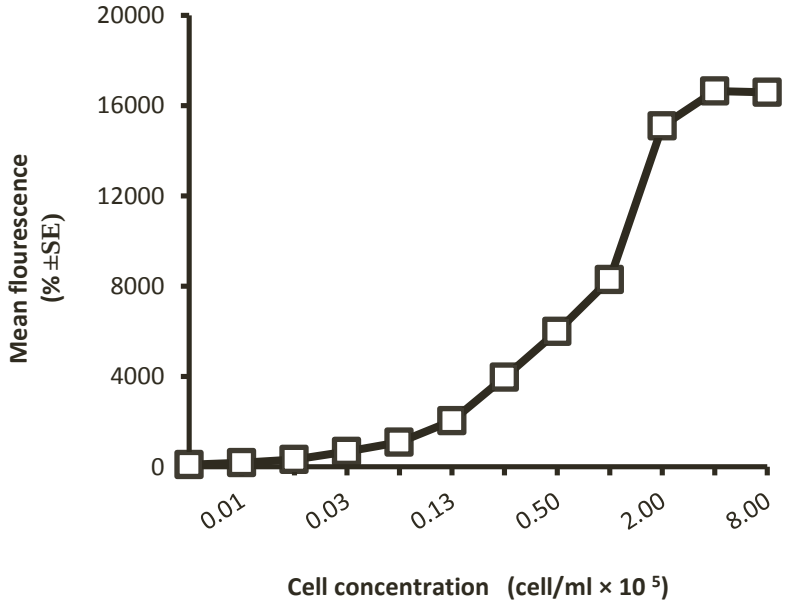

Figure 6.2 The effect of cell concentration on measurement of the proliferation of B16 F0 Luc cells at concentration range $0.01\text{-}8\times10^5$ cells/ml after 24 hours incubation with cells. B16 F0 Luc cells were added to the wells of a 96 well tissue culture plate. The cells were serially diluted (1:1) with complete DMEM medium. The fluorescence of the wells (n = 6/treatment) was determined at 570 and 600 nm.

In the luciferin assay, a higher cell concentration (0.01-8 $\times 10^6$ cells/ml) was required to get sufficient bioluminescence signals (10 times that used in the resazurin assay). The maximum bioluminescence was achieved at a concentration of 4×10^6 cells/ml and 50% of bioluminescence was achieved at 1×10^6 cells/ml (Figure 6.3). Therefore, the luciferin assay was not more sensitive than the resazurin assay.

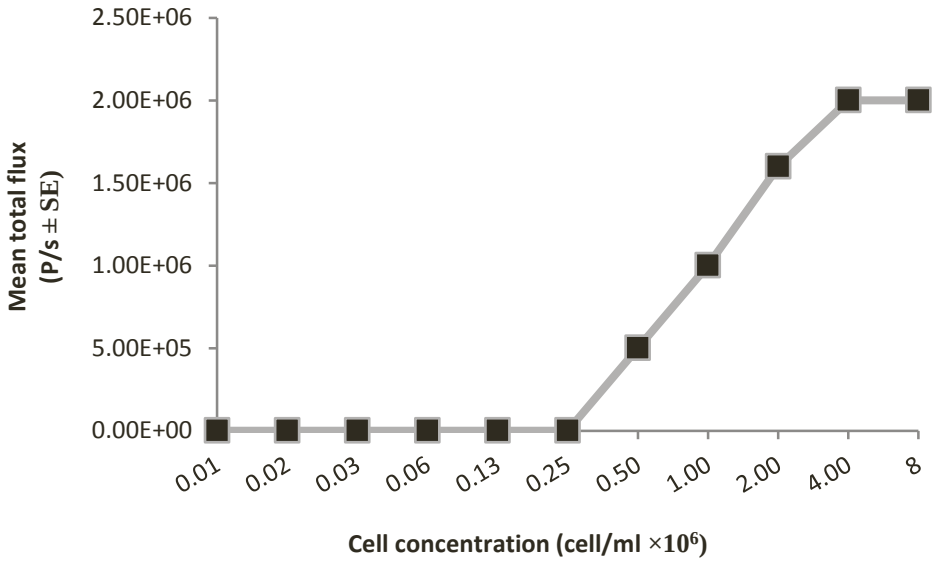

Figure 6.3 The effect of cell concentration on measurement of the proliferation of B16 F0 Luc cells at concentration range 0.01-8 $\times 10^6$ cells/ml after 24 hours incubation with cells. B16 F0 luciferase cells were added to the wells of a 96 well tissue culture plate. The cells were serially diluted (1:1) with complete DMEM medium. The bioluminescence of luciferin of the wells (n = 6/treatment) was determined using an IVIS®.

The *in vitro* cytotoxicity of Gem at concentration range of 0.1-14mg/ml was prepared in various forms including: Gem solution, Gem-NIV (30mM lipid) or empty NIV (30mM lipid) was compared using B16 F0 Luc cells. Fluorescence data was used in this study because the estimation of mean suppression % from those data could be done more rapidly than estimation using absorbance data and both of them gave the same results. Cells treated with empty NIV had no IC_{50} over the concentration range tested and Gem-NIV were more cytotoxic than Gem solution with an IC_{50} that was four times lower than that of Gem solution (Figure 6.4)

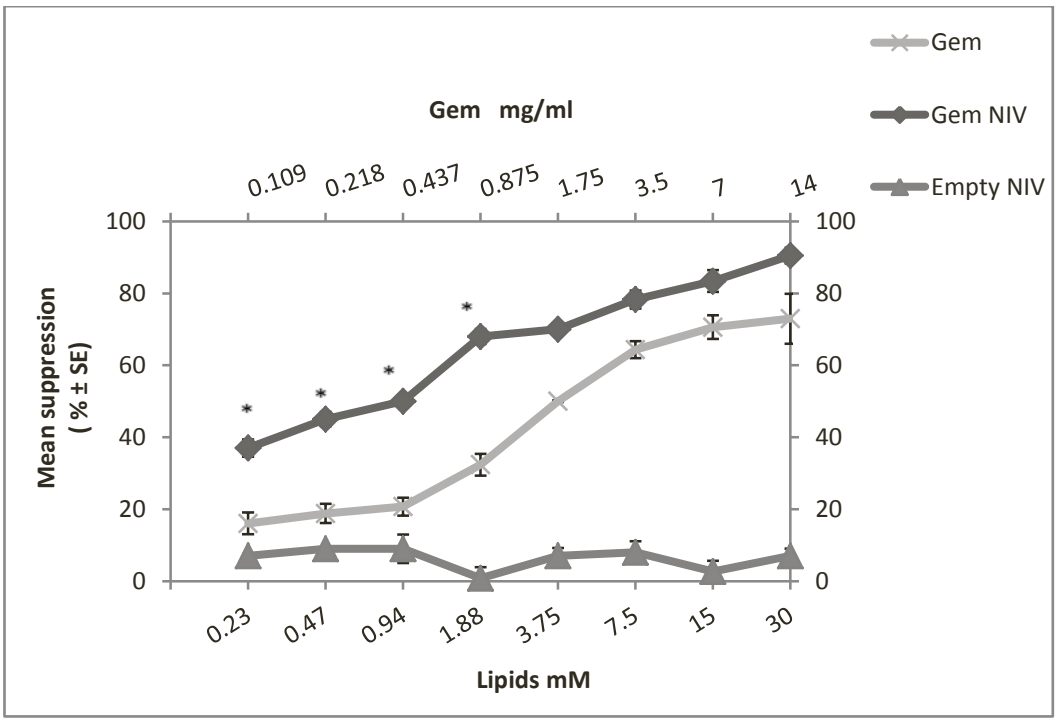

Figure 6.4 The effect of treatment with different formulations on the survival of B16 F0 Luc cells. B16 F0 Luc cells (1×10^5 cells/ml) were incubated with medium alone (control), Gem or Gem-NIV (30 mM; vesicle size ± SD, 300 nm ± 5; zeta potential ± SD, -87 mV ± 7.3, entrapment efficiency ± SD, 45% ± 4) or Empty NIV (30mM, vesicle size 280 nm ± 3; zeta potential ± SD, -50 mV ± 1) for 24 hours. Then, the amount of fluorescence emitted by cells was determined at 570 and 600 nm. The mean suppression in cell survival compared to control values was determined for each treatment. IC_{50} of free Gem is 1.75 ± 0.5 mg /ml whereas of Gem NIV is 0.44 ± 0.02mg/ml. $^{*}P < 0.05$ comparing Gem and Gem-NIV at the concentration shown.

Studies using bioluminescence showed that Gem-NIV significantly ($p < 0.05$) improved the cytotoxic activity of Gem (IC_{50} value: Gem-NIV 3.5 ± 0.04 mg/ml; Gem solution 5.75 ± 0.07 mg/ml) (Figure 6.5).

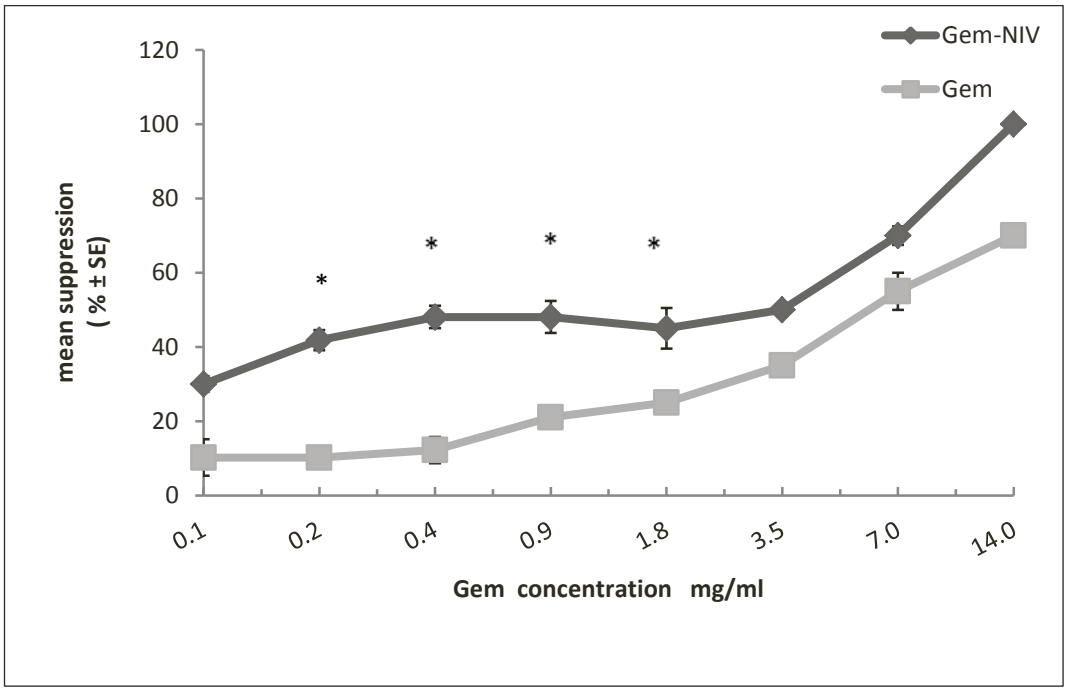

Figure 6.5 A comparison of the cytotoxicity of Gem solution and Gem-NIV on the survival of B16 F0 Luc cells. B16 F0 luciferase cells (1×10^6 cells/ml) were incubated with medium alone (control), Gem or Gem-NIV (30 mM; vesicle size ± SD, 304 ± 2.1nm; zeta potential ± SD, -88 ± 6.3mV and entrapment efficiency ± SD, 43% ±1.5) and Empty NIV (30mM; vesicle size ± SD, 282 ± 1nm; zeta potential ± SD, -50 ± 3mV) for 24 hours. Then, the amount of bioluminescence was determined. The mean suppression in cell survival compared to the control values was determined for each treatment. IC_{50} of free Gem is 5.75 ± 0.07mg /ml whereas of Gem-NIV is 3.5 ± 0.04 mg/ml. $^{*}P < 0.05$ comparing Gem and Gem-NIV at the concentration shown.

Increasing the lipid concentration used to prepare NIV led to a significant ($p < 0.01$) increase in their efficacy in comparison with the corresponding drug solution with no IC_{50} value for empty NIV (Figure 6.6). At a lipid content of 60 mM, Gem-NIV IC_{50} was 0.87 mg/ml whereas the IC_{50} of Gem solution was 4.45 mg/ml.

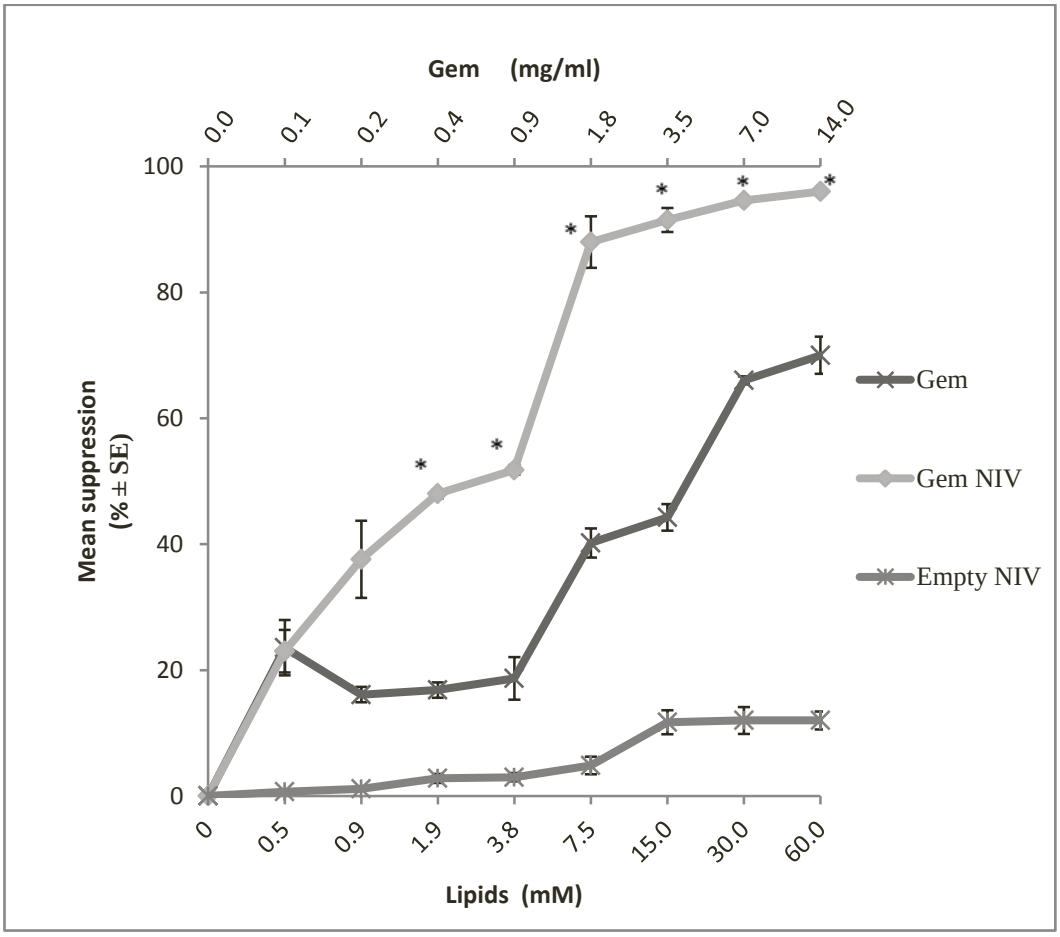

Figure 6.6 The effect of treatment with different formulations on the survival of B16 F0 Luc cells (1×10^6 cells/ml). B16 F0 Luc cells were incubated with medium alone (control), Gem, Gem-NIV (60 mM; vesicle size ± SD, 511 ± 24.1nm ; zeta potential ± SD, -70 ± 4.4mV and entrapment efficiency ± SD, 80% ± 2.2) and Empty NIV (60 mM; vesicle size ± SD , 500 ± 18 nm; zeta potential ± SD, -75 ± 1 mV) for 24 hours. Then, the amount of bioluminescence emitted by the cells was determined. The mean suppression in cell survival compared to controls was determined for each treatment. IC_{50} of free Gem is 4.45 ± 0.03 mg /ml whereas of Gem-NIV is 0.87 ± 0.01 mg/ml. $^{*}P < 0.01$ comparing Gem and Gem-NIV at the concentration shown.

To assess the effect of size on the efficiency of Gem-NIV prepared using 60 mM, lipid were homogenised for different times and speeds, in order to create vesicles of different times and speeds. The size of the vesicles used had no significant impact on the survival rates of B16 F0 Luc cells (Figure 6.7).

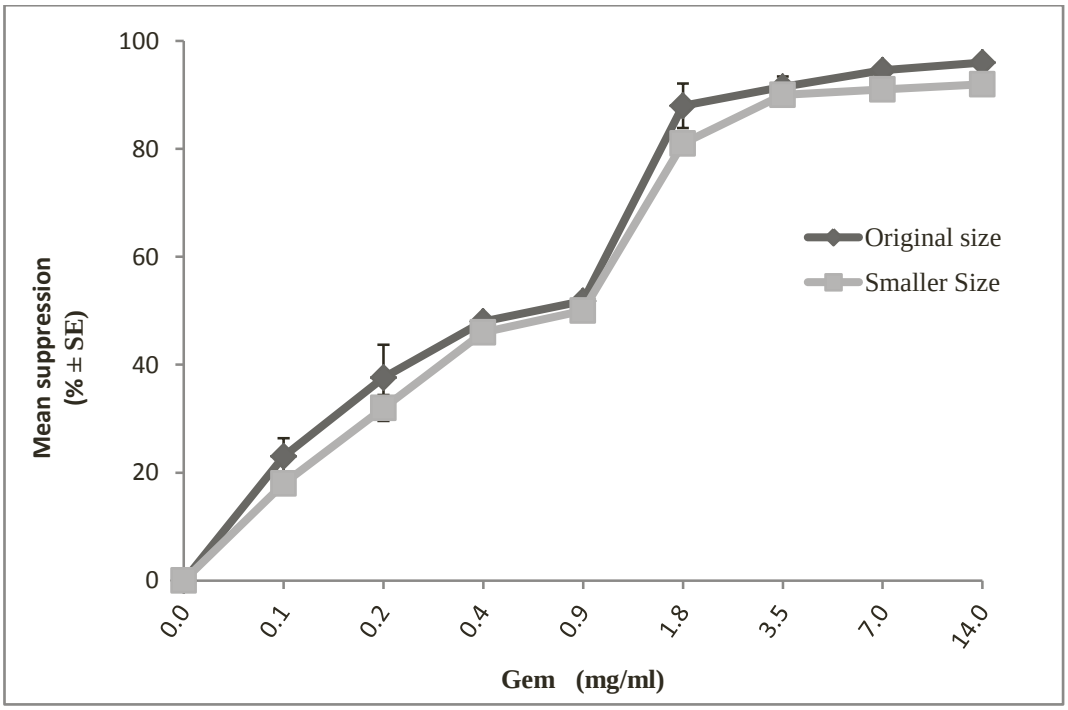

Figure 6.7 The effect of treatment with Gem-NIV formulations having different vesicle size on the survival of B16 F0 Luc cells (1×10^6 cells/ml). B16 F0 Luc cells were incubated with medium alone (control), original size Gem-NIV (vesicle size ± SD, 511 ± 24.1nm) or smaller size one (vesicle size ± SD, 255 ± 7 nm) for 24 hours. Then, the amount of bioluminescence emitted by the cells was determined.

Empty NIV with a different surface charge were produced to determine whether or not they had similar effects on the survival of B16 F0 Luc cells. The treatment of B16 F0 Luc cells with empty NIV prepared using DCP, was carried out to give vesicles with a net negative charge, and was not toxic to cells when compared with similar treatment with empty-NIV prepared with SA, producing vesicles with a net positive charge ($p < 0.05$, Figure 6.8).

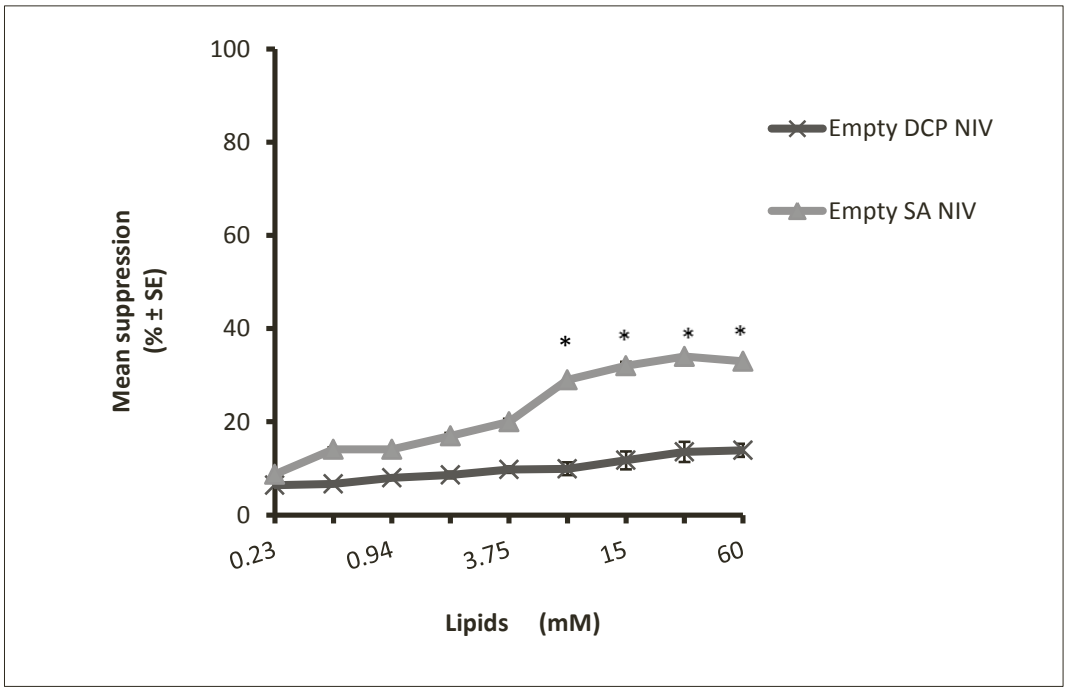

Figure 6.8 The effect of treatment with Empty NIV formulations of different surface charge on the survival of B16 F0 Luc cells (1×10^6 cells/ml). B16 F0 Luc cells were incubated with medium alone (control), negatively charged NIV (prepared using DCP) or positive charged NIV (prepared using SA) for 24 hours. Then, the amount of bioluminescence emitted by the cells was determined. $^{*}P < 0.05$ comparing two formulations at the concentration shown.

6.4 Discussion

In vitro cytotoxicity studies on B16 F0 Luc cell line demonstrated that 30 and 60 mM Gem-NIV significantly affected cell proliferation as compared to the Gem solution as shown by lower IC_{50} values, in agreement with previous observations (Cosco *et al.*, 2009). Moreover, the previous observations showed an efficient interaction of lipid-based vesicles (Gem-liposomes) with the cell membrane, which suggests a greater drug internalisation and activity as compared to free Gem (Celia *et al.*, 2008).

There are two factors that have an influence on activity of lipid based vesicles against tested cells *in vitro*: (1) an effective entrapment efficiency of drug inside vesicles and (2) uptake of these vesicles by tested cells (Cosco *et al*., 2009; Celia *et al*., 2008). The uptake of pharmaceutically active substances into living cells is affected by many factors including the lipophilic nature of the target bio-membrane and formulation properties of those substances (e.g. lipid composition, surface charge and size, Foster *et al*., 2001; Miller *et al.*, 1998). Results have shown that increasing the lipid concentration used to prepare Gem-NIV improved *in vitro* cytotoxicity against B16 F0 Luc cells compared to treatment with identical concentration of Gem solution. Increasing the amount of lipid has shown that it increases drug entrapment efficiency (see Chapter 4).

In general, negatively charged vesicles containing DCP, phosphatidylserine, phosphatidylglycerol or phosphatidic acid were taken up faster and more fully than neutral particles, because of electrostatic interactions with the receptors available on viable cells (Lee *et al*., 1992; Allen *et al*., 1991; Allen *et al*., 1988). However, the effect of surface charge on drug delivery seems to depend on the cell line used and surface properties of vesicles. Thus, positively charged liposomes are taken up to a greater extent by Hela (ovarian carcinoma) cells than negatively charged or neutral liposomes, but J774 (mononuclear macrophage) cells phagocytised both positive and negative charged liposomes to a similar extent, but also that both were taken up better than uncharged liposomes (Miller *et al*., 1998). Therefore, negatively charged Gem-NIV seemed to be taken up by B16 F0 Luc cells more efficiently than neutral free Gem in solution form.

The size preference for uptake may also depend on the cell studied; therefore KLN 205 squamous carcinoma cell line preferentially internalized particles with a size of 20-600 nm whereas the Hepa 1-6 hepatoma and HepG2 human hepatocyte cell lines internalized particles with mean sizes of 20-100 nm (Zauner *et al*., 2001). In our study, B16 F0 Luc cells showed similar responses when treated with 60 mM Gem-NIV of ~ 500 nm or those which were homogenised to ~ 250 nm. Moreover, the smallest vesicle size, which could be obtained by homogenization for Gem-NIV was approximately 250 nm and this will limit any investigation on the study of the influence of small sized vesicles.

Chapter 7: *In vivo* assessment of the anti-tumour activity of nebulized Gem-NIV using bioluminescence imaging

7.1 Introduction

Animal models are commonly used in the investigation of anticancer drugs and the animals may be healthy, diseased, genetically manipulated and/or altered by prior treatment (Zhang and Wu, 2009). Animal studies can produce information about the progression of cancer, drug activity, metabolism and the kinetic features of drugs. One of the most useful tools for investigating and discovering efficacious and novel treatments are mouse cancer models (Cui *et al*., 2006). There are two types of murine models used by researchers to study cancer; the ectopic cancer model, where cancer cells are seeded subcutaneously into mice, and the orthotropic cancer model, where tumour cells are seeded into a specific organ (Kubota, 1994).

An orthotropic cancer model allows cells to grow in a suitable microenvironment, a factor that can play a vital role on the growth of cancer cells (Paget, 1989). In addition, metastatic spread, which can be an important feature of some cancers, is more efficient if cancer cells are seeded in the orthotropic organ rather than subcutaneously (Glinsk, 2003; Hoffman, 1999; Madero *et al.*, 2012).

However, in ectopic cancer models, cells generally grow rapidly after inoculation (Kuo *et al*., 1993; Wilmanns *et al*., 1992). The orthotropic model allows delivery of the drug to the origin of the cancer observed in human patients and makes it more relevant to studies investigating how drug delivery systems can improve

therapeutics. For example, fluorouracil nanoparticles accumulated mostly in hepatic cancer tissues by factors many times that of normal liver, kidney, heart and blood

respectively, show that the orthotropic liver cancer mouse model can be effectively used to evaluate targeting of hepatic cancer cells to inhibit tumour growth (Cheng *et al.*, 2012). Various imaging technologies have been used to determine the outcome of anti-cancer treatments (Table 7.1), including pulmonary-targeted chemotherapy (Zarogoulidis *et al*., 2012; Park *et al*., 2012).

Imaging technique	Formulation types	Subjects	References
BL imaging	Liposome/Doxorubicin Liposome/Doxorubicin	Animals Animals and Cells	(Garbuzenko *et al.*, 2005) (Garbuzenko *et al.*, 2010)
FL imaging	Nanoparticles/Doxorubicin Liposome/Doxorubicin	Animals Animals and Cells	(Al-Hallak *et al.*, 2012) (Garbuzenko *et al.*, 2005)
Confocal microscopy	Nanoparticles/Doxorubicin	Animals	(Al-Hallak *et al.*, 2012)
MRI	Micelles/Doxorubicin	Cells	(Guthi *et al.*, 2010)

Table 7.1 Formulations types of various anticancer drugs, evaluated by imaging techniques. Bioluminescence (BL), fluorescence (FL) and magnetic resonance imaging (MRI).

A variety of imaging systems are available; for example, non-optical imaging includes magnetic resonance imaging (MRI), computing tomography (CT), positron-emission tomography (PET) and single-photon-emission computed tomography (SPECT). In MRI, a magnetic resonance is generated from the angular spin of protons in the water of living tissues (Willmann *et al.*, 2008) and the protons provide a signal which gives anatomical and molecular imaging details. However, a low water content can limit MRI signals and variations caused by air interfaces in alveoli and bronchioles can cause image degradation (Leach, 2006; Willmann *et al.*, 2008).

Optical imaging includes confocal microscopy, multiphoton microscopy, fluorescence (FL) imaging and bioluminescence (BL) imaging. BL imaging is commonly used, as good quality images can be produced with a low background and the strength of the signal quantitatively correlates with the cell number (Ballou *et al*., 2005). However, the optimum imaging condition must be identified for each application as *in vivo* conditions can affect BL, e.g. the availability of luciferin, which depends on its *in vivo* pharmacokinetics (Close *et al.*, 2010 and 2011) and oxygen and adenosine triphosphate (ATP) availability, all of which are essential for luciferase enzyme activity (Dothager *et al.*, 2009; Sadikot and Blackwell, 2005; Yu and Hales, 2011). In cancer research, BL imaging can monitor tumour growth in mice and show the viability of a few thousands cells (Madero-Visbal *et al*., 2012).

Studies have shown that neither the inherent luciferase-expression of the cells or their interaction with luciferin substrate has any deleterious effects on *in vivo* tumour growth (Tiffen *et al.*, 2010). The luciferase gene incorporated into cancer cells can

be isolated from the North American fireflies (*Photinuspyralis;* FLuc), jellyfish (*Aequorea*), sea pansies (*Renilla*; RLuc), corals (*Tenilla*), click beetles (*Pyrophorus plagiophthalamus*) or from some bacterial species (Lipshutz *et al.*, 2001; Nguyen *et al.*, 1988). The light spectrum from firefly luciferase is within a 530–640 nm range, peaking at 562 nm, and its intensity ranges from blue (least intense) to red (most intense). Low light sensing luminometers can be used to quantify emitted photons (Colin *et al.*, 2000; Lee and Camilli, 2000; Lipshutz *et al.*, 2001), but for *in vivo* studies BL imaging equipment such as the IVIS® is used (Contag *et al.*, 1997). The IVIS® allows a digital photograph to be integrated with BL emissions and the software provided allows BL to be detected within the animal tissues (*in vivo* and *ex vivo*) with a high sensitivity (Luker and Luker, 2008; Zhang *et al.*, 1994). The earliest studies of BL technology were for cancer using a mouse xenograft model of human cervical carcinoma cells implanted into immune deficient (SCID) mice where it was shown that 1×10^{3} cells could be detected after intraperitoneal injection, 1×10^{4} cells after subcutaneous injection and 1×10^{6} cells could be detected in the lungs directly after the intravenous injection (Edinger *et al.*, 1999). In addition, studies using BALB/c mice showed that leukaemia and lymphoma cells could be detected with high sensitivity in internal organs such as the lung, liver, spleen, lymph nodes and bone marrow. Cancer penetration of the spleen was observed earlier and with a higher sensitivity by BL technology in comparison with flow cytometry (Edinger *et al*., 2002). The ability to carry out *in vivo* and *ex vivo* measurements aligned with the ability to examine many animals simultaneously with very short scanning times makes BL an ideal technology for drug evaluation and efficiency studies.

The gender of the animals used in studies may also be important. Many studies have shown that gender can influence the cancer burden. For example, women are more likely to have lung cancer than men (Kiyohara, 2010; Patel, 2004; Stabile and Siegfried, 2003), as the presence of α and β oestrogen receptors on normal and cancerous cells of the lung allows endogenous and exogenous oestrogen to stimulate the lung cancer cells and increase proliferation. Furthermore, *in vitro* studies have shown that oestrogen stimulates the proliferation of lung cancer cells (Dougherty, 2006; Kaiser, 1996; Stabile and Siegfried, 2003). In a genetically modified murine model of lung adenocarcinoma, females had higher cancer burdens than males and this variation was eliminated if females were given an ovariectomy, indicating that oestrogen promoted cancer growth (Hammoud, 2008; Jackson, 2005).

The mouse strain used in the studies is also important. Nude mice have no competent immune system because of the lower number of T cells due to the fact that they are athymic; this enables them to receive many types of cancer tissues while retaining the histological appearance as well as the biomedical patterns of the original tissues (Kim *et al*., 2007). They also lack hair, which makes them more efficient at emitting BL as hair can absorb the emitted photons (Zinn, 2008). However, nude mice can be very susceptible to infection and in cancer studies, the outcome of drug treatment is often based on the percentage of animals that have survived by a given time point (Croy *et al*., 2007).

7.2 Results

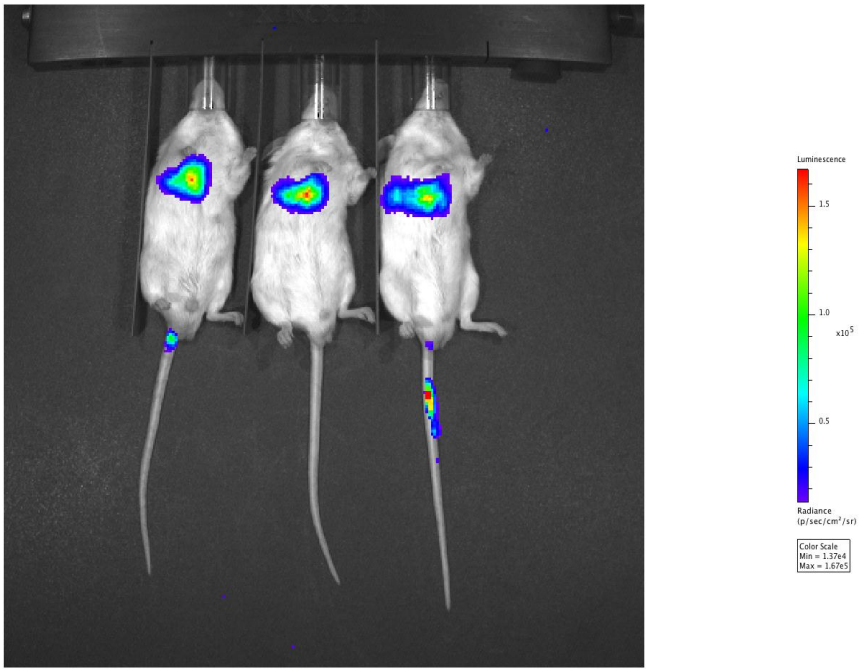

Figure 7.1 Bioluminescent imaging of lung cancer in BALB/c male mice. 5×10^5 B16 F0 Luc cells were injected via the tail vein into BALB/c male mice. Each mouse was injected intraperitoneally with luciferin solution (0.2 ml; 150 mg/ml). Ten minutes later bioluminescence imaging was performed with a CCD camera (IVIS®, Xenogen). Data are expressed as photon flux (p/s).

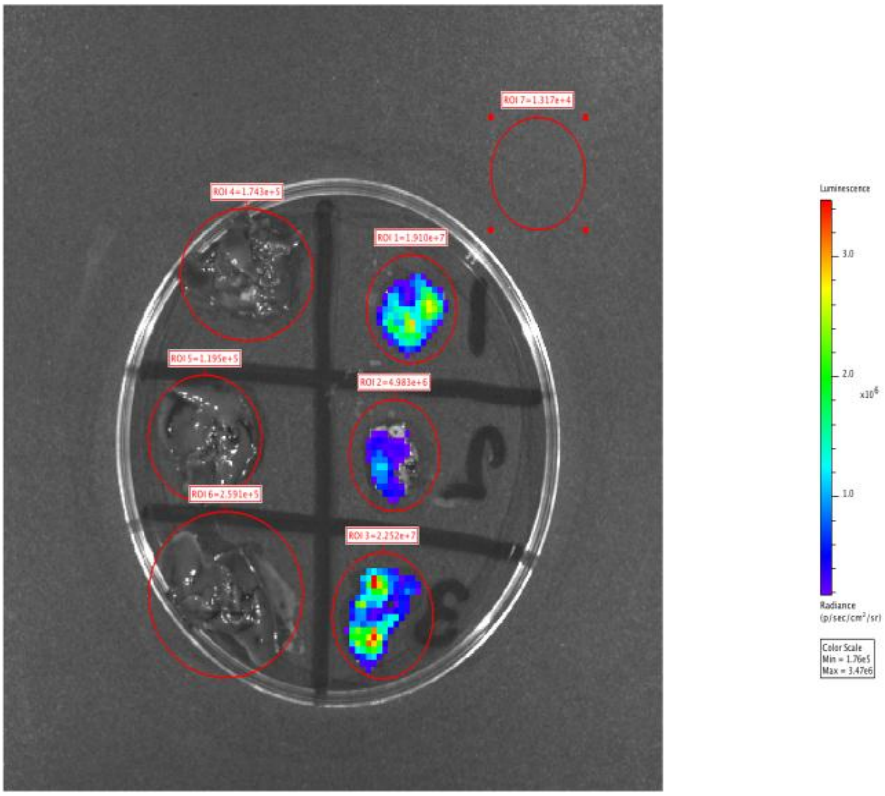

Figure 7.2 *Ex vivo* bioluminescence imaging of lungs (left) and liver (right) isolated from the mice after soaking in luciferin solution at a concentration of 150 µg /ml for 1 min.

There was no significant difference in the progression of lung cancer in male and female BALB/c based on BL, however the male mice had significantly heavier lung weights than the female mice post-mortem (Figure 7.3).

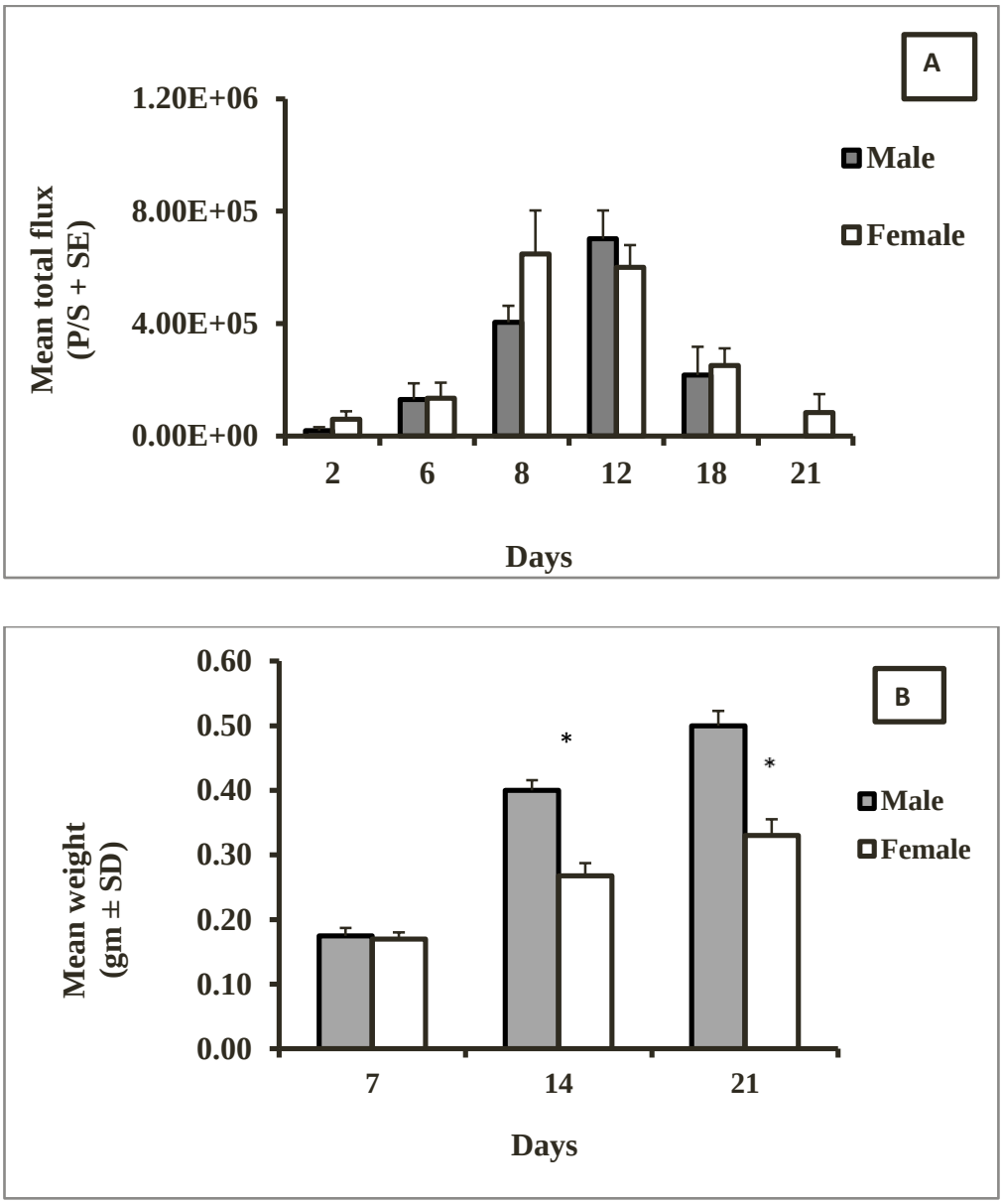

Figure 7.3 *In vivo* comparison of the progression of lung cancer in mice. BALB/c male or female mice (n =12 / gender) were injected intravenously into the tail vein with B16 F0 Luc cells (5×10^5 cells / mouse). BL data (A), and weights data (B).

The most interesting finding was a reduction in BL after day 14 *in vivo* (Figure 7.3) whereas *ex vivo* signals for the lung were much higher on day 21 than they had been on day 14, indicating that there was an increase in cancer growth in the organ (Figure 7.4).

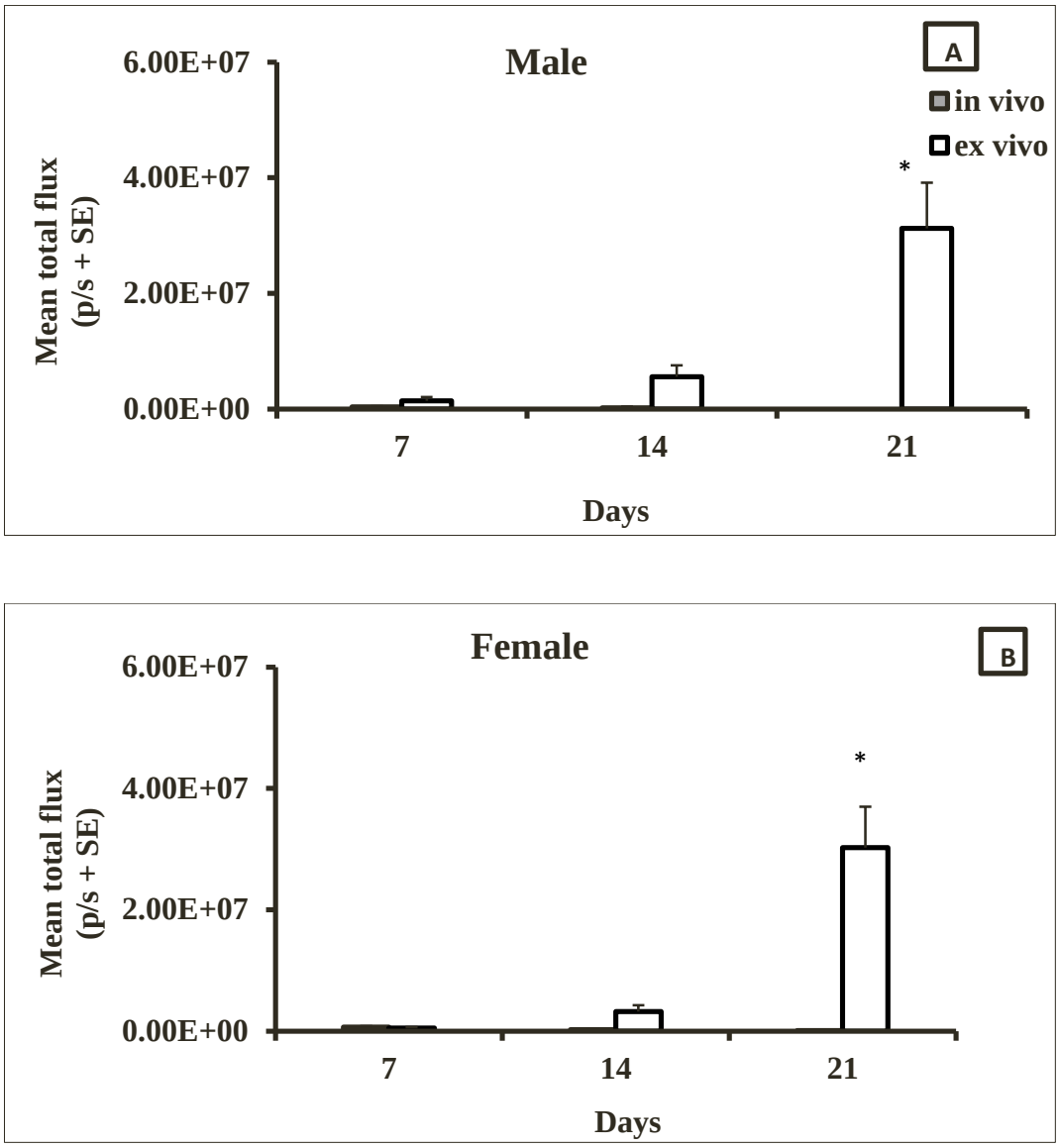

Figure 7.4 *In vivo* and *ex vivo* comparison of the progression of lung cancer in mice. BALB/c male or female mice (n=12 / gender) were injected intravenously into the tail veins with B16 F0 Luc cells (5×10^5 cells / mouse). *Ex vivo* bioluminescence of the lungs after soaking in luciferin solution at a concentration of 150 µg /ml for 1 min. Male (A) and female (B).

The same phenomenon was observed with nude mice but these mice became ill over the course of experiment and only one mouse survived until day 21 (Figure 7.5). Therefore, BALB/c male mice were chosen for the anticancer drug studies.

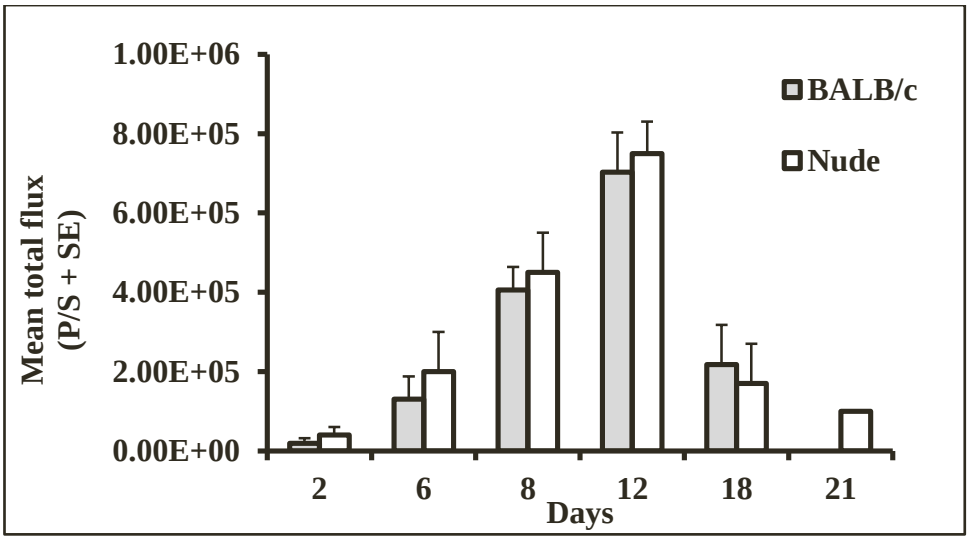

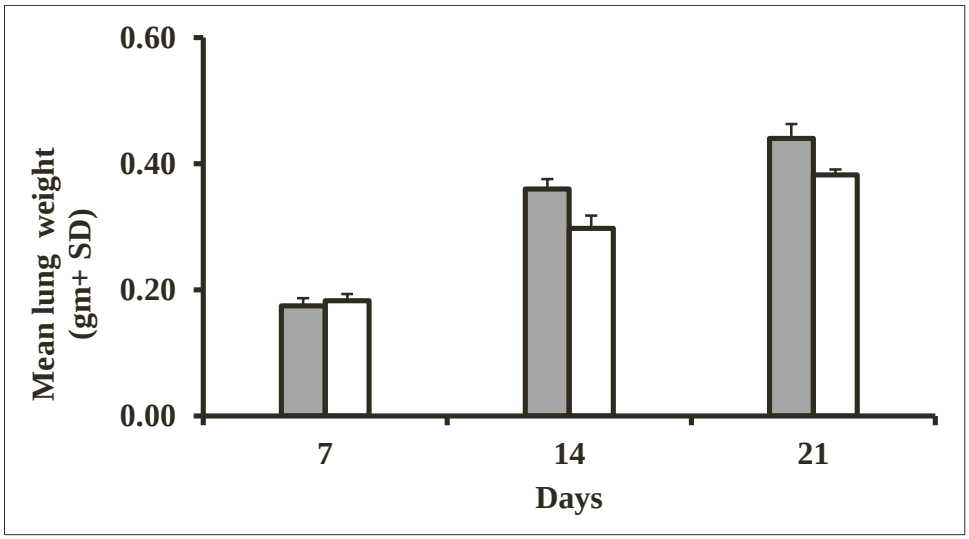

Figure 7.5 *In vivo* comparison of the progression of lung cancer in mice. BALB/c or Nude male mice were injected intravenously into the tail vein with B16 F0 Luc cells (5×10^5 cells /mouse, n=12). There is no signal at 21 days in BALB/c mice.

Initial studies showed that Gem-NIV prepared using 150 mM lipid and hydrated with 14 mg Gem/ml could not be nebulised as they were too viscous (Niven and Schreier, 1990; Taylor *et al.*, 1990; Bridges *et al*., 2000). Therefore, Gem-NIV were prepared using a lipid content less than 150 mM. Treatments with Gem-NIV (30mM) or Gem solution were equally effective at significantly inhibiting cancer progression ($p < 0.05$) compared to controls, whereas treatment with empty-NIV had no significant effect on cancer growth (Figures 7.6-7.8).

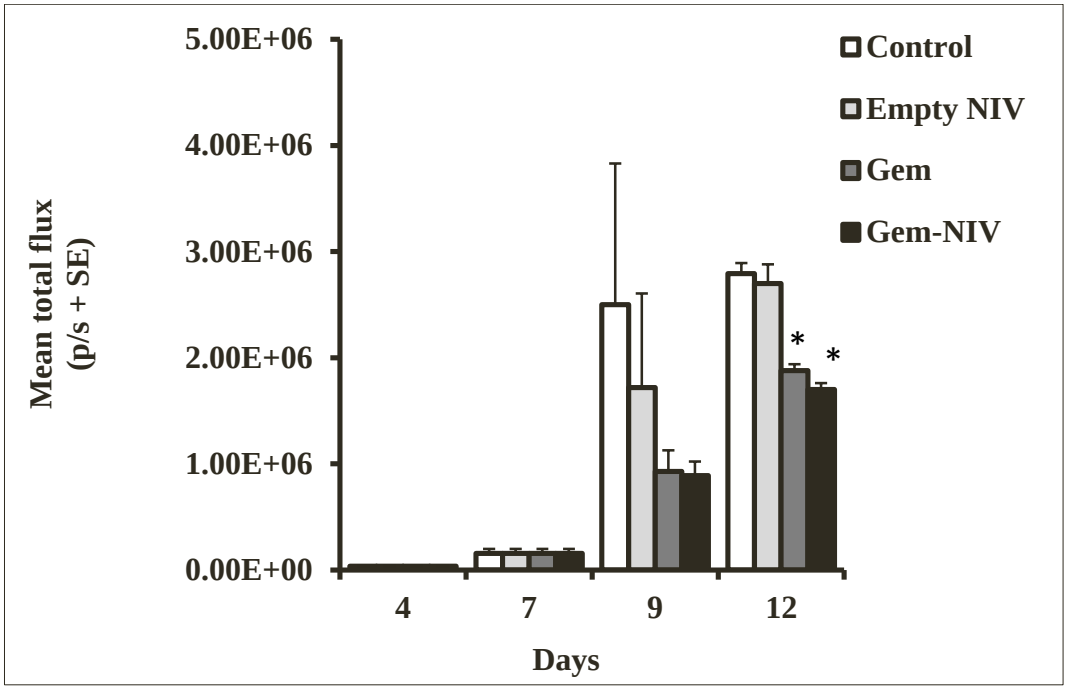

Figure 7.6 Evaluation of tumour inhibition for different Gem formulations. Treatment was started on day 3 after mice were inoculated with B16 F0 Luc cells (5×10^5/ mouse) on day 0. On day 3 the mice were treated by inhalation using a nebuliser with Gem solution (0.5 ml, 14 mg/ml) or Gem NIV (0.5 ml, prepared using 30 mM lipid and 14 mg Gem/ml: Vesicle size, 302 ± 5.7 nm; Zeta potential, -40.3 ± 5.1mV and entrapment efficiency, 49.0 ±1.0%) and Empty NIV was prepared using 30 mM lipid (particle size, 299.1 ± 7.6 nm; Zeta potential, -48.1 ± 6.2mV) (n= 6). The amount of bioluminescence emitted *in vitro* from lungs was determined in the mice at different time points. $^{*}P < 0.05$ Gem-NIV and Gem compared to control.

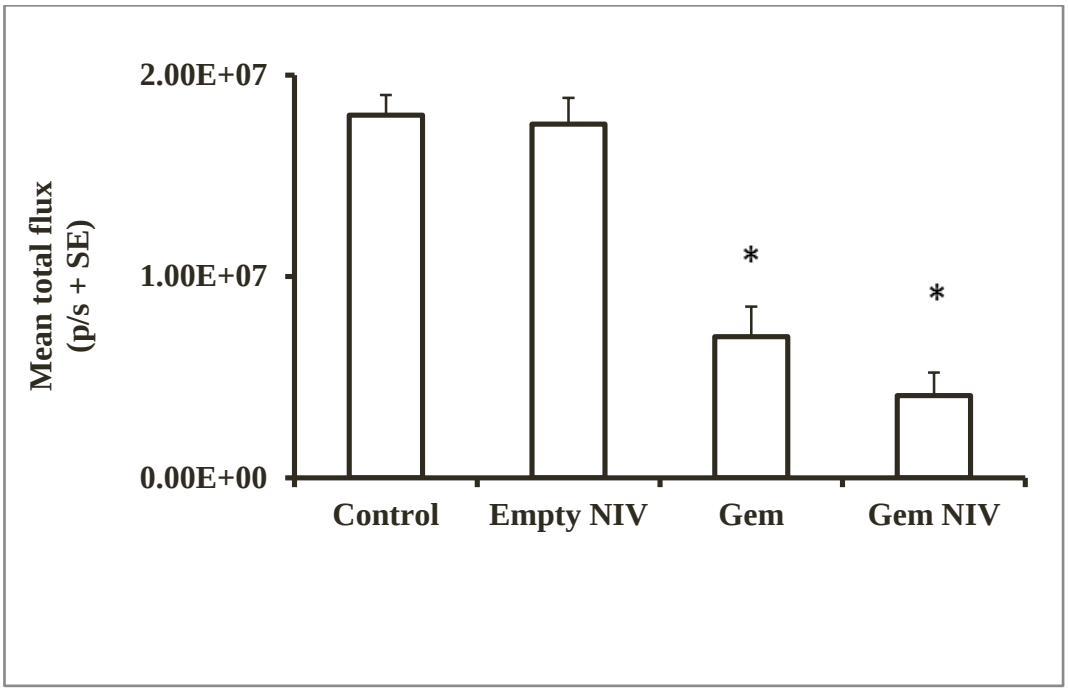

Figure 7.7 Evaluation of tumour inhibition for different Gem formulations. Treatment was started on day 3 after mice were inoculated with B16 F0 Luc cells (5 × 10^5/ mouse) on day 0. On day 3 the mice were treated by inhalation using a nebuliser with Gem solution (0.5 ml, 14 mg/ml) or Gem NIV (0.5 ml, prepared using 30 mM lipid and 14 mg Gem/ml: Vesicle size, 302 ± 5.7 nm; Zeta potential, -40.3 ± 5.1mV and entrapment efficiency, 49.0 % ±1.0) and Empty NIV prepared using 30 mM lipid (particle size, 299.1nm ± 7.6; Zeta potential, -48.1mV ± 6.2). The amount of bioluminescence emitted from the lungs was determined in the mice at different time points in the lungs which had been isolated from the mice on day 12 (*ex vivo*). $^*P < 0.05$ Gem and Gem-NIV compared to control and Empty NIV (n = 6/treatment).

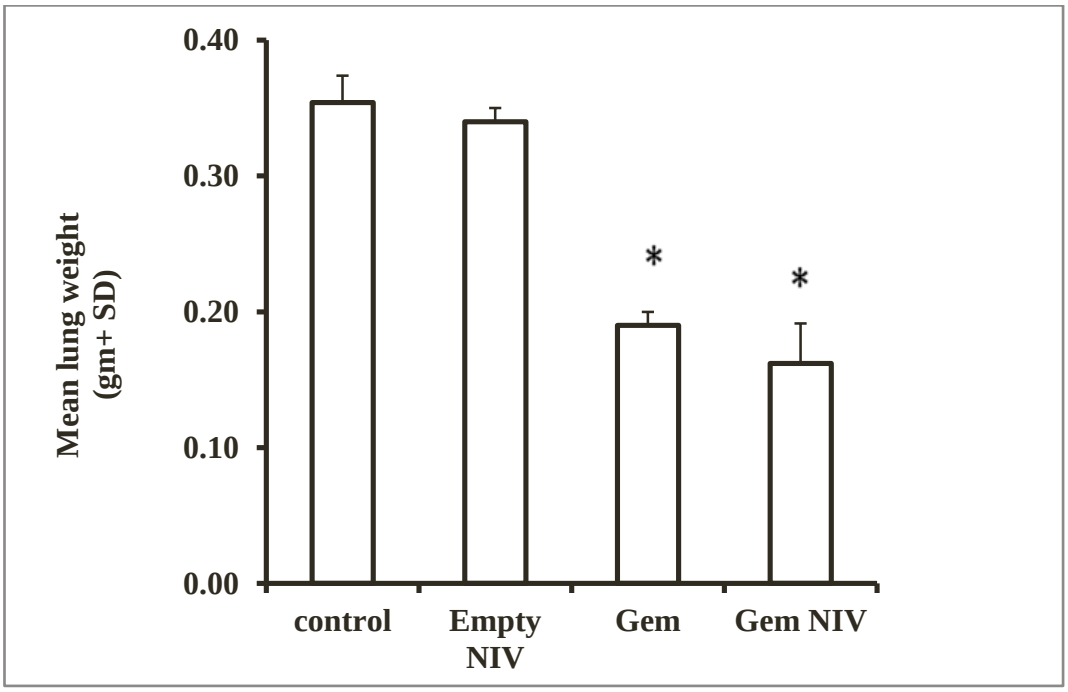

Figure 7.8 Evaluation of tumour inhibition for different Gem formulations. Treatment was started on day 3 when mice were inoculated with B16 F0 Luc cells (5 × 10^5 / mouse). On day 3 the mice were treated by inhalation using a nebuliser with Gem solution (0.5 ml, 14 mg/ml) or Gem NIV (0.5 ml, prepared using 30 mM lipid and 14 mg Gem/ml: Vesicle size, 302 ± 5.7 nm; Zeta potential, -40.3 ± 5.1mV and entrapment efficiency, 49.0%±1.0) and Empty NIV prepared using 30 mM lipid (particle size, 299.1nm ± 7.6; Zeta potential, -48.1mV ± 6.2). The weights of the lungs were determined in the mice at different time points in the lungs which had been isolated from the mice on day 12. $^{*}P < 0.05$ Gem and Gem-NIV compared to control and Empty NIV (n = 6/treatment).

Mouse weight was monitored over the course of the experiment as this can be used as a parameter to indicate the potential toxicity of treatments (Talmadge *et al*., 2007). There was a significant reduction in body weight by the end of the experiment for the two Gem formulations, but not for empty NIV treatment compared to controls (Figure7.9).

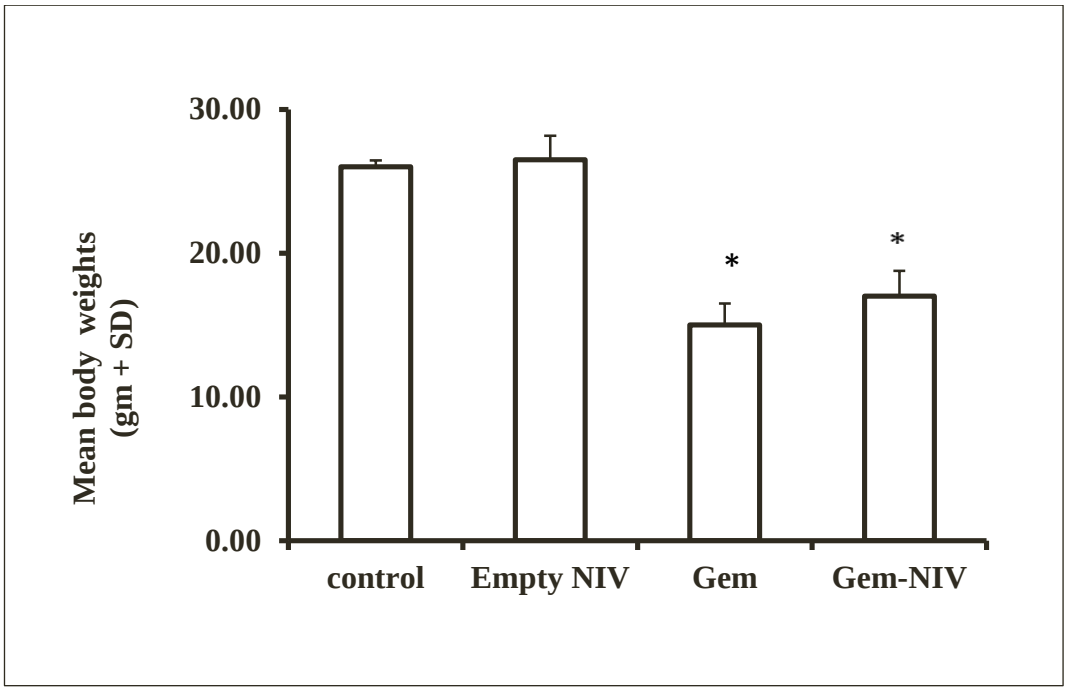

Figure 7.9 Evaluation of mice weights for different Gem formulations. Treatment was started on day 3 after mice were inoculated with B16 F0 Luc cells (5×10^5 / mouse) on day 0. On day 3 the mice were treated by inhalation using a nebuliser with Gem solution (0.5 ml, 14 mg/ml) or Gem NIV (0.5 ml, prepared using 30 mM lipid and 14 mg Gem/ml: Vesicle size, 302 ± 5.7 nm; Zeta potential, -40.3 ± 5.1mV and entrapment efficiency, 49.0 % ±1.0) and Empty NIV prepared using 30 mM lipid (particle size, 299.1nm ± 7.6; Zeta potential, -48.1mV ± 6.2).. The weight of the mice was determined on day 12. * $P < 0.05$ Gem and Gem-NIV compared to control and Empty NIV (n = 6/treatment).

These results indicated that the drug concentration used to treat mice had to be lowered to minimise acute toxicity and that the lipid content used to form Gem-NIV should be increased to improve their entrapment efficacy. Treatment with Gem-NIV (60mM lipid) resulted in a greater reduction in cancer growth compared to control (Figures 7.10-7.12) whilst decreasing the hydrating concentration of Gem used to prepare NIV from 14 mg/ml to 7 mg/ml or 3.5 mg/ml prevented the weight losses observed in the initial experiment. Treatment with Gem-NIV (60mM lipid) prepared using 7 mg/ml Gem was observed to be the most effective treatment compared to controls based on BL over the course of the study.

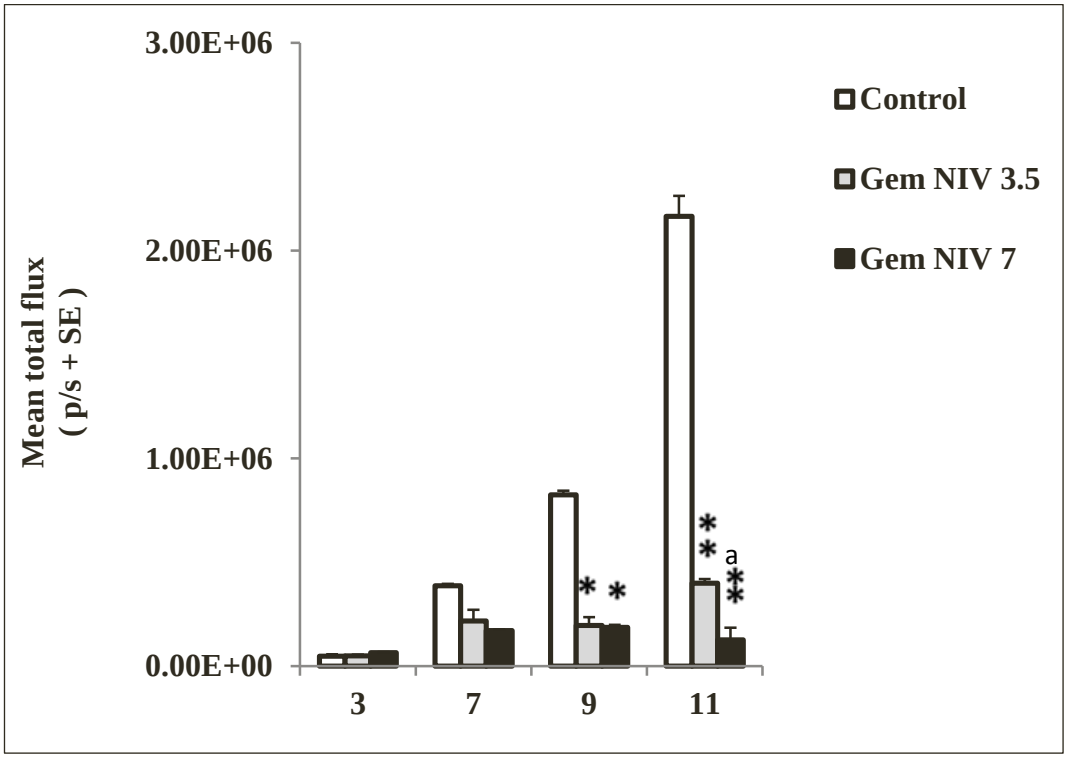

Figure 7.10 Evaluation of tumour inhibition and mouse weights for different Gem formulations. Treatment was started on day 3 after inoculation of the mice with B16 F0 Luc cells (5×10^5/ mouse) on day 0. On day 3 the mice were treated by inhalation using a nebuliser with Gem NI.V (0.5 ml, prepared using 60 mM lipid and 7 or 3.5 mg Gem/ml: Vesicle size, 545.1nm ± 2.8; Zeta potential, -70.2 mV ± 9.4 and entrapment efficiency, 80.1% ±4.8). The amount of bioluminescence emitted from the lungs was determined in the mice at different time points (*in vivo*). $^{*}P < 0.05$ Gem-NIV compared to control values. $^{**}P < 0.01$ Gem-NIV compared to control and $^{a}P < 0.05$ Gem-NIV 7 mg/ml compared to Gem NIV 3.5mg/ml. The number of mice per group was 6.

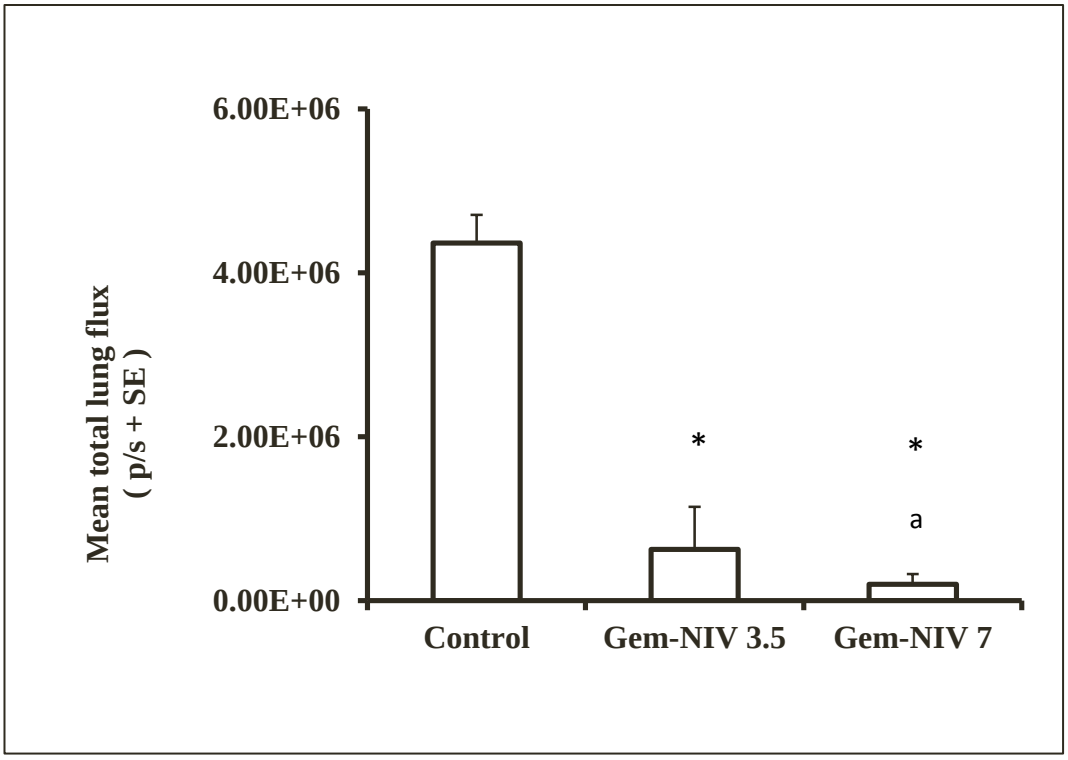

Figure 7.11 Evaluation of tumour inhibition for different Gem formulations. Treatment was started on day 3 after of the mice were inoculated with B16 F0 Luc cells (5×10^{5}/ mouse) on day 0. On day 3 the mice were treated by inhalation using a nebuliser with Gem NI.V (0.5 ml, prepared using 60 mM lipid and 7 or 3.5 mg Gem/ml: Vesicle size, 545.1nm ± 2.8; Zeta potential, -70.2 mM ± 9.4 and entrapment efficiency, 80.1% ±4.8). The amount of bioluminescence emitted from the lungs was determined in the mice at different time points in the lungs which had been isolated from the mice on day 11 (*ex vivo*). $^{*}P < 0.05$ Gem-NIV compared to control values and $^{a}P < 0.05$ Gem NIV 7 mg/ml compared to Gem NIV 3.5 mg/ml values. The number of mice per group was 6.

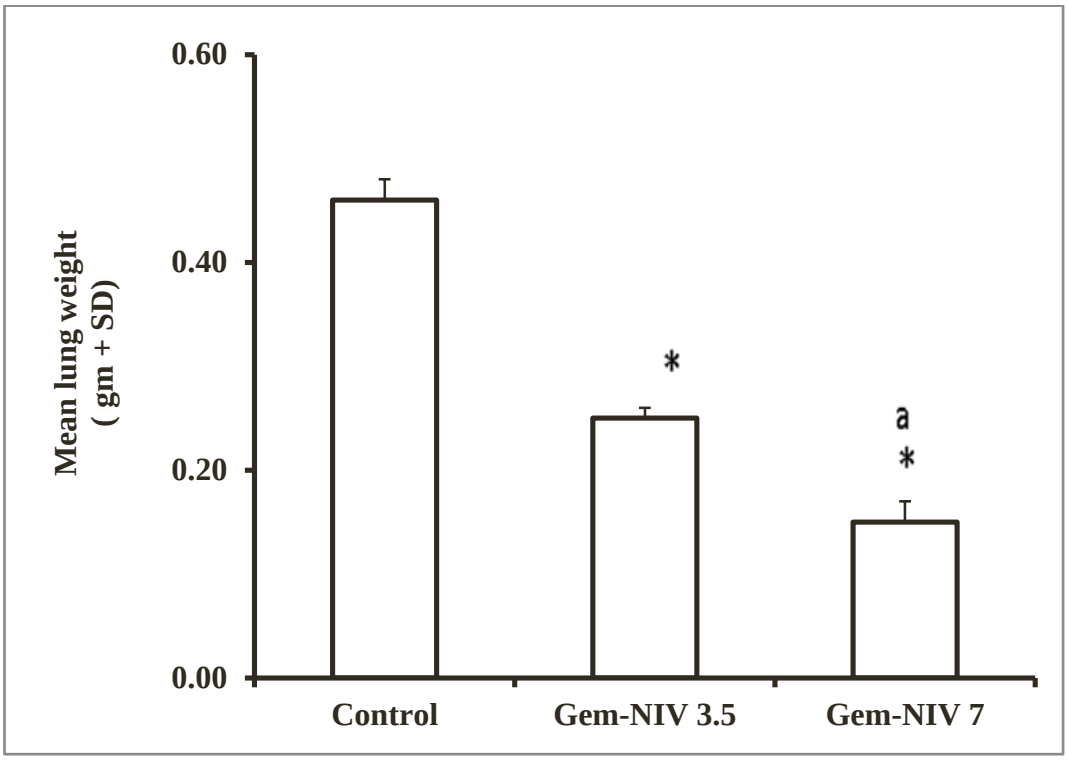

Figure 7.12 Evaluation of tumour inhibition for different Gem formulations. Treatment was started on day 3 after the mice were inoculated with B16 F0 Luc cells (5×10^5/ mouse) on day 0. On day 3 the mice were treated by inhalation using a nebuliser with Gem-NIV (0.5 ml, prepared using 60 mM lipid and 7 or 3.5 mg Gem/ml: Vesicle size, 545.1nm ± 2.8; Zeta potential, -70.2mV ± 9.4 and entrapment efficiency, 80.1% ± 4.8). The lungs were removed and weighed on day 11. $^{*}P < 0.05$ Gem NIV compared to control values and $^{a}P < 0.05$ Gem-NIV 7 mg/ml compared to Gem NIV 3.5 mg/ml values. The number of mice per group was 6.

The above experiment was repeated with a Gem solution control arm and an extension of the study to 14 days. All Gem formulations significantly ($p < 0.05$) inhibited cancer growth compared to controls by day 10. However, by day 14, treatment with the Gem solution at 3.5 mg/ml did not continue to inhibit cancer growth. At day 14, Gem-NIV (60mM lipid, 7mg/ml Gem) was the most effective treatment, causing a significant ($p < 0.01$) reduction in BL compared to controls (Figure 7.13).

The *ex vivo* and lung weights from these animals supported the *in vivo* results (Figure 7.14 and 15). Treatment with 7mg/ml Gem solution caused a significant ($p <0.05$) reduction in mouse weight by day 14 to starting body weight (Figures 7.16).

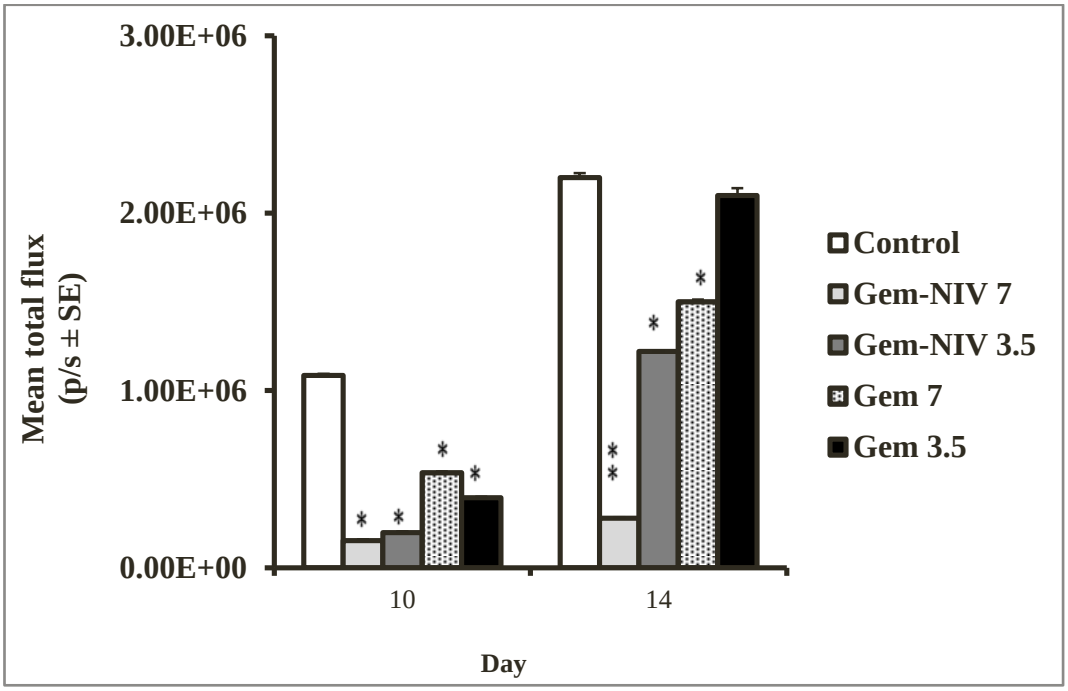

Figure 7.13 Evaluation of tumour growth inhibition for different Gem formulations. Treatment was started on day 3 after the inoculation of the mice with B16 F0 Luc cells (5×10^5/ mouse) on day 0. On day 3 the mice were treated by inhalation using a nebuliser with Gem solution (0.5ml, 3.5 mg or 7 mg/ml) and Gem-NIV (0.5 ml, prepared using 60 mM lipid and Gem 3.5 or 7mg/ml: Vesicle size, 540.1nm ± 2; Zeta potential, -75.2 ± 3mV and entrapment efficiency, 77.1% ± 4). The amount of bioluminescence emitted from the lungs was determined in mice at different time points (*in vivo*). $^{*}P < 0.05$ control compared to treatments values. $^{**}P < 0.01$ control compare to treatments. The number of mice per group was 6.

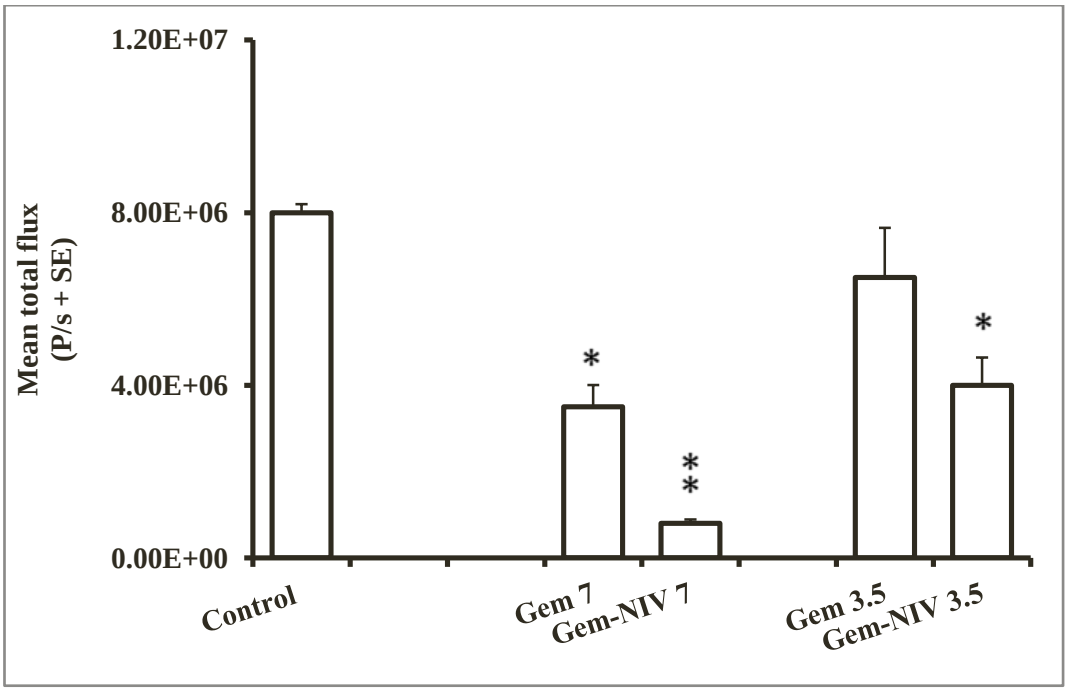

Figure 7.14 Evaluation of tumour growth inhibition and mouse weights for different Gem formulations. Treatment was started on day 3 after the mice were inoculated with B16 F0 Luc cells (5×10^{5} / mouse) on day 0. On day 3 the mice were treated by inhalation using a nebuliser with Gem solution (0.5ml, 3.5 mg or 7 mg/ml) and Gem-NIV (0.5 ml, prepared using 60 mM lipid and Gem 3.5 or 7mg/ml: Vesicle size, 540.1nm ± 2; Zeta potential, -75.2 mV ± 3 and entrapment efficiency, 77.1% ±4). The amount of bioluminescence emitted from the lungs was determined in the mice at different time points in lungs which had been isolated from the mice on day 14 (*ex vivo*). $^{*}P < 0.05$ control compared to treatments values. $^{**}P < 0.01$ control compare to treatments. The number of mice per group was 6.

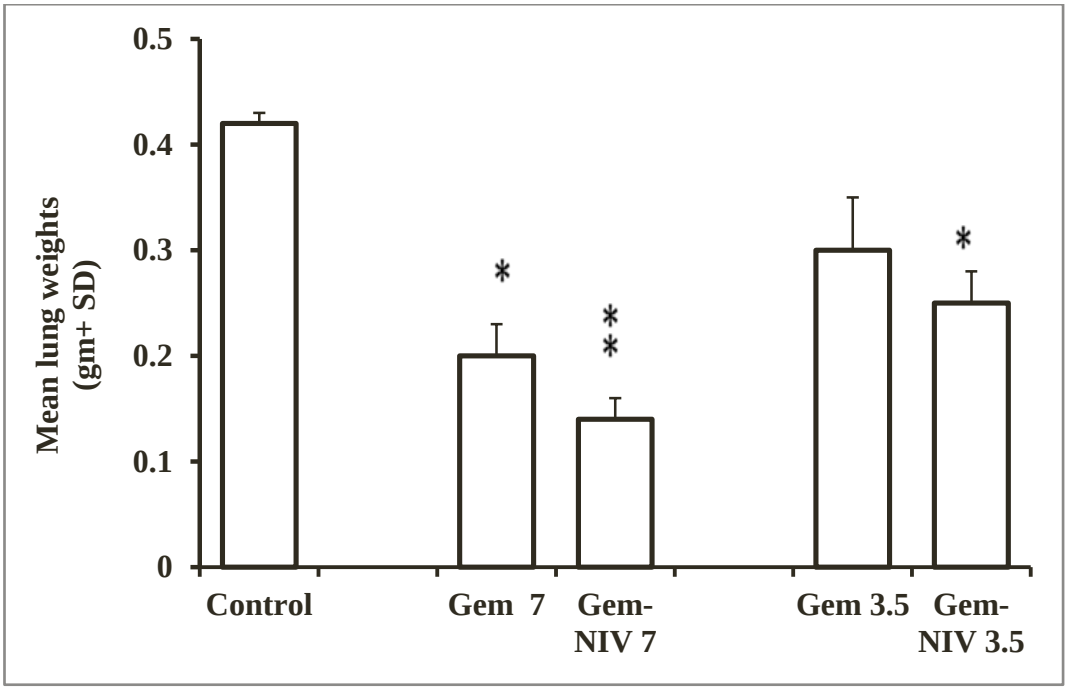

Figure 7.15 Evaluation of tumour growth inhibition for different Gem formulations. Treatment was started on day 3 after the mice were inoculated with B16 F0 Luc cells (5×10^5/ mouse) to mice on day 0. On day 3 the mice were treated by inhalation using a nebuliser with Gem solution (0.5ml, 3.5 mg or 7 mg/ml) and Gem-NIV (0.5 ml, prepared using 60 mM lipid and Gem 3.5 or 7mg/ml: Vesicle size, 540.1nm ± 2; Zeta potential, -75.2 mV ± 3 and entrapment efficiency, 77.1% ± 4). The amount of bioluminescence emitted from the lungs was determined in the mice at different time points in lungs which had been isolated from the mice on day 14 (*ex vivo*). $^{**}P < 0.01$. Gem-NIV 7 mg/ml compared to control. $^{*}P < 0.05$ Gem-NIV 3.5 mg/ml compared to control. The number of mice per group was 6.

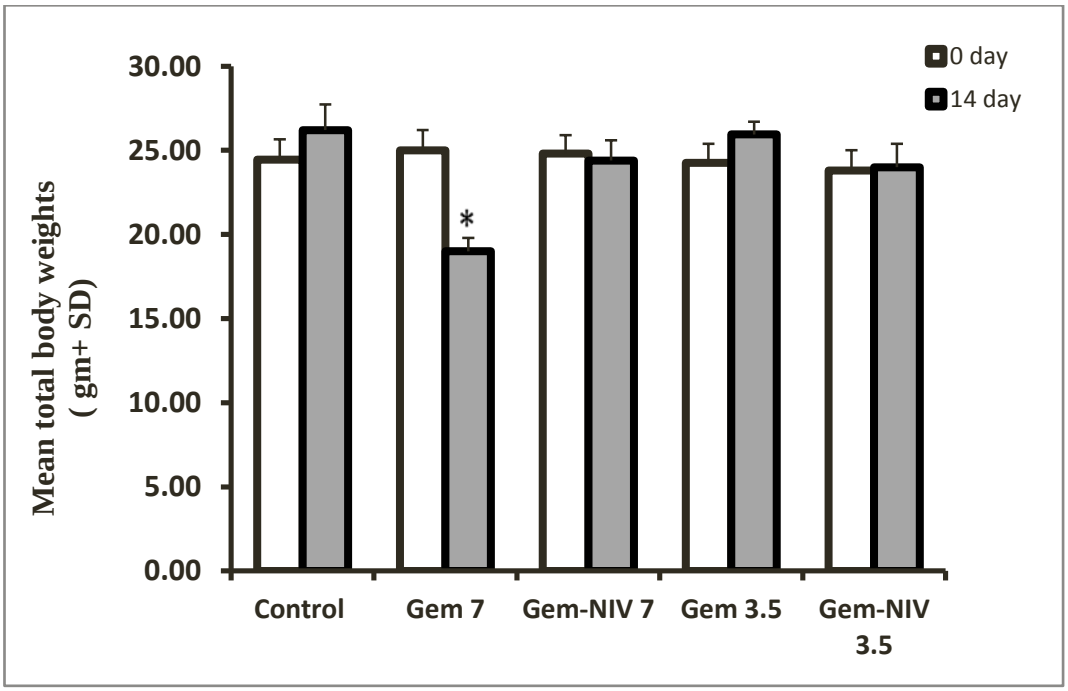

Figure 7.16 Evaluation of mice weights for different Gem formulations. Treatment was started on day 3 after the mice were inoculated with B16 F0 Luc cells (5×10^{5} / mouse) on day 0. On day 3 the mice were treated by inhalation using a nebuliser with Gem solution (0.5ml, 3.5 mg or 7 mg/ml) and Gem-NIV (0.5 ml, prepared using 60 mM lipid and Gem 3.5 or 7mg/ml: Vesicle size, 540.1 ± 2 nm; Zeta potential, -75.2 ± 3mV and entrapment efficiency, 77.1% ±4). The mice were weighed on days zero and 14. $^{*}P < 0.05$ day 14 compared to day zero. The number of mice per group was 6.

Empty NIV had no effect on cancer progression compared to controls and it can therefore be deduced that the reduction in cancer growth was attributable to Gem entrapped in the NIV formulation. Gem-NIV (60 mM lipid) in both doses (3.5 or 7 mg/ml) was more active than the corresponding Gem solution on day 12 and 14 according to *in vivo* mean total bioluminescence flux (Figure 7.17). Ex *vivo* data showed that, Gem NIV 7mg/ml was significant compared to Gem solution (Figure 7.18) and supported by lung weights (Figure 7.19). Treatment with 7mg/ml Gem solution caused a significant reduction in mouse weight by days 7 and 14 to starting body weight (Figures 7.20).

The effect of vesicle size on the anticancer activity of Gem-NIV was determined using Gem-NIV (60 mM, 7mg/ml Gem) manufactured at differ vesicle sizes. Both vesicle sizes of NIV (60 mM lipid, 7mg/ml Gem) significantly reduced cancer growth compared to controls, although treatment with the larger Gem-NIV (540 ± 3 nm) was significantly more active than reduced size (269 nm ± 4) ($p < 0.01$, Figures 7.21 and 22). However, although the isolated lung weights from mice on day 14 post-treatment showed no significant difference between the two vesicle sizes, both were still significantly lower than those of the control values ($p < 0.05$, Figure 7.23). Neither Gem-NIV treatments had an effect on the body weight of mice compared to controls indicating that administration was not associated with any overt toxicity.

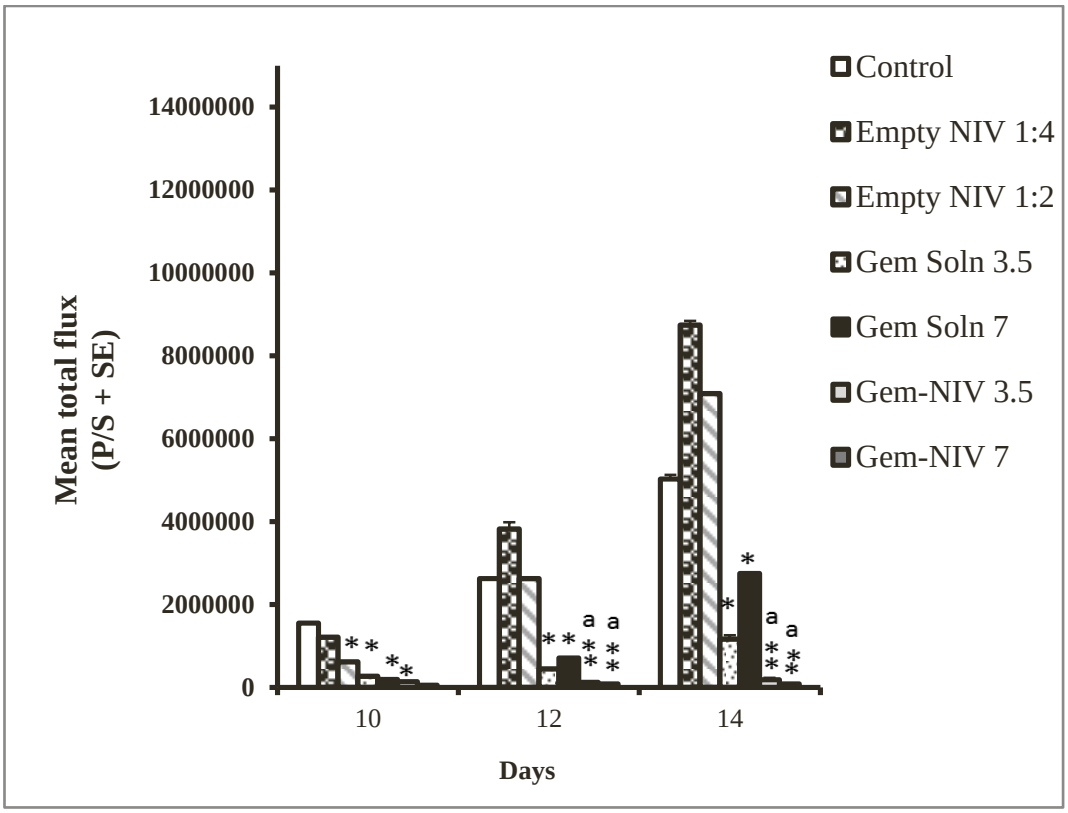

Figure 7.17 Evaluations of tumour growth inhibition for different Gem-NIV formulation. Treatment was started on day 3 after the mice were inoculated with B16 F0 Luc cells (5 $\times 10^5$/ mouse) on day 0. On day 3 the mice were treated by inhalation using a nebuliser with Gem solution (0.5ml, 3.5 mg or 7 mg/ml), Gem- NIV (0.5 ml, prepared using 60 mM lipid and 3.5 or 7mg/ml Gem-NIV (0.5 ml, prepared using 60 mM lipid and Gem 3.5 or 7mg/ml: Vesicle size, 542 nm ± 3; Zeta potential, -70 mV ± 5 and entrapment efficiency, 78 % ±3) and Empty NIV (1:4 and 1:2 dilutions). The amount of bioluminescence emitted from the lungs was determined in the mice at different time points (*in vivo*). $^{*}P < 0.05$ Gem compared to control and Empty. $^{**}P < 0.01$ Gem-NIV compared to control and Empty. $^{a}P < 0.05$ Gem-NIV compared Gem solutions. The number of mice per group was 6.

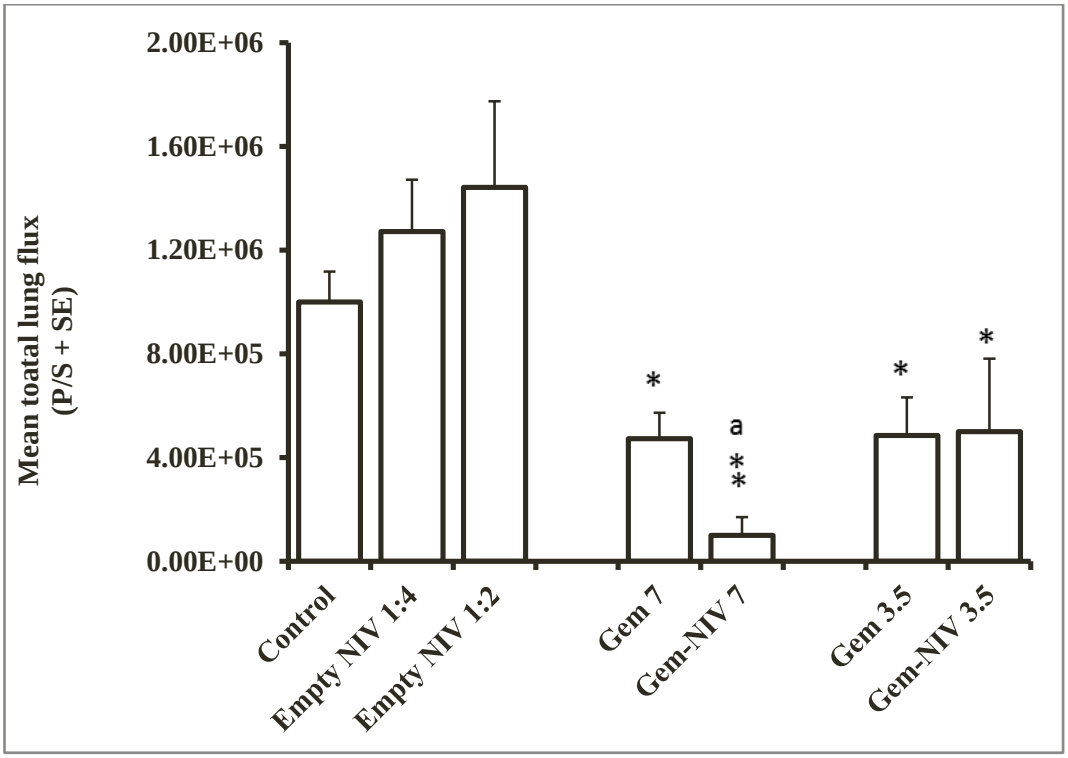

Figure 7.18 Evaluations of tumour inhibition for different Gem- NIV formulation. Treatment was started on day 3 after the mice were inoculated with B16 F0 Luc cells (5×10^{5}/ mouse) on day 0. On day 3 the mice were treated by inhalation using a nebuliser with Gem solution (0.5ml, 3.5 mg or 7 mg/ml), Gem-NI.V (0.5 ml, prepared using 60 mM lipid and 3.5 or 7mg/ml; Vesicle size, 542 nm ± 3; Zeta potential, -70 mV ± 5 and entrapment efficiency, 78 % ±3) and Empty NIV (1:4 and 1:2 dilutions). The amount of bioluminescence emitted from the lungs which had been isolated from the mice on day 14 was measured (*ex vivo*). $^{*}P < 0.05$ treatments compared to control and empty NIV. $^{**}P < 0.01$ Gem-NIV 7mg/ml compared to control and Empty NIV. $^{a}P < 0.05$ Gem-NIV compared to Gem solutions. The number of mice per group was 6.

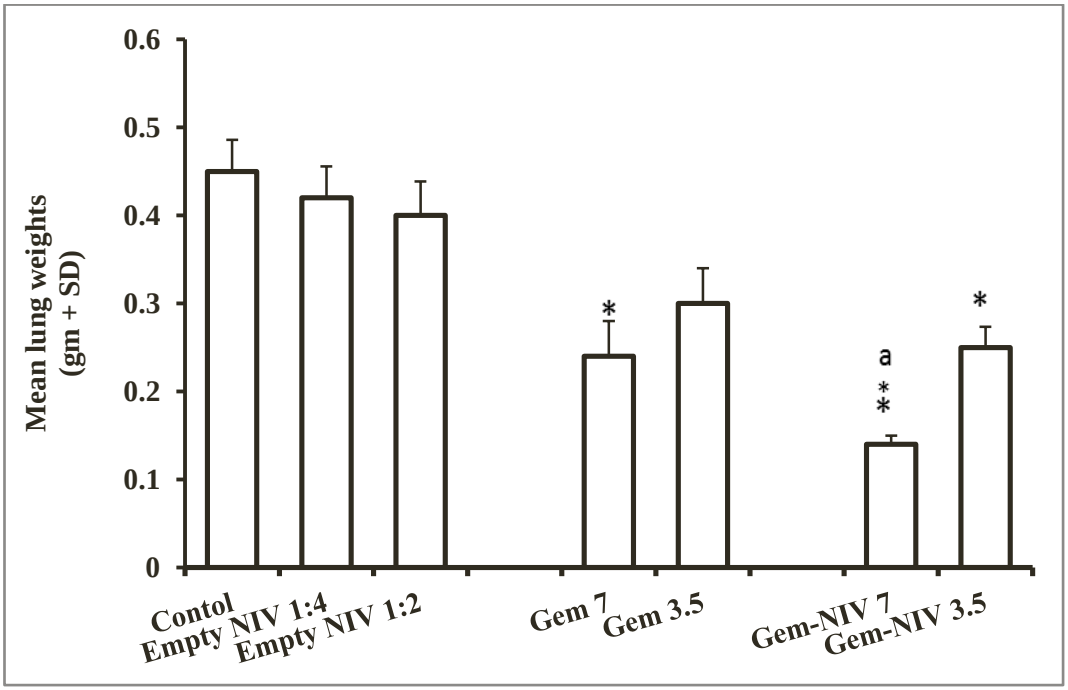

Figure 7.19 Evaluations of tumour inhibition for different Gem formulations. Treatment was started on day 3 after the inoculation of the mice with B16 F0 Luc cells (5×10^5/mouse) on day 0. On day 3 the mice were treated by inhalation using a nebuliser with Gem solution (0.5ml, 3.5 mg or 7 mg/ml), Gem-NIV (0.5 ml, prepared using 60 mM lipid and 3.5 or 7mg/ml; Vesicle size, 542 ± 3 nm ; Zeta potential, -70 mV± 5 and entrapment efficiency, 78 % ±3) and Empty NIV (1:4 and 1:2 dilutions). The removed lungs were weighed on day 14.). $^{*}P < 0.05$ treatments compared to control and empty NIV. $^{**}P<0.01$ Gem-NIV 7mg/ml compared to control and Empty NIV. $^{a}P < 0.05$ Gem-NIV compared to Gem solutions. The number of mice per group was 6.

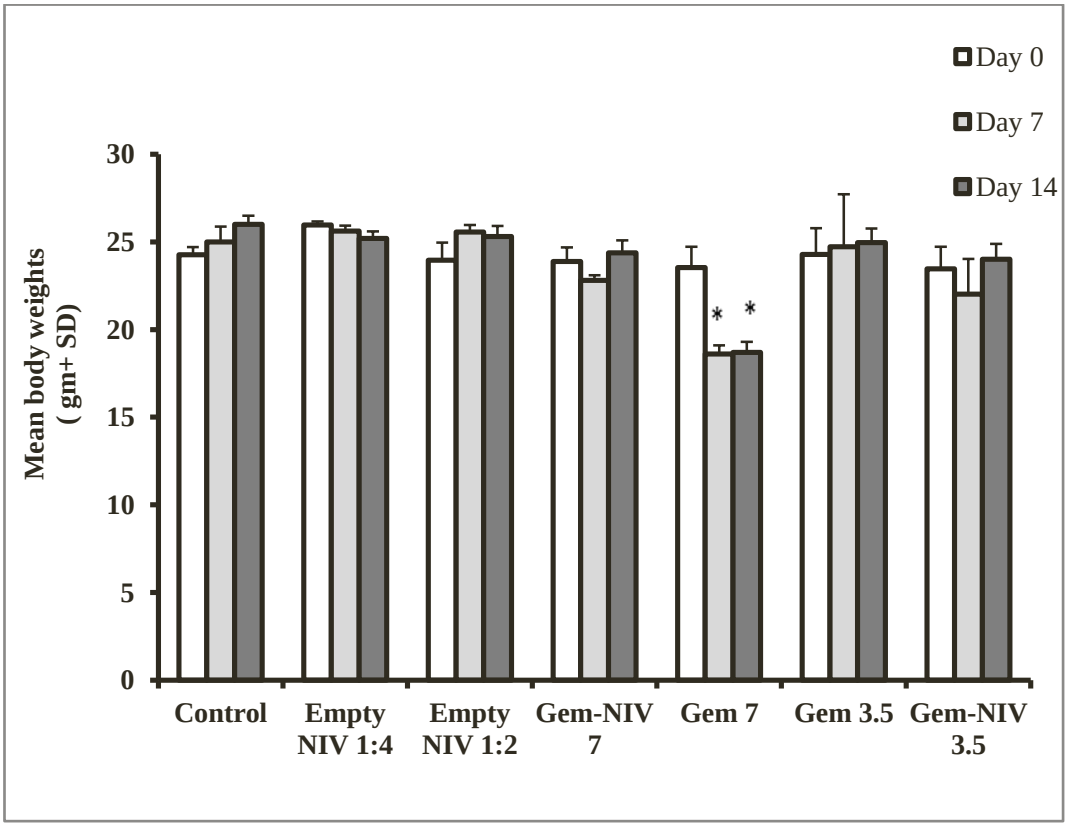

Figure 7.20 Evaluations of mice weights for different Gem formulations. Treatment was started on day 3 after the mice were inoculated with B16 F0 Luc cells (5×10^5/ mouse) on day 0. On day 3 the mice were treated by inhalation using a nebuliser with Gem solution (0.5ml, 3.5 mg or 7 mg/ml), Gem-NIV (0.5 ml, prepared using 60 mM lipid and 3.5 or 7 mg/ml; Vesicle size, 542 nm ± 3; Zeta potential, -70 mV ± 5 and entrapment efficiency, 78 % ±3) and Empty NIV (1:4 and 1:2 dilutions). The mice were weighed on days 0, 7 and 14. $^*P < 0.05$ Gem Solution 7 mg/ml at day 7 and 14 compared to days 0. The number of mice per group was 6.

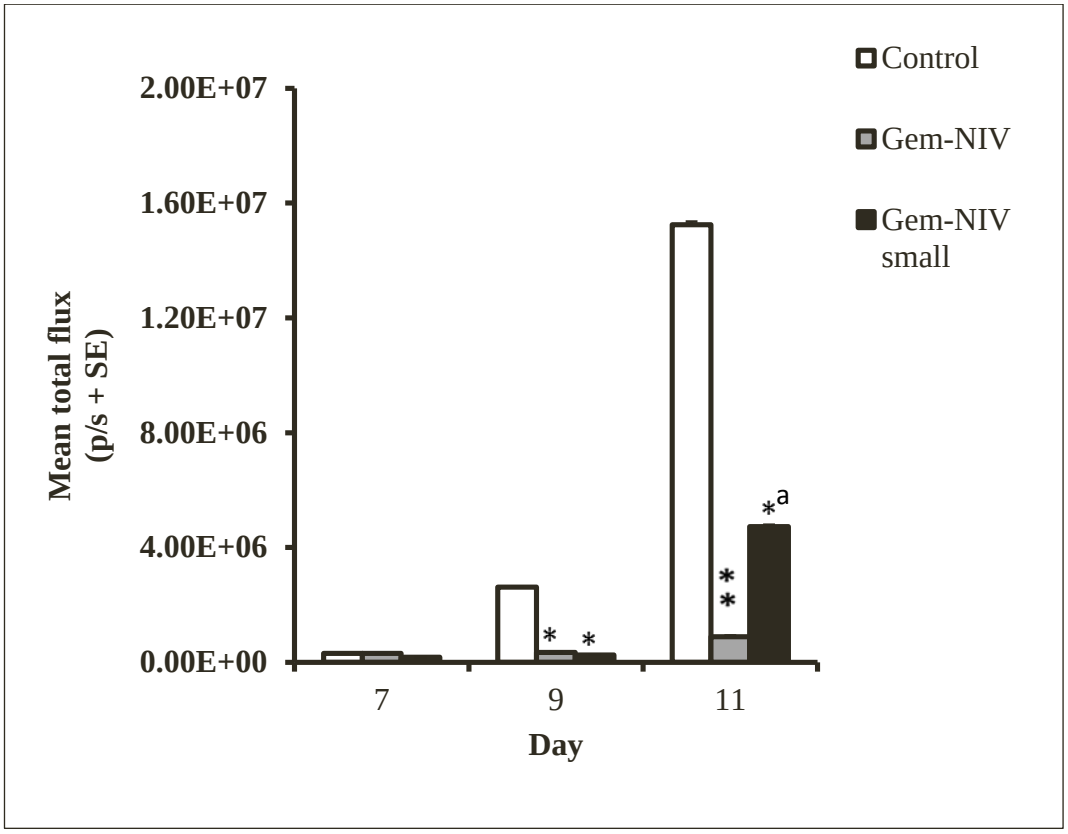

Figure 7.21 Evaluation of tumour growth inhibition for small Gem-NIV. Treatment was started on day 3 after the mice were inoculated with B16 F0 Luc cells (5×10^5/ mouse) on day 0. On day 3 the mice were treated by inhalation using a nebuliser with Gem-NIV (0.5 ml, prepared using 60 mM lipid and 7mg/ml Gem of 540 nm ± 3 or 269 nm ± 4). The amount of bioluminescence emitted from the lungs was determined in the mice at different time points (*in vivo*). $^{*}P < 0.05$ Gem-NIV compared to control values. $^{**}P < 0.01$ Gem-NIV compared to control and $^{a}p < 0.05$ Gem-NIV small compared to Gem-NIV values. The number of mice per group was 6.

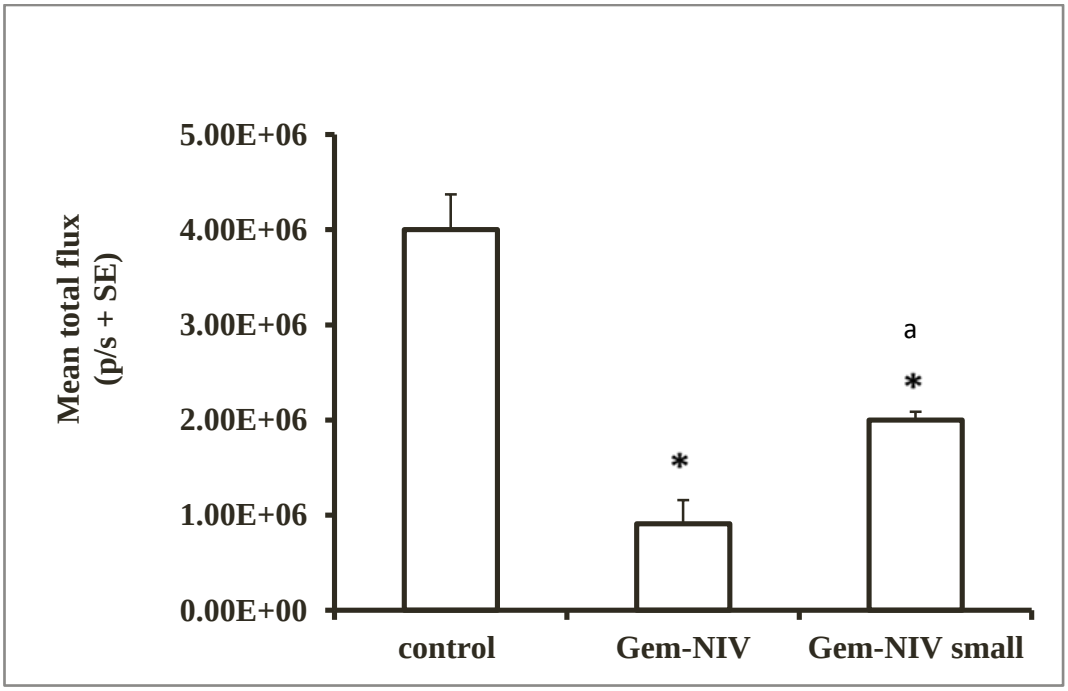

Figure 7.22 Evaluation of tumour growth inhibition for different small Gem-NIV formulation. Treatment was started on day 3 after the inoculation of the mice with B16 F0 Luc cells (5 x 10^5/ mouse) on day 0. On day 3 the mice were treated by inhalation using a nebuliser with Gem-NIV (0.5 ml, 60 mM lipid, 7mg/ml Gem) using sizes of 540 nm ± 3 or 269 nm ± 4±). The amount of bioluminescence emitted from the lungs was determined in the mice at different time points in lungs which had been isolated from the mice on day 11 (ex *vivo*). $^{*}P < 0.05$ Gem NIV compared to control values. $^{a}P < 0.05$ Gem-NIV small compared to Gem-NIV values. The number of mice per group was 6.

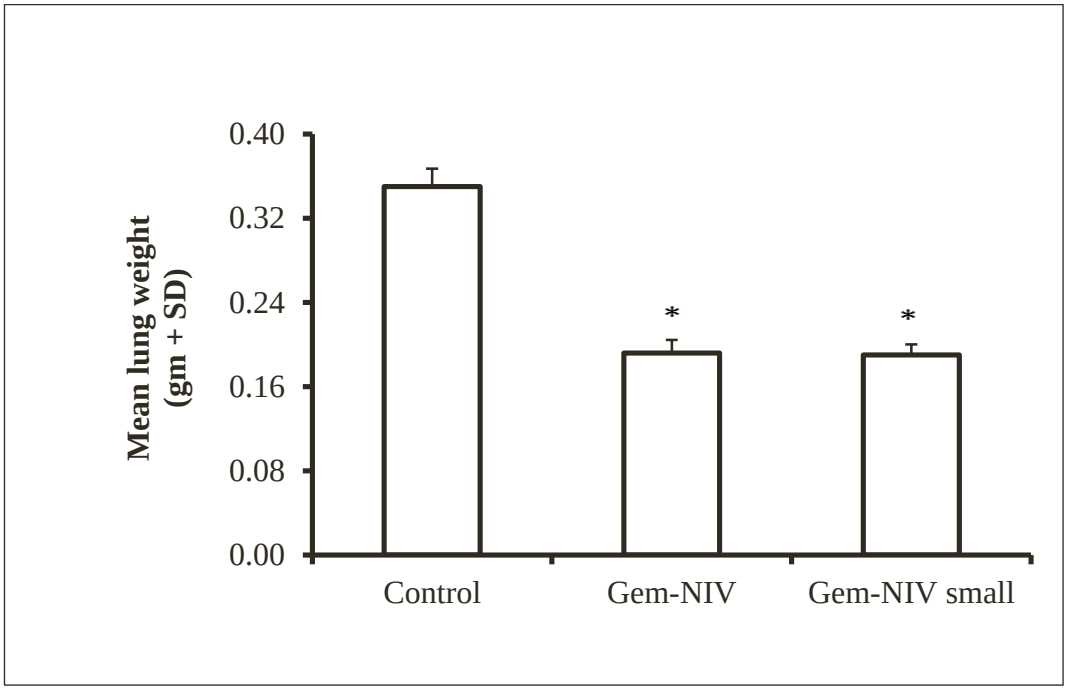

Figure 7.23 Evaluation of tumour growth inhibition for different small Gem-NIV formulation. Treatment was started on day 3 after the inoculation of the mice with B16 F0 Luc cells (5 x 10^5/ mouse) on day 0. On day 3 the mice were treated by inhalation using a nebuliser with Gem-NIV (0.5 ml, prepared using 60 mM lipid and 7mg/ml Gem of 540 ± 3 nm or smaller size of 269 ± 4 nm). Removed lungs were weighed on day 11. $^*P < 0.05$ Gem NIV compared to control. The number of mice per group was 6.

7.3 Discussion

In this study, male BALB/c mice had higher lung cancer burdens than females. However, many studies in humans and animals have shown the opposite effect. This may be attributable to the mouse strain and cell line used in this study. Differences in metabolism, DNA repair, expression of oncogenes and tumour suppressor genes may affect cancer burdens (Bartsch, 1996). For example, the BALB/c mice were resistant to lung cancer induced by cigarette smoke (Santiago, 2009) whereas A/J mice showed a strong tendency to develop lung cancer (Witschi, 2002). In this study, most of the nude mice had died by day 21. Based on these results it was decided to use BALB/c male mice and to assess tumour progression up as it represented a less severe animal model, which was aligned to the principles of the 3Rs and is more ethically appropriate. However, BALB/c showed a reduction in BL signals after day 14 and a similar reduction in BL signalling in an orthotopic mouse model has been reported in a previous study which showed an inhibition of BL signals in a bladder cancer model, starting 14 days after cancer cell transplantation (Jurczok, 2007).

Other studies have shown that BL data does not correlate with an increase in tumour weight, which is also used as an indication of cancer progression (Black, 2010; Sarraf-Yazdi *et al*., 2004; Zabala *et al*., 2009). It has been proposed by many literatures that tissue hypoxia is responsible for this lack of correlation between *in vivo* and *ex vivo* readings in advanced tumours (Moriyama, 2008; Zabala *et al.*, 2009). Advanced tumours contain large hypoxic regions, leading to changes in

cancer cell metabolism. The hypoxic and necrotic areas arise from poor oxygenated blood supply and with BL utilising luciferase imaging being oxygen dependent, hypoxia therefore detrimentally affects signal production (Black, 2010). If a lack of oxygenation within the tumour mass limits BL signalling then BL light emission should be restored in *ex vivo* samples.

Mice treated with Gem-NIV (30 mM, 14 mg/ml Gem) and Gem solution (14 mg/ml) showed less cancer burden than untreated mice (control) but the drug concentration used to prepare the solution and Gem-NIV had an important effect. At the highest concentration tested (14 mg/ml), signs of toxicity were evident based on mouse body weight loss for both treatments (Gem solution and Gem-NIV). As the un-entrapped drug is not removed from the Gem-NIV formulation during manufacture, this could be an explanation for the effect with un-entrapped drug causing acute toxicity similar to that of free Gem in solution. Gem-NIV prepared using 60 mM lipid, as this formulation gave a high level of drug entrapment. Drug entrapment has already been shown to be an important factor in efficacy of lipid-based vesicles, which is used as a carrier for drugs (Chan *et al.*, 2004; Ramana *et al.*, 2010). For example, Gem liposomes (5mg/ml) prepared by 660 mM total lipid concentration had a greater anti-tumour activity than that of free Gem in Gem solution (15 mg/ml) when studied in a xenograft mouse model of human pancreatic carcinoma, in which BxPC-3 or PSN-1 cells were injected into CB-17 SCID mice intraperitoneally (Cosco *et al*., 2009). Free Gem is rapidly inactivated to difluorouridine by cytidine deaminase, causing the short plasma half-life of free Gem (8-17 min). The present study has shown that NIV protects Gem from being metabolised (Chapter 5), therefore the higher efficacy

of Gem-NIV is also related to its higher and more prolonged availability to the lung tumour (Abbruzzese *et al*., 1991; Moog *et al.*, 2002; Soloman and Gabizon, 2008).

Additionally, in another study, Gem liposomes cause a reduction in pancreatic tumour size of 68 % in comparison with free Gem, which reduced the tumour by 7% and this was successfully monitored by BL technology (Graeser, *et al.*, 2009). This has been confirmed in a more recent study by Ma *et al.* (2012), evaluating a nano-micelles formulation of docetaxel and BL optical imaging used to evaluate the anti-cancer activity of docetaxel in mice bearing B16 melanoma tumour. Therefore, the observed results are commensurate with these observations.

The present studies indicate that Gem-NIV treatment can reduce toxic side effects, as treatment with Gem-NIV (60mM, 7 mg/ml Gem) was not associated with weight loss whereas treatment with corresponding Gem solution caused weight loss. Gem doses >12mg/kg are associated with more appreciable toxicity and can cause fatal pulmonary oedema in mice (Gordon and Kleinerman, 2010). Furthermore, previous pharmacokinetic studies (see Chapter 5) showed that systemic levels were much lower using Gem-NIV in comparison to Gem solution.

Chapter 8: Stability of Gem-NIV formulation upon storage

8.1 Introduction

This study was carried out in order to predict the stability of the candidate Gem-NIV formulation. The chemical and physical stability of pharmaceutical products are influenced by their storage conditions, which will then determine the shelf-life and storage conditions that have to be used for the finished product. Commercial products should generally have a shelf-life of approximately two years or greater. The content should not drop below 90% under the recommended storage conditions and the product should still have the same appearance as it had when first manufactured (Aulton, 2007). This can be determined experimentally by monitoring the physical and chemical characteristics of a drug formulation over time and measuring any degradative changes. Hydrolysis and oxidation are the most common pathways of chemical degradation. Chemical degradation is affected by the thermal conditions during storage, for example, if the temperature increases by 10°C then degradation can be accelerated by a two to five fold factor (Aulton, 2007).

The stability of a vesicular delivery system can be determined by the measurement of particle size, zeta potential, entrapment efficiency and lipid content at various temperatures over a certain period of time. The chemical degradation of lipids may affect the entrapment efficiency of vesicular formulation causing drug leakage as a result of changes in the permeability of the vesicular bilayers (Lasic, 1998;Ozer and Talsma, 1989; Uchegbu and Vyas, 1998). Degradation may produce a number of products with highly different chemical natures from the original lipids (Grit and

Crommelin, 1993). For example, phospholipids within liposomes usually undergo peroxidation and hydrolysis causing defects in the stability of liposomes (Cortesi *et al.*, 2007). Some surfactants such as polyethers have a tendency to be oxidised by atmospheric oxygen into hydroperoxides, peroxides, and formaldehyde and other carbonyl compounds (Bergh *et al.*, 1998). The physical characteristics of a vesicle formulation may also change; for example, changes in vesicle size or surface charge may produce other colloidal structures as a result of aggregation (Heurtault *et al.*, 2003). Lyophilisation was developed to increase the stability of formulations to thermal effects during long storage (Lo *et al*., 2004; Mishima, 2008; Sankar *et al*., 2007) and the addition of cholesterol and negatively charged lipids to vesicular products can reduce drug leakage and/or aggregation during storage (Chen *et al*., 2010).

Another parameter that can be used to assess the stability of a formulation is to monitor its flow characteristics over time (Manca *et al*., 2012). In stress-free conditions, pharmaceutical formulations have a viscosity that may change when exposed to an external stress. Most formulations have viscosities, which vary with shear rate (Non-Newtonian flow). Products that demonstrate Non-Newtonian flow have pseudoplastic characteristics allow flow without resistance during administration (shear thinning) in contrast to those which demonstrate dilatant (shear thickening) characteristics and which resist flow with an increasing shear rate (Aulton, 2007).

8.2 Results

The entrapment efficiency did not change significantly over 90 days with storage at 4°C and 25°C temperatures for the Gem-NIV suspension and did not change for the lyophilised Gem-NIV formulation stored at -20°C. A decrease in entrapment efficiency occurred for Gem-NIV stored at 37°C, but it was only observed after day 90. The concentration of Gem present in the supernatant as well as the pellet was determined as part of the drug entrapment studies. An increase in the concentration of Gem in the supernatant (un-entrapped) was obtained in the Gem-NIV, which was stored at 37ºC on day 90 whereas a decrease in the concentration of Gem in the supernatant was obtained in the lyophilised product on day 90. The results indicated that Gem is chemically stable over 90 days because there were no changes in the total concentration of Gem at all storage temperatures (Figure 8.1).

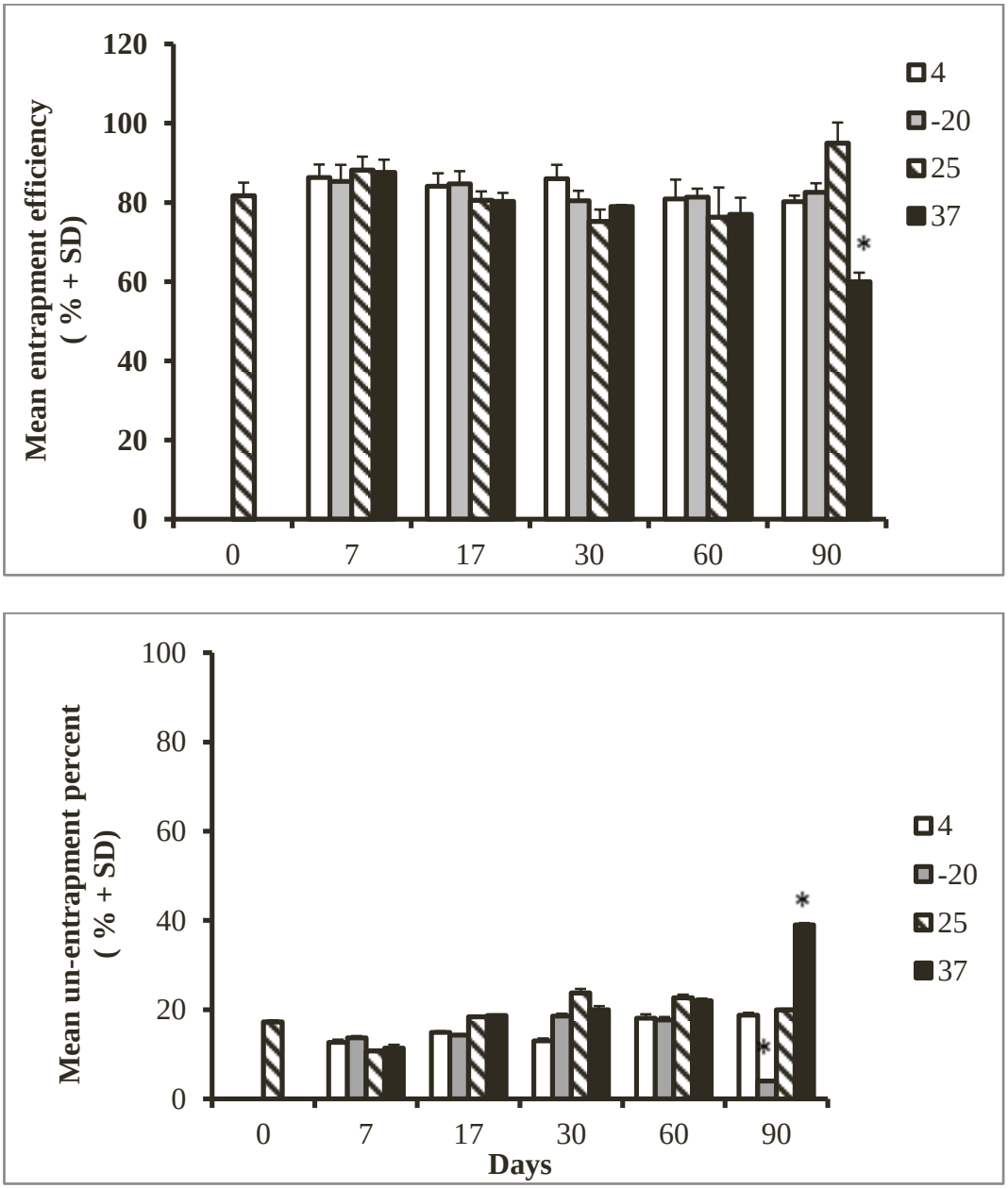

Figure 8.1 The entrapment efficiency of Gem-NIV and un-entrapped Gem in the supernatant stored at 4, -20 (lyophilised Gem-NIV), 25 and 37°C determined over time at 0, 7, 17, 30, 60 and 90 days post-preparation. $^{*}P < 0.05$ stored samples compared to the day zero value.

The particle size of Gem-NIV was stable during storage at 4°C and 25°C, even after 90 days. However, the vesicle size significantly ($p < 0.05$) increased for Gem-NIV stored at 37°C for 90 days. The lyophilised Gem-NIV had vesicles that were significantly ($p < 0.05$) larger upon rehydration compared to the initial particle size but the vesicles had a similar size over the course of the study (Figure 8.2).

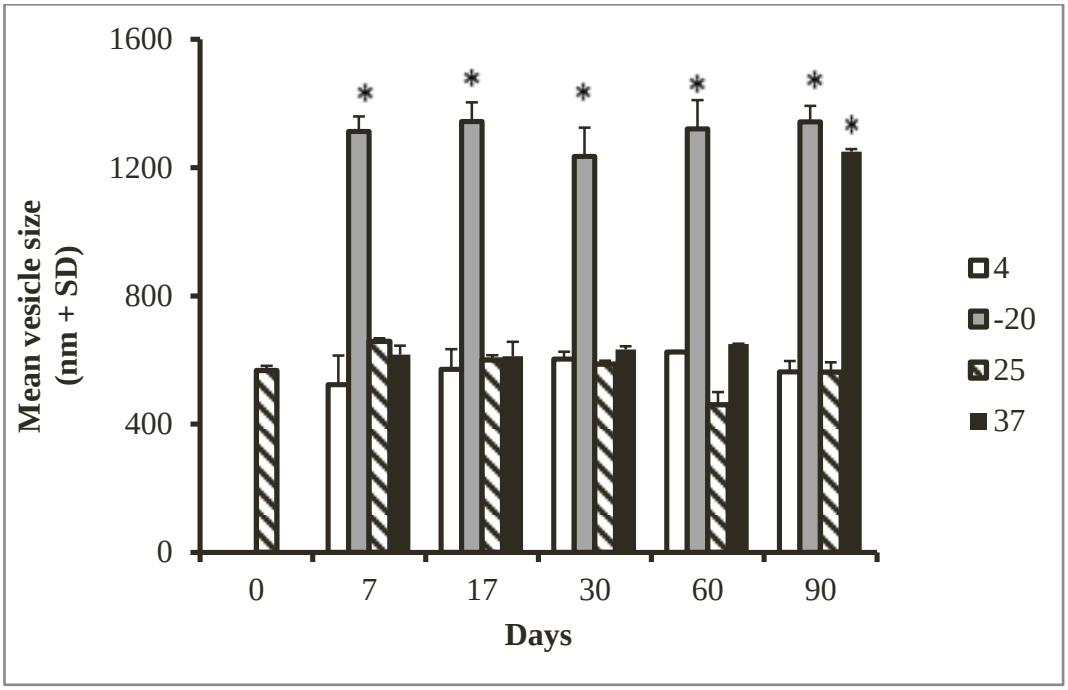

Figure 8.2 The size of Gem-NIV stored at 4, -20 (lyophilised Gem-NIV post hydration), 25 and 37°C determined over time at 0, 7, 17, 30, 60 and 90 days post-preparation. *P < 0.05 samples stored at -20 and 37°C compared to the day zero value.

The decrease in DCP concentration was associated with a decrease in vesicle surface charge at the same time points for Gem-NIV stored at 37°C (Figure 8.3). DCP content dropped during storage at 37°C by day 60 and 90 (Figure 8.4).

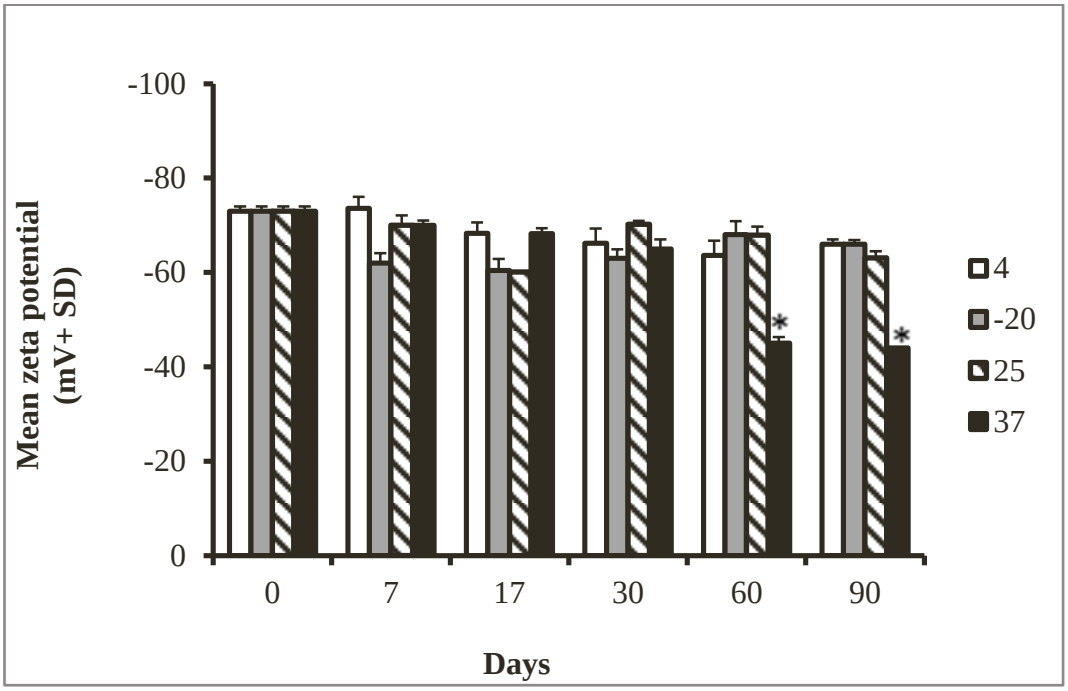

Figure 8.3 The zeta potential of Gem NIV stored at 4°, -20° (lyophilised Gem-NIV post hydration), 25° and 37°C determined over time at 0, 7, 17, 30,60 and 90 days post-preparation. $^{*}P < 0.05$ compared to the day zero value.

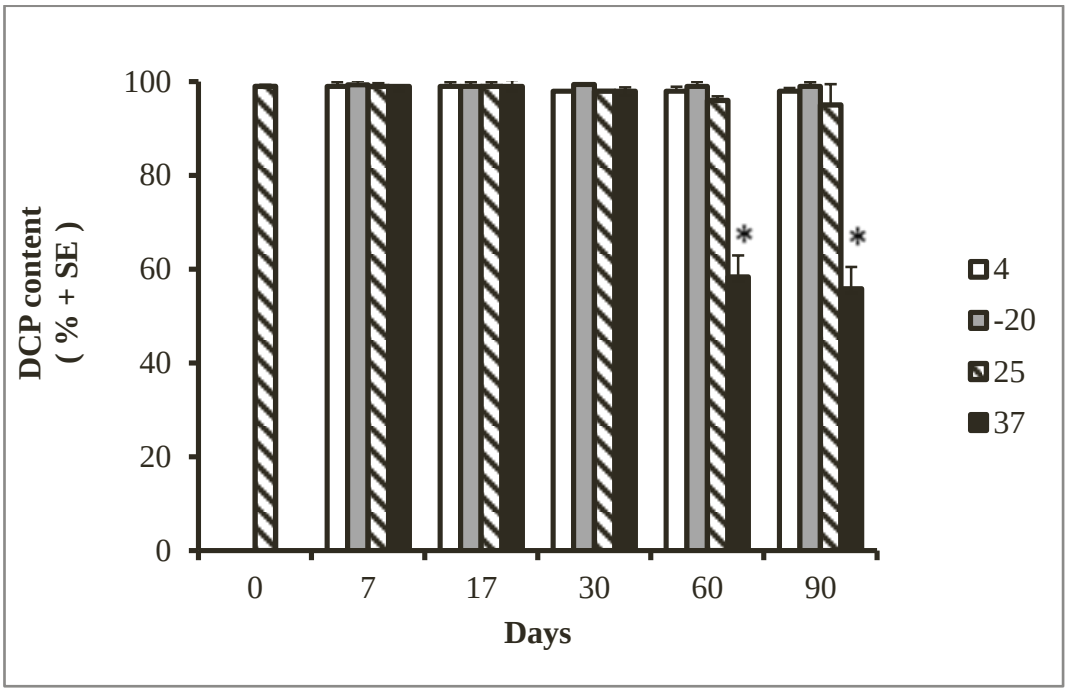

Figure 8.4 DCP content percentage stored at 4°, -20° (lyophilised post-hydration), 25° and 37°C determined over time at 0, 7, 17, 30, 60 and 90 days post-preparation. * $P < 0.05$ stored samples compared to the original sample.

However, the surfactant and cholesterol content of Gem-NIV did not significantly change over time.

The viscosity of Gem-NIV decreased with increased temperature and inversely increased with decreased temperature (Figure 8.5a). Lyophilisation after rehydration resulted in a change in the rheological behaviour of Gem-NIV, from pseudoplastic to Newtonian behaviour (Figure 8.5b).

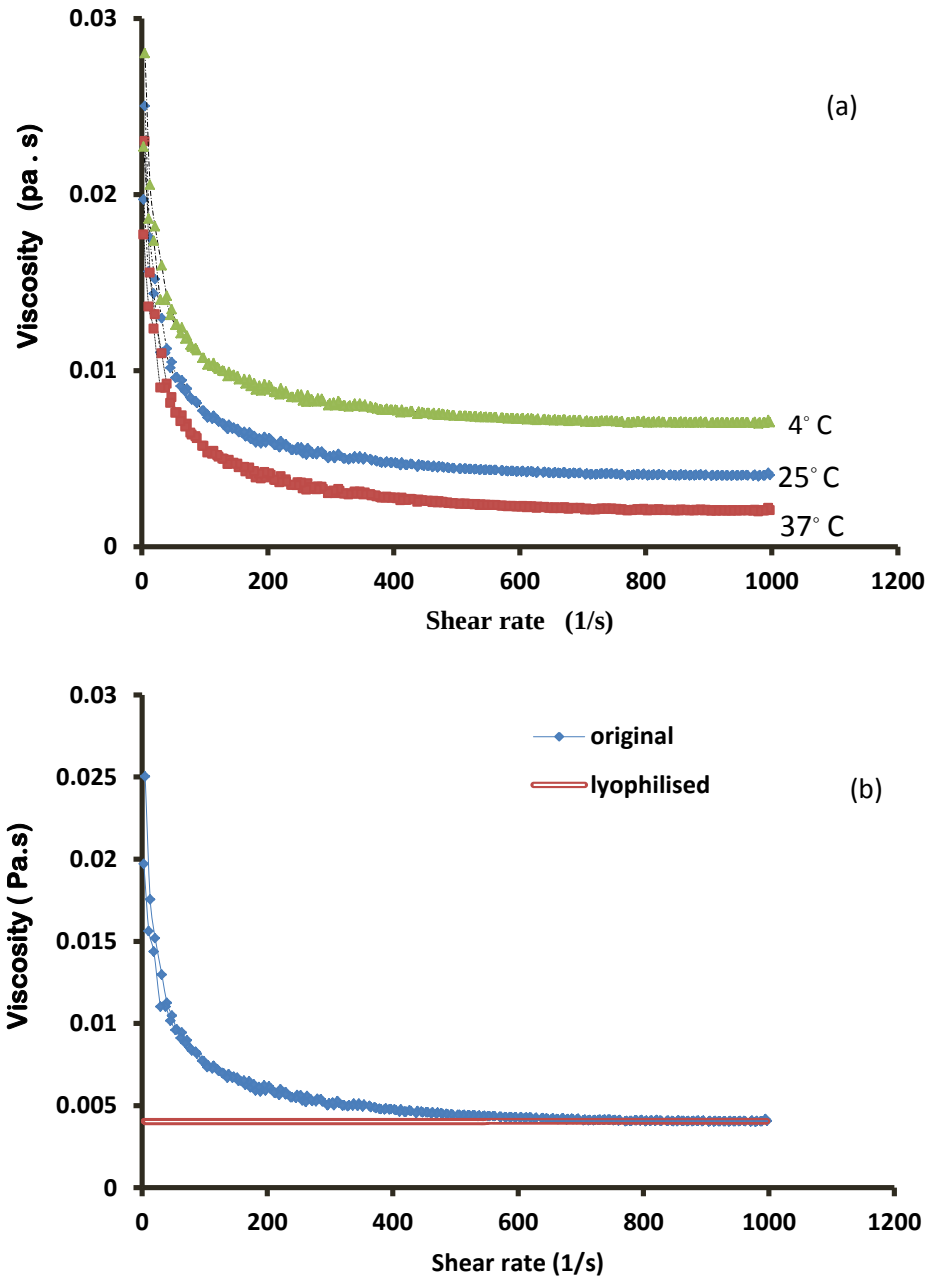

Figure 8.5 Effects of storage conditions on the viscosity of NIV for a period of 90 days, expressed as (a) temperatures (b) lyophilisation.

8.3 Discussion

The results from this study suggest that storage of Gem-NIV at 4 and 25°C was the best condition to maintain the chemical and physical stability of the formulation. Storage at 37ºC led to a significant reduction in Gem entrapment efficiency, vesicle size and DCP content at day 90. The reduction in DCP content was associated with a significant reduction in vesicle surface charge. The finding concerning entrapment efficiency was in agreement with a previous study on stability of cytarabine NIV prepared from cholesterol and Span 60, where the formulation was stored over a period of one month at the same temperatures used in our study. The percentage of entrapped cytarabine in NIV stored at 37°C was 36.2% which was lower than NIV stored at 4°C (90.4%) or at room temperature (68.1%). However, using Tween 20 instead of Span 20 in NIV preparation led to an increase in the percentage of entrapped cytarabine in NIV which had been stored at 37°C, to 59%. Therefore, the stability of the lipid used in preparation of NIV is an important factor in maintaining the percentage of drug retention in NIV. In particular, the significant decrease seen in the entrapment efficiency of Gem stored at high temperature, which was associated with increase in percentage of un-entrapped Gem, indicates that there is a leakage of Gem from NIV into surrounding medium due to increase bilayer permeability due to increase in the temperature (Ruckmani *et al*., 2000). A similar finding was observed when examining griseofulvin NIV consisting of a lipid mixture of surfactant, cholesterol, and DCP. Griseofulvin leakage and a decrease in the number of vesicles were detected at 25 ± 2°C whereas storage at 4 ± 1°C resulted in a minimum leakage of griseofulvin (Jadon *et al*., 2009).

The exposure of the NIV bilayer to the higher temperature of 37°C may lead to oxidation or hydrolysis of the charged lipid (DCP) present in the Gem-NIV formulation. Therefore, affected vesicles may aggregate/fuse due to drop in their zeta potential. The significant change in NIV size may indeed indicate that fusion occurred in NIV stored at 37°C by days 60 and 90 respectively. However, the particles were stable when Gem-NIV were stored at 4°C even after 90 days. This may be due to the decreased mobility and reduced permeability of the vesicle bilayer at lower temperatures (Balasubramaniam *et al.*, 2002). Fusion is an irreversible process because the original vesicle structure is fundamentally changed and forms a new colloidal structure. Fusion can be induced by many physical and chemical factors, including prolonged storage at a high temperature (Kreuter, 2010).

Previous studies have indicated that the most suitable storage temperature for colloidal lipid formulations is 4°C or 20°C, depending on the formulation characteristics (Heiati *et al.*, 1998; Pietzyk and Henschke, 2000). For example, a six month storage study showed that vesicle size of a liposomal system was more stable at 4°C compared to 25°C (Duplessis *et al.*, 1996) and griseofulvin NIV vesicle size was also more stable at 4°C compared to 25°C when stored for 30 days (Jadon *et al*., 2009). Daunorubicin NIV showed no change in its particle size distribution at 4°C whereas there was a moderate and wide change in size distribution at 25°C and 37°C, respectively (Balasubramaniam *et al*., 2002). Storage of Gem-NIV at 37°C was associated with a significant decrease in vesicle zeta potential which could affect the electrostatic charge repulsion that prevents vesicle aggregation (Freitas and Müller, 1998).

A non-ionic surfactant is less susceptible to oxidation than unsaturated phospholipids. Furthermore, cholesterol oxidation is highest in liposomes containing unsaturated phospholipids and lowest in NIV prepared with non-ionic surfactant and cholesterol (Sevanian, 1987). In this study the surfactant and cholesterol in Gem-NIV was stable at all temperatures over the course of the study.

The lyophilised Gem-NIV formulation was stable but a significant increase in vesicle size upon rehydration was observed, which is known to occur for other vesicular formulations. Freezing and rehydration during the lyophilisation process caused the formation of larger vesicles without a change in entrapment efficiency, probably due to the growth of ice crystals in between the head groups of NIV membranes during freezing and to the increasing size of NIV after rehydration with water (Chen *et al.*, 2010; Zhang *et al.*, 1997b). Aminoglycosides vesicles also had larger vesicles from 163.4 $\pm$ 38.4 to 259.8 $\pm$ 11.8 nm after the freezing-drying and hydration processes (Mugabe *et al.*, 2006). However, the addition of sucrose as a lyoprotectant can prevent an increase in size. For example, pirarubicin liposomes were significantly larger than those prepared with sucrose (1000 nm versus 400 nm) (Kawano, 2003).

There was a significant decrease in the percentage of un-entrapped Gem present in lyophilised Gem-NIV, which may be due to the formation of large crystals of free Gem which did not re-dissolve upon warming to room temperature. The formation of crystals was reported in another study, where the physical and chemical stability of Eli Lilly product Gemraz®, containing Gem hydrochloride, was evaluated over a period of 35 days. Gemraz® 200mg or 1 gm vials were used in the study and the

powdered product was reconstituted at a concentration of 38mg/ml in 0.9 % sodium chloride or sterile water. The reconstituted samples were stored at 4°C, 23°C and 32°C. HPLC studies showed that the samples stored at 23°C were chemically stable, clear and odourless for 35 days, whereas the samples stored at 32°C were only stable for 7 days. Refrigerated solutions had Gem losses of 20-35% due to the formation of large colourless crystals after 14 days of storage in vials, whereas packaging in plastic syringes prevented their formation (Xu, 1999).

In the present study, Gem-NIV showed shear thinning flow and lyophilized and rehydrated Gem-NIV showed Newtonian flow. Previous studies have shown that the flow features of vesicle formulations are dependent on their composition. For example, paroxetine liposomes, prepared using soya lecithin, cholesterol and drug at different weight ratios, exhibited shear thinning flow behaviour, where there was a decrease in viscosity when the shear rate was increased (Mohamed *et al.*, 2012). Meanwhile, rifampicin liposomes prepared using phosphatidylcholine, cholesterol and oleic acid showed Newtonian behaviour, where the viscosity is independent on shear stress and this is ideal for nebulisation (Manca *et al*., 2012).

Chapter 9: Conclusions

9.1 Summary of results

The developed HPLC analysis method was simple, sensitive and rapid, and offers economical Gem determination in plasma and tissues. The lipid analysis method used was also sensitive, simple, rapid and reliable in the quantification of the lipid content of NIV composed of cholesterol, surfactant VIII and DCP.

Gem entrapment efficiency was increased with increasing lipid concentration. However, NIV nebulisation efficiency decreased with increasing lipid concentration. No change in NIV sizes and ZP were caused after incorporation into the vesicle, except in the case of NIV prepared with low lipid concentration (30 mM). Lyophilisation caused an increase in NIV sizes due to the effect of rehydration after freeze drying, but the zeta potential did not change after lyophilisation.

MSLI studies allowed prediction of aerosolisation performance of Gem-NIV and solution. Although the size of the droplets resulting from aerosolisation of Gem solution could not be determined using a Zeta sizer, it was indirectly assessed by quantifying entrapment at each part of MSLI using HPLC analysis. According to this analysis, Gem-NIV passed to stages 1 and 2, whereas most of the Gem solution was lost in the MP of the MSLI. Vesicle size analysis showed that nebulisation resulted in size reduction during nebulisation and these smaller vesicles tended to deposit in the mouthpiece of MSLI. Nebulisation did not significantly affect the zeta potential of Gem-NIV. The lead formulation was identified to be Gem-NIV prepared using 60 mM lipid.

Localization of Gem in lungs can be obtained by using NIV formulated with 60 mM lipids. Increases in lipid concentration produced Gem-NIV with a higher vesicle size, zeta potential and entrapment efficiency. The well formulated Gem-NIV would target the lung and even if they distribute into blood circulation, they are rapidly cleared from the blood by macrophages and mainly distributed to the spleen, leading to a decrease in the side effects which result from the exposure of other tissues to Gem cytotoxicity.

Gem-NIV was more cytotoxic than Gem solution against B16 F0 Luc cells and the greatest cytotoxicity was obtained with Gem-NIV formulated using 60mM lipid. NIV should be prepared using DCP rather than SA because the later showed toxic effect against B16 F0 Luc cells when used in preparation of empty NIV.

The limitation in IVIS bioluminescence imaging instrument is that only small mice can be used. Therefore, the evaluation of Gem-NIV and Gem solution *activity in vivo* was limited on mice rather than rats. The result was that Gem-NIV treatment was more effective than Gem-solution using a murine model of lung cancer and the optimum NIV formulation was Gem-NIV (60mM lipid, 7 mg/ml Gem). The stability studies indicated that: storage at 25°C is the most suitable for Gem-NIV and Gem-NIV are stable for up to 90 days. Lyophilisation of Gem-NIV gives good flow properties that would be suitable for nebulisation. A lyoprotectant is required to control the vesicle size of the lyophilised Gem-NIV formulation on rehydration.

9.1. Future studies

Vesicle size and ZP measurements can be conducted in simulated lung fluid at 37 ºC to confirm the stability of NIV structure *in vivo.* Furthermore, there are a number of studies that can be carried out to try and improve the current lead Gem-NIV formulation to be more efficient. For example surface modifications to the Gem-NIV may increase the residence time of NIV in the lung and thus increase the efficacy of the formulation e.g. through the coating of NIV by mucoadhesive agents (e.g. chitosan).

A variety of nebulisers should be assessed to determine the most efficient and their potential to improve pulmonary delivery assessed *in vitro* (MSLI) or *in vivo* (mice and rats). Especially there is limitation in this study that the nebulisation to lungs of rats was conducted using the nose only where a chamber for whole body exposure was used in the nebulisation to the lungs of mice.

The distribution and metabolism of Gem-NIV can be monitored directly using positron emission tomography (PET), which provides three dimensional images generated by loading NIV with radiolabeled traces inhaled in non-pharmacological doses. These traces are natural biochemical labelled with the radionuclides of carbon, nitrogen, oxygen and fluorine. Thus, more information about Gem-NIV distribution through *in vivo* can be obtained.

The cellular uptake of Gem-NIV and free Gem can be studied by using fluorescence microscopy (Oh *et al.,* 1995). B16 F0 luciferase cells can be seeded on glass

coverslips and incubated with free Gem or Gem-NIV for 24 hours. After incubation the live cells, Gem can be detected by fluorescence microscope using suitable band pass excitation filter.

Sonication can be tried instead of homogenization to get irreversible and smaller NIV (less than 250 nm) to investigate the effect of vesicle size on the in vitro uptake by B16 F0 Luc. In particular, probe sonication which is described by Sezgin-Bayindir and Yuksel (2012) as following: NIV were placed in an ice-water bath to prevent overheating, and sonication was applied by a probe sonicator for 0, 5, 10, 20, 30, and 60 min. Sonicated NIV can be coded as N1, N2, N3, N4, N5, and N6, respectively. The size measurements should be repeated after 24 hours to confirm the irreversibility of the size reduction process.

Before clinical studies on human, evaluations of Gem-NIV should be prepared on a large scale and the chemical and physical stability assessed over a longer-term stability study. This study could prepare 'ready to use Gem-NIV' and lyophilised formulation and the effect of addition of lyoprotectants such as sucrose on vesicle size and drug entrapment can be determined. The long-term stability for lipid based vesicles can vary between 12 (Lasic, 1998) and 18-24 months (Watwe and Bellare, 1995), ideally a NIV formulation which meets or exceeds this shelf life is required. To make a commercial product, four to five ml of the Gem NIV containing Gem 1000 mg is optimally used and normal saline can be added if the fill volume is lower. In addition, the choice of device is important because not all devices are suitable for anticancer drugs. For example, physicians may not select PMDI or DPI inhalers for patients who have problems with their coordination or memory and single dose

which given in the hospital using nebuliser is recommended and it may be the most appropriate choice. A mouthpiece should be used to improve lung deposition and avoid eye injury, and aerosolised anticancer drugs should be delivered in a well-ventilated room with an effective air filtering system (Gagnadoux *et al.,* 2008; Wittgen *et al.,* 2006).

9.3 Concluding Remarks

The main achievements of this project are that NIV provide a novel carrier for Gem when administered by the pulmonary route, particularly with regard to high delivery of drug into the lungs and the avoidance of systemic exposure to Gem. Consequently, the vital organs such as the heart and kidney are protected from the adverse side effects of this cytotoxic drug. Furthermore, improvements of Gem-NIV were achieved with respect to their physicochemical properties, including surface charge, lipid concentration and particle size in order to target cancer cells. Concerning the stability of the formulations, Gem-NIV were stable in terms of particle size, zeta potential, drug and lipid content and rheological properties. Taken together, this data provides encouragement for this technology to proceed to clinical trial.

References

Abbruzzese, J.L., Grunewald, R., Weeks, E.A., Gravel, D., Adams, T., Nowak, B., Mineishi, S., Tarassoff, P., Satterlee, W., Raber, M.N., 1991. A phase I clinical, plasma, and cellular pharmacology study of gemcitabine. Journal of Clinical Oncology, 9, 491-498.

Abra, R.M., Hunt, C.A., 1981. Liposome disposition in vivo. III. Dose and vesicle-size effects. Biochimica et Biophysica Acta, 666, 493-503.

Achiwa, H., Oguri, T., Sato , S., Maeda , H., Niimi, T., Ueda, R., 2004, Determinants of sensitivity and resistance to gemcitabine: the roles of human equilibrative nucleoside transporter 1 and deoxycytidine kinase in non-small cell lung cancer. Cancer Science ,95, 753-757.

Ahmad, K.R., Kumar, A., Sadouki, F., Lorenz, C., Forbes, B., Dailey, L., Collins, H., 2012. The delivered dose: Applying particokinetics to in vitro investigations of nanoparticle internalization by macrophages. Journal of Controlled Release, 162, 259-266.

Agarwal, S., Udupa, Guruprasad, Uma Devi, 2001. Niosomal daunorubicin with reduced toxicity and improved anticancer activity in swiss mice bearing fibro sarcoma. Indian Drugs, 38, 21-26.

Ahuja, S. 2007. Overview of HPLC method development for pharmaceuticals, In: Satinder, A., Henrik, R. (Eds.) Separation Science and Technology. Academic Press, 1-11.

Ajithkumar, T., Parkinson, C., Shamshad, F., Murray, P., 2007. Ifosfamide Encephalopathy. Clinical Oncology, 19, 108-114.

Al-Hallak, M.H., Sarfraz, M.K., Azarmi, S., Roa, W.H., Finlay, W.H., Rouleau, C., Lobenberg, R., 2012. Distribution of effervescent inhalable nanoparticles after pulmonary delivery: an *in vivo* study. Ther. Deliv. 3, 725-734.

Alici-Evcimen, Y., Breitbart, W.S., 2007. Ifosfamide neuropsychiatric toxicity in patients with cancer. Psycho-Oncology 16, 956-960.

Allen, T.M., Chonn, A., 1987. Large unilamellar liposomes with low uptake into the reticuloendothelial system. FEBS Letters FEBS Letters 223, 42-46.

Allen, T.M., Cullis, P.R., 2004. Drug Delivery Systems: entering the mainstream. science (New York, N.Y.), 303, 1818-1822.

Allen, T.M., Everest, J.M., 1983. Effect of liposome size and drug release properties on pharmacokinetics of encapsulated drug in rats. The Journal of Pharmacology and Experimental Therapeutics, 226, 539-544.

Allen, T.M., Martin, F.J., 2004. Advantages of liposomal delivery systems for anthracyclines. Seminars in Oncology, Supplement, 13, 5-15.

Allen, T.M., Murray, L., MacKeigan, S., Shah, M., 1984. Chronic liposome administration in mice: effects on reticuloendothelial function and tissue distribution. The Journal of Pharmacology and Experimental Therapeutics, 229, 267-275.

Allen, T. M., Austin, G. A., Chonn, A., Lin, L., Lee, K. C., 1991, Uptake of liposomes by cultured mouse bone marrow macrophages: influence of liposome composition and size. Biochimica et Biophysica Acta (BBA) - Biomembranes, 1061, 56-64.

Allen, T. M., Williamson, P., Schlegel, R. A., 1988, Phosphatidylserine as a determinant of reticuloendothelial recognition of liposome models of the erythrocyte surface. Proceedings of the National Academy of Sciences 85, 8067-8071.

Ahlin,P., Kristl,J. and Smid-Kobar, J., 1998, Optimization of procedure parameters and physical stability of solid lipid nanoparticles in dispersions. Acta Pharmaceutica 48no, 259-267.

Anoopkumar-Dukie, S., Carey, J.B., Conere, T., O'Sullivan, E., van Pelt, F.N., Allshire, A., 2005. Resazurin assay of radiation response in cultured cells. The British Journal of Radiology, 78, 945-947.

Arriagada, R., Bergman, B., Dunant, A., Le Chevalier, T., Pignon, J.P., Vansteenkiste, J., International Adjuvant Lung Cancer Trial Collaborative, G., 2004. Cisplatin-based adjuvant chemotherapy in patients with completely resected non-small-cell lung cancer. The New England Journal of Medicine, 350, 351-360.

Arriagada, R., Dunant, A., Pignon, J.P., Bergman, B., Chabowski, M., Grunenwald, D., Kozlowski, M., Le Pechoux, C., Pirker, R., Pinel, M.I.S., Tarayre, M., Le Chevalier, T., 2010. Long-term results of the international adjuvant lung cancer trial evaluating adjuvant cisplatin-based chemotherapy in resected lung cancer. J. Clin. Oncol. Journal of Clinical Oncology, 28, 35-42.

Aulton, M.E., 2007. Pharmaceutics : The design and manufacture of medicines. Churchill Livingstone Elsevier, Hungary,650-666.

Baban, D.F.S.L.W., 1998. Control of tumour vascular permeability. Advanced Drug Delivery Reviews Advanced Drug Delivery Reviews, 34, 109-119.

Baillie, A.J., Florence, A.T., Hume, I.R., Murihead, G.T. and Rogerson, A.,1985. The preparation and properties of niosomes-Nonionic surfactant vesicles, J. Pharm. Pharmacol., 37, 863-868.

Balasubramaniam, A., Kumar, V.A., Pillai, K.S., 2002. Formulation and *in vivo* evaluation of niosome-encapsulated daunorubicin hydrochloride. Drug Development and Industrial Pharmacy, 28, 1181-1193.

Ballou, B., Ernst , L.A., Waggoner , A.S., 2005. Fluorescence imaging of tumors *in vivo*. Current Medicinal Chemistry, 12, 795-805.

Bartlett, G.R., 1959. Phosphorus assay in column chromatography. The Journal of Biological Chemistry, 234, 466-468.

Bartsch, H., Hietanen, E., 1996. The role of individual susceptibility in cancer burden related to environmental exposure. Environmental Health Perspectives ,104, 569-577.

Bapiro, T.E., Richards, F.M., Goldgraben, M.A., Olive, K.P., Madhu, B., Frese, K.K., Cook, N., Jacobetz, M.A., Smith, D.-M., Tuveson, D.A., Griffiths, J.R., Jodrell, D.I., 2011, A novel method for quantification of gemcitabine and its metabolites 2,2-difluorodeoxyuridine and gemcitabine triphosphate in tumour tissue by LCMS/MS: comparison with 19F NMR spectroscopy. Pharmacol Cancer Chemotherapy and Pharmacology, 68, 1243-1253.

Bharali, D.J., Khalil , M., Gurbuz , M., Simone , T.M., Mousa , S.A., 2009. Nanoparticles and cancer therapy: A concise review with emphasis on dendrimers. Int. J. Nanomed. International Journal of Nanomedicine, 4, 1-7.

Bragagni, M., Mennini, N., Mura , P., Ghelardini , C., 2012. Development and characterization of niosomal formulations of doxorubicin aimed at brain targeting. J. Pharm. Pharm. Sci. Journal of Pharmacy and Pharmaceutical Sciences, 15, 184-196.

Bergh, M., Shao, L.P., Hagelthorn, G., Gäfvert, E., Nilsson, J.L., Karlberg, A.T., 1998. Contact allergens from surfactants. Atmospheric oxidation of polyoxyethylene alcohols, formation of ethoxylated aldehydes, and their allergenic activity. Journal of Pharmaceutical Sciences, 87, 276-282.

Beumer, J.H., Eiseman, J.L., Parise, R.A., Joseph, E., Covey, J.M., Egorin, M.J., 2008. Modulation of gemcitabine (2',2'-difluoro-2'-deoxycytidine) pharmacokinetics, metabolism, and bioavailability in mice by 3,4,5,6-tetrahydrouridine. American Association for Cancer Research, 14, 3529-3535.

Birnbaum, D., Brannon-Peppas, L. 2004. Microparticle Drug Delivery Systems, In: Brown, D. (Ed.) Drug Delivery Systems in Cancer Therapy. Humana Press, 117-135.

Bilensoy, E., Gürkaynak, O., Ertan , M., Sen , M., Hincal , A.A., 2008. Development of nonsurfactant cyclodextrin nanoparticles loaded with anticancer drug paclitaxel. Journal of Pharmaceutical Sciences 97, 1519-1529.

Boe, J., Dennis, J.H., O'Driscoll, B.R., Bauer, T.T., Carone, M., Dautzenberg, B., Diot, P., Heslop, K., Lannefors, L., European Respiratory Society Task Force on the use of, n., 2001. European Respiratory Society Guidelines on the use of nebulizers. The European respiratory journal 18, 228-242.

Borra, R.c., Lotufo, M.A., Gagioti , S.M., Barros , F.M., Andrade, P.M., 2009, A simple method to measure cell viability in proliferation and cytotoxicity assays. Brazilian Oral Research, 23, 255-62

Bouffard, D.Y., Laliberté, J., Momparler, R.L., 1993. Kinetic studies on 2',2'-difluorodeoxycytidine (Gemcitabine) with purified human deoxycytidine kinase and cytidine deaminase. Biochemical Pharmacology,45, 1857-1861.

Bridges, Paul, A., Taylor, Kevin, M.G., 2000. An investigation of some of the factors influencing the jet nebulisation of liposomes. International Journal of Pharmaceutics,204, 69-79.

Brown, R.A., Jr., Schanker, L.S., 1983. Absorption of aerosolized drugs from the rat lung. Drug mMetabolism and Disposition,11,355-60.

Black , P.C., Shetty , A., Brown , G.A., Esparza-Coss, E., Metwalli , A.R., Agarwal, P.K., McConkey, D.J., Hazle , J.D., P., D.C., 2010. Validating bladder cancer xenograft bioluminescence with magnetic resonance imaging: the significance of hypoxia and necrosis. BJU International 106, 1799-1804.

Buja, L.M., Ferrans, V.J., Mayer, R.J., Roberts, W.C., Henderson, E.S., 1973. Cardiac ultrastructural changes induced by daunorubicin therapy. Cancer 32, 771-788.

Buszewski, B., Noga, S., 2012. Hydrophilic interaction liquid chromatography (HILIC)--a powerful separation technique. Analytical and Bioanalytical chemistry 402, 231-247.

Calvagno, M.G., Celia, C., Paolino, D., Cosco, D., Iannone, M., Castelli, F., Doldo, P., Frest, M., 2007. Effects of lipid composition and preparation conditions on physical-chemical properties, technological parameters and in vitro biological activity of gemcitabine-loaded liposomes. Current Drug Delivery, 4, 89-101.

Carozzi, V.A., Marmiroli, P., Cavaletti, G., 2010. The role of oxidative stress and anti-oxidant treatment in platinum-induced peripheral neurotoxicity. Current Cancer Drug Targets, 10, 670-682.

Chan, Y.H., Chen, B.H., Chiu, C.P., Lu, Y.-F., 2004. The influence of phytosterols on the encapsulation efficiency of cholesterol liposomes. Int J Food Sci Tech International Journal of Food Science and Technology, 39, 985-995.

Chang, M.Y., Mentzer, S.J., Colson, Y.L., Linden, P.A., Jaklitsch, M.T., Lipsitz, S.R., Sugarbaker, D.J., 2007. Factors predicting poor survival after resection of stage IA non–small cell lung cancer. The Journal of Thoracic and Cardiovascular Surgery, 134, 850-856.

Chang , D.K. ,Lin ,C.T, Wu, C.H.,Wu , H.C.,2009. A novel peptide enhances efficacy of liposomal –anticancer drugs in mice models of human lung cancer.PLoS One ,4 ,1,4171.

Chen, C., Han, D., Zhang, Y., Yuan, Y., Tang, X., 2010. The freeze-thawed and freeze-dried stability of cytarabine-encapsulated multivesicular liposomes. International Journal of Pharmaceutics, 387, 147-153.

Chen, C., Han, D., Cai, C., Tang, X., 2010. An overview of liposome lyophilization and its future potential. Journal of Controlled Release ,142, 299-311.

Chen , L., Sha , X., Jiang, X., Chen , Y., Ren , Q., Fang, X., 2012. Pluronic P105/F127 mixed micelles for the delivery of docetaxel against Taxol-resistant non-small cell lung cancer: Optimization and in vitro, *in vivo* evaluation. Int. J. Nanomed. International Journal of Nanomedicine, 8, 73-84.

Chen,W.,Meng,F.,Cheng,R.,Zhong,Z., 2009.PH-sensetive degradable polymersomes for triggered release of anticancer drugs.Journal of Controlled Release,3,1-13.

Cheng, M., Han, J., Li, Q., He, B., Zha, B., Wu, J., Zhou, R., Ye, T., Wang, W., Xu, H., Hou, Y., 2012. Synthesis of galactosylated chitosan/5-fluorouracil nanoparticles and its characteristics, in vitro and *in vivo* release studies. Journal of Biomedical Materials Research. Part B, Applied Biomaterials, 100, 2035-2043.

Chimote, G., Banerjee , R., 2010. In vitro evaluation of inhalable isoniazid-loaded surfactant liposomes as an adjunct therapy in pulmonary tuberculosis. Journal of Biomedical Materials Research. Part B, Applied Biomaterials, 94, 1-10.

Chimote, G., Banerjee, R., 2009, Evaluation of antitubercular drug-loaded surfactants as inhalable drug-delivery systems for pulmonary tuberculosis. Journal of Biomedical Materials Research. Part A, 89, 281-292.

Chougule, M.B., Padhi, B.K., Jinturkar, K.A., Misra, A., 2007. Development of dry powder inhalers. Recent patents on drug delivery & formulation, 1, 11-21.

Chrai,S.S., Murari, R., Ahmad,I., 2001. Liposomes (a Review), Part One: Manufacturing Issues. Biopharm -Eugene, 14, 10-27.

Chono , S., Tanino, T., Seki , T., Morimoto, K., 2006. Influence of particle size on drug delivery to rat alveolar macrophages following pulmonary administration of ciprofloxacin incorporated into liposomes. Journal of Drug Targeting, 14, 557-566.

Chono, S., Tanino , T., Seki, T., Morimoto , K., 2008. Efficient drug targeting to rat alveolar macrophages by pulmonary administration of ciprofloxacin incorporated into mannosylated liposomes for treatment of respiratory intracellular parasitic infections. Journal of Controlled Release,127, 50-58.

Chrystyn, H., 2000. Methods to determine lung distribution of inhaled drugs - could gamma scintigraphy be the gold standard. British Journal of Clinical Pharmacology 49, 525-528.

Celia, C, Calvagno, M.G, Paolino, D., Bulotta, S, Ventura, C.A, Russo, D., Fresta ,M. ,2008. Improved in vitro anti-tumoral activity, intracellular uptake and apoptotic induction of gemcitabine-loaded pegylated unilamellar liposomes. J Nanosci Nanotechnol ,8,2102–2113.

Croy, B. Anne, S., James, P., Manz, M., Bankert, R. B., 2007, Chapter 13 - Mouse Models of Immunodeficiency, In: James, G., Fox, M., T., Davisson, Fred, W., Quimby, S. W., Barthold, C. E. Newcomer, Abigail, L.,Smith,A. The Mouse in Biomedical Research (Second Edition). Academic Press, Burlington, 275-289.

Colin, M., Moritz, S., Schneider, H., Capeau, J., Coutelle, C., Brahimi-Horn, M.C., 2000. Haemoglobin interferes with the ex vivo luciferase luminescence assay: consequence for detection of luciferase reporter gene expression in vivo. Gene Therapy 7, 1333-1336.

Colombo, P., Traini, D., Buttini, F., 2013. Inhalation Drug Delivery : techniques and products. Wiley-Blackwell, Chichester, West Sussex; Hoboken, NJ.,Chapter 6.

Colthorpe, P., Farr, S.J., Smith, I.J., Wyatt, D., 1995. The Influence of Regional Deposition on the Pharmacokinetics of Pulmonary-Delivered Human Growth Hormone in Rabbits. Pharm. Res., 12, 356.

Colthorpe, P., Farr, S.J., Taylor, G., Smith, I.J., Wyatt, D., 1992. The pharmacokinetics of pulmonary-delivered insulin: a comparison of intratracheal and aerosol administration to the rabbit. Pharm. Res., 9, 764-768.

Conhaim, R.L., Eaton, A., Staub, N.C., Heath, T.D., 1988. Equivalent pore estimate for the alveolar-airway barrier in isolated dog lung. Journal of Applied Physiology , 64, 1134-1142.

Contag, C.H., Spilman, S.D., Contag, P.R., Oshiro, M., Eames, B., Dennery, P., Stevenson, D.K., Benaron, D.A., 1997. Visualizing gene expression in living mammals using a bioluminescent reporter. Photochemistry and Photobiology, 66, 523-531.

Cortesi, R., Esposito, E., Corradini, F., Sivieri, E., Drechsler, M., Rossi, A., Scatturin, A., Menegatti, E., 2007. Non-phospholipid vesicles as carriers for peptides and proteins: Production, characterization and stability studies. International Journal of Pharmaceutics 339, 52-60.

Cosco, D., Bulotta, A., Ventura, M., Celia, C., Calimeri, T., Perri, G., Paolino, D., Costa, N., Neri, P., Tagliaferri, P., Tassone, P., Fresta, M., 2009. *In vivo* activity of gemcitabine-loaded PEGylated small unilamellar liposomes against pancreatic cancer. Cancer Chemotherapy and Pharmacology 64, 1009-1020.

Cosco, D., Federico, D., Morittu, D., Britti, D., Trapasso, D., 2012. Gemcitabine-loaded liposomes: rationale, potentialities and future perspectives. IJN International Journal of Nanomedicine, 7, 5423-36

Cosco , D., Paolino , D., Muzzalupo , R., Celia , C., Citraro, R., D., C., Picci , N., Fresta , M., 2009. Novel PEG-coated niosomes based on bola-surfactant as drug carriers for 5-fluorouracil. Biomedical Microdevices,11, 1115-1125.

Cui, Z.y., Ahn , J.S., Lee, J.Y., Kim , W.S., Lim , H.Y., Jeon, H.J., Suh , S.W., Kim , J.H., Kong , W.H., Kang, J.M., Nam do, H., Park , K., 2006. Mouse orthotopic lung cancer model induced by PC14PE6. Cancer Research and Treatment ,38, 234-239.

Davis, S.S., 1978. Physico-chemical studies on aerosol solutions for drug delivery I. Water-propylene glycol systems. International Journal of Pharmaceutics,1, 71-83.

Decosterd, L.A., Cottin , E., Chen , X., Lejeune, F., Mirimanoff , R.O., Biollaz , J., Coucke, P.A., 1999, Simultaneous Determination of Deoxyribonucleoside in the Presence of Ribonucleoside Triphosphates in Human Carcinoma Cells by High-Performance Liquid Chromatography. Analytical Biochemistry Analytical Biochemistry, 270, 59-68.

Dong, M.W., 2006. Modern HPLC for practicing scientists. Wiley-Interscience, Hoboken, Study of the pilot production process of long-circulating and pH-sensitive liposomes containing cisplatin. Journal of Liposome Research, 21, 60-69.

Dong, M.W., Passalacqua, P.V., Choudhury, D.R., 1990, Liquid Chromatographic Considerations for High Sensitivity Impurity and Stability Testing of Pharmaceuticals. Journal of Liquid Chromatography , 13, 2135-2160.

Dothager, R.S., Flentie, K., Moss, B., Pan, M.H., Kesarwala, A., Piwnica-Worms, D., 2009. Advances in bioluminescence imaging of live animal models. Current Opinion in Biotechnology, 20, 45-53.

Dougherty ,S., Mazhawidza ,W. ,Bohn ,A. R. ,Robinson, K. A., Mattingly, K. A. Blankenship, K. A., Huff ,M. O., Mcgregor, W. G., Klinge, C. M., 2006, Gender difference in the activity but not expression of estrogen receptors alpha and beta in human lung adenocarcinoma cells. Endocrine-Related Cancer ,13, 113-134.

Douillard, J.Y., Rosell, R., De Lena, M., Carpagnano, F., Ramlau, R., Gonzales-Larriba, J.L., Grodzki, T., Pereira, J.R., Le Groumellec, A., Lorusso, V., Clary, C., Torres, A.J., Dahabreh, J., Souquet, P.J., Astudillo, J., Fournel, P., Artal-Cortes, A., Jassem, J., Koubkova, L., His, P., Riggi, M., Hurteloup, P., 2006. Adjuvant vinorelbine plus cisplatin versus observation in patients with completely resected stage IB-IIIA non-small-cell lung cancer (Adjuvant Navelbine International Trialist Association [ANITA]): a randomised controlled trial. Lancet Oncology, 7, 719-727.

Drummond, D., Kirpotin, D., Benz, C., Park, J., Hong, K. 2004. Liposomal Drug Delivery Systems for Cancer Therapy, In: Brown, D. (Ed.) Drug Delivery Systems in Cancer Therapy. Humana Press, 191-213.

Duplessis, J., Ramachandran, C., Weiner, N., Muller, D., 1996. The influence of lipid composition and lamellarity of liposomes on the physical stability of liposomes upon storage. International Journal of Pharmaceutics ,127, 273-278.

Edinger, M., Sweeney, T.J., Tucker, A.A., Olomu, A.B., Negrin, R.S., Contag, C.H., 1999. Noninvasive assessment of tumor cell proliferation in animal models. Neoplasia , 1, 303-310.

Edinger, M., Cao, Y., Hornig , Y.S., Jenkins , D.E., Verneris, M.R., Bachmann, M.H., Negrin , R.S., Contag , C.H., 2002. Advancing animal models of neoplasia through *in vivo* bioluminescence imaging. European Journal of Cancer European Journal of Cancer, 38, 2128-2136.

Edwards, K.A., Baeumner, A.J., 2006, Analysis of liposomes. Talanta ,68, 1432-1441.

Ehtezazi, T., Saleem, I., Shrubb, I., Allanson, D.R., Jenkinson, I.D., O'Callaghan, C., 2010. The Interaction Between the Oropharyngeal Geometry and Aerosols via Pressurised Metered Dose Inhalers. Pharm. Res., 27, 175-186.

El-Araud, K.A., Clark, B.J., Kaahwa, C., Anum, P., Chrystyn, H., 1998. The effect of dose on the characterization of aerodynamic particle-size distributions of

beclomethasone dipropionate metered-dose inhalers. The Journal of Pharmacy and Pharmacology, 50, 1081-1085.

Essa, E., 2010. Effect of formulation and processing variables on the particle size of sorbitan monopalmitate niosomes. Asian Journal of Pharmaceutics, ,4, 227-233.

Elstad, N.L., Fowers, K.D., 2009. OncoGel (ReGel/paclitaxel) — Clinical applications for a novel paclitaxel delivery system. Advanced Drug Delivery Reviews, 61, 785-794.

Fang, J., Hong , C.T., Chiu , W.T., Wang , Y.Y., 2001. Effect of liposomes and niosomes on skin permeation of enoxacin. International Journal of Pharmaceutics ,219, 1-2.

Fatouros,D.g., Antimisiaris, S.G., 2002. Effect of amphiphilic drugs on the stability and zeta-potential of their liposome formulations: a study with prednisolone, diazepam, and griseofulvin. Journal of Colloid and Interface Science, 251, 271-277.

Fauvel, M., Farrugia, C., Tsapis , N., Gueutin , C., Cabaret , O., Bories , C., Bretagne , S., Barratt , G., 2012. Aerosolized liposomal amphotericin B: Prediction of lung deposition, in vitro uptake and cytotoxicity. International Journal of Pharmaceutics ,436, 106-110.

Flieder, D.B., 2005. Tumor Size Is a Determinant of Stage Distribution in T1 Non-Small Cell Lung Cancer. Chest Journal, 128, 2304.

Forbes, B., Asgharian, B., Dailey, L.A., Ferguson, D., Gerde, P., Gumbleton, M., Gustavsson, L., Hardy, C., Hassall, D., Jones, R., Lock, R., Maas, J., McGovern, T., Pitcairn, G.R., Somers, G., Wolff, R.K., 2011. Challenges in inhaled product development and opportunities for open innovation. Advanced Drug Delivery Reviews, 63, 69-87.

Forbes, B., 2000, Human airway epithelial cell lines for in vitro drug transport and metabolism studies. Pharmaceutical Science & Technology Today, 3, 18-27.

Foster, K. A., Yazdanian, M., Audus, K. L., 2001, Microparticulate uptake mechanisms of in-vitro cell culture models of the respiratory epithelium. Journal of Pharmacy and Pharmacology, 53, 57-66.

Fossella, F., Pereira, J.R., von Pawel, J., Pluzanska, A., Gorbounova, V., Kaukel, E., Mattson, K.V., Ramlau, R., Szczesna, A., Fidias, P., Millward, M., Belani, C.P., 2003. Randomized, multinational, phase III study of docetaxel plus platinum combinations versus vinorelbine plus cisplatin for advanced non-small-cell lung cancer: the TAX 326 study group. Journal of Clinical Oncology, 21, 3016-3024.

Freeman, K.B., Anliker, S., Hamilton, M., Osborne, D., Dhahir, P.H., Nelson, R., Allerheiligen, S.R., 1995. Validated assays for the determination of gemcitabine in human plasma and urine using high-performance liquid chromatography with ultraviolet detection. Journal of Chromatography. B, Biomedical applications, 665, 171-181.

Friedl, P., Alexander, S., 2011. Cancer invasion and the microenvironment: plasticity and reciprocity. Cell, 147, 992-1009.

Freitas, C., Müller, R.H., 1998, Effect of light and temperature on zeta potential and physical stability in solid lipid nanoparticle (SLN) dispersions. International Journal of Pharmaceutics International Journal of Pharmaceutics ,168, 221-229.

Gabizon, A., Papahadjopoulos, D., 1988. Liposome formulations with prolonged circulation time in blood and enhanced uptake by tumors. Proceedings of the National Academy of Sciences of the United States of America, 85, 6949-6953.

Gabizon, A.A., Shmeeda, H., Zalipsky, S., 2006. Pros and Cons of the Liposome Platform in Cancer Drug Targeting. Journal of Liposome Research, 16, 175-183.

Gagnadoux, F., Hureaux, J., Vecellio, L., Urban, T., Le Pape, A., Valo, I., Montharu, J., Leblond, V., Boisdron-Celle, M., Lerondel, S., Majoral, C., Diot, P., Racineux, J.L., Lemarie, E., 2008. Aerosolized chemotherapy. Journal of Aerosol Medicine and Pulmonary Drug Delivery, 21, 61-70.

Garbuzenko, O., Barenholz, Y., Priev, A., 2005. Effect of grafted PEG on liposome size and on compressibility and packing of lipid bilayer. Chem. Phys. Lipids, 135, 117-129.

Garbuzenko, O.B., Saad, M., Pozharov, V.P., Minko, T., Reuhl, K.R., Mainelis, G., 2010. Inhibition of lung tumor growth by complex pulmonary delivery of drugs with oligonucleotides as suppressors of cellular resistance. Proc. Natl. Acad. Sci. U. S. A. Proceedings of the National Academy of Sciences of the United States of America, 107, 10737-10742.

Gatzemeier, U., Shepherd, F.A., Le Chevalier, T., Weynants, P., Cottier, B., Groen, H.J., Rosso, R., Mattson, K., Cortes-Funes, H., Tonato, M., Burkes, R.L., Gottfried, M., Voi, M., 1996. Activity of gemcitabine in patients with non-small cell lung cancer: a multicentre, extended phase II study. European Journal of Cancer (Oxford, England : 1990), 32, 243-248.

Glinskii Ab, Smith B. A. Jiang P. Li X. M. Yang M. Hoffman R. M. Glinsky G. V., 2003, Viable circulating metastatic cells produced in orthotopic but not ectopic prostate cancer models. Cancer Research, 63, 4239-4243.

Gheorgheosu, D., Dehelean, C., Muntean, D., Cristea, M., 2011, Development of the B16 murine melanoma model. Ann. Rom. Soc. Cell Biol. Annals of the Romanian Society for Cell Biology, 16, 148-152

Goerner M, S.T.Y.S.H., 2010. Molecular targeted therapies in head and neck cancer--an update of recent developments. Head & Neck Oncology 2.

Goje, A., Doijad, R.C., Sompur, C.K., 2011. Design and characterization of long circulating lyophilized vesicular drug delivery system for antineoplastic agents. Intl. J. Pharma Bio Sci. International Journal of Pharma and Bio Sciences 2, 238-247.

Gude, R.P., Jadhav , M.G., Rao , S.G.A., Jagtap , A.G., 2002. Effects of Niosomal Cisplatin and Combination of the Same with Theophylline and with Activated Macrophages in Murine B16F10 Melanoma Model. Cancer Biotherapy & Radiopharmaceuticals, 17, 183-192.

Guo, C., Gillespie, S.R., Kauffman, J., Doub, W.H., 2008. Comparison of delivery characteristics from a combination metered-dose inhaler using the Andersen cascade impactor and the next generation pharmaceutical impactor. Journal of Pharmaceutical Sciences 97, 3321-3334.

Gordon, N., Kleinerman, E.S., 2010. Aerosol therapy for the treatment of osteosarcoma lung metastases: targeting the Fas/FasL pathway and rationale for the use of gemcitabine. Journal of Aerosol Medicine and Pulmonary Drug Delivery, 23, 189-196.

Gotfredsen, C.f., Van Berkel , T.J., Kruijt, J.K., Goethals , A., 1983, Cellular localization of stable solid liposomes in the liver of rats. Biochemical Pharmacology, 32, 3389-3396.

Graeser, R., Esser, N., Schaechtele, C., Bornmann, C., Hopt, U.T., Von Dobschuetz, E., Ziroli, V., Jantscheff, P., Unger, C., Massing, U., 2009. Antimetastatic effects of liposomal gemcitabine and empty liposomes in an orthotopic mouse model of pancreatic cancer. Pancreas Pancreas, 38, 330-337.

Grit, M., Crommelin, D.J., 1993. Chemical stability of liposomes: implications for their physical stability. Chemistry and Physics of lipids, 64, 1-3.

Groneberg, D.A., Witt, C., Wagner, U., Chung, K.F., Fischer, A., 2003. Fundamentals of pulmonary drug delivery. Respiratory Medicine, 97, 382-387.

Guchelaar, H.J., Richel, D.J., van Knapen, A., 1996. Clinical, toxicological and pharmacological aspects of gemcitabine. Cancer Treatment Reviews, 22, 15-31.

Gupta, P.K., Hickey, A.J., 1991. Contemporary approaches in aerosolized drug delivery to the lung. Journal of Controlled Release, 17, 127-147.

Guthi, J.S., Yang, S.G., Huang, G., Li, S., Khemtong, C., Kessinger, C.W., Peyton, M., Minna, J.D., Brown, K.C., Gao, J., 2010. MRI-visible micellar nanomedicine for targeted drug delivery to lung cancer cells. Mol. Pharm., 7, 32-40.

Hathout, Rania, Mansour, Samar, Mortada, Nahed, Guinedi, Ahmed, 2007, Liposomes as an ocular delivery system for acetazolamide: *In vitro* and *in vivo* studies. AAPS Pharm.Sci.Tech., 8, 1.

Hamada, A., Kawaguchi, T., Nakano, M., 2002. Clinical pharmacokinetics of cytarabine formulations. Clinical Pharmacokinetics, 41, 705-718.

Hamid, R., Rotshteyn, Y., Rabadi, L., Parikh, R., Bullock, P., 2004. Comparison of alamar blue and MTT assays for high through-put screening. Toxicology *in vitro*, 18, 703-710.

Hammond, E. W. 1993. High performance liquid chromatography. In E. W. Hammond (Ed.), Chromtography for The Analysis of Lipids , CRC Press, Inc., Florida, USA., 113-153.

Hammoud ,Z., Tan , B. , Badve, S., Bigsby, R. M., 2008, Estrogen promotes tumor progression in a genetically defined mouse model of lung adenocarcinoma. Endocrine-Related Cancer, 15, 475-483.

Harashima, H., Sakata, K., Kiwada, H., 1993. Distinction between the depletion of opsonins and the saturation of uptake in the dose-dependent hepatic uptake of liposomes. Pharm. Res., 10, 606-610.

Heiati, H., Tawashi, R., Phillips, N.C., 1998. Drug retention and stability of solid lipid nanoparticles containing azidothymidine palmitate after autoclaving, storage and lyophilization. Journal of Microencapsulation, 15,173-84.

Heinemann, V., Xu, Y.Z., Chubb, S., Sen, A., Hertel, L.W., Grindey, G.B., Plunkett, W., 1992. Cellular elimination of 2',2'-difluorodeoxycytidine 5'-triphosphate: a mechanism of self-potentiation. Cancer Research, 52, 533-539.

Hess, D.R., 2008. Aerosol delivery devices in the treatment of asthma. Respiratory Care, 53, 699-723.

Heurtault, B., Saulnier, P., Pech, B., Proust, J.E., Benoit, J.P., 2003. Physico-chemical stability of colloidal lipid particles. Biomaterials, 24, 4283-4300.

Hickey, A.J., 2003. Pharmaceutical inhalation aerosol technology, Marcel Dekker, Inc., New York.,81-142.

Hobbs, S. K., Monsky, W. L., Yuan, F., Roberts, W., G., Griffith, L., Torchilin, V.P., Jain, R. K., 1998. Regulation of transport pathways in tumor vessels: Role of tumor type and microenvironment. Proceedings of the National Academy of Sciences of the United States of America, 95, 4607.

Hong, M., Zhu, S., Jiang, Y., Tang, G., Pei, Y., 2009. Efficient tumor targeting of hydroxycamptothecin loaded PEGylated niosomes modified with transferrin. Journal of Controlled Release, 133, 96-102.

Hood, E., Gonzalez, M., Plaas, A., Strom, J., VanAuker, M., 2007. Immuno-targeting of nonionic surfactant vesicles to inflammation. International Journal of Pharmaceutics, 339, 222-230.

Hosny, K.M., Ciprofloxacin as ocular liposomal hydrogel. AAPS Pharm.Sci.Tech. , 11, 241-246.

Hoffman, R. M., 1999, Orthotopic metastatic mouse models for anticancer drug discovery and evaluation: a bridge to the clinic. Investigational New Drugs 17, 343-359.

Huang, P., Chubb, S., Hertel, L.W., Grindey, G.B., Plunkett, W., 1991. Action of 2',2'-difluorodeoxycytidine on DNA synthesis. Cancer Research, 51, 6110-6117.

Hureaux, J., Lagarce, F., Gagnadoux, F., Vecellio, L., Clavreul, A., Roger, E., Kempf, M., Racineux, J.-L., Diot, P., Benoit, J.-P., Urban, T., 2009. Lipid nanocapsules: Ready-to-use nanovectors for the aerosol delivery of paclitaxel. European Journal of Pharmaceutics and Biopharmaceutics, 73, 239-246.

Immordino, M.L., Brusa, P., Rocco, F., Arpicco, S., Ceruti, M., Cattel, L., 2004. Preparation, characterization, cytotoxicity and pharmacokinetics of liposomes containing lipophilic gemcitabine prodrugs. Journal of Controlled Release ,100, 331-346.

Islam, N., Rahman, S., 2008. Pulmonary drug delivery: Implication for new strategy for pharmacotherapy for neurodegenerative disorders. Drug Discoveries & Therapeutics, 2, 264-76

Jackson, E.l., Olive, K. P., Tuveson, D. A., Bronson ,R. ,Crowley, D., Brown, M. ,Jacks, T., 2005, The differential effects of mutant p53 alleles on advanced murine lung cancer. Cancer Research, 65, 10280-10288.

Jadon , P.S., Jadon , R.S., Gajbhiye, K.R., Ganesh , N., 2009. Enhanced Oral Bioavailability of Griseofulvin via Niosomes. AAPS Pharm.Sci.Tech.,10, 1186-1192.

Jain, R.K., 1994. Barriers to drug delivery in solid tumors. Scientific American, 271, 58-65.

Jain, R.K., 1996. Whitaker Lecture: delivery of molecules, particles, and cells to solid tumors. Annals of Biomedical Engineering, 24, 457-73

Jinturkar, K.A., Anish, C., Kumar, M.K., Bagchi, T., Panda, A.K., Misra, A.R., 2012. Liposomal formulations of Etoposide and Docetaxel for p53 mediated enhanced cytotoxicity in lung cancer cell lines. Biomaterials, 33, 2492-2507.

Jones A, H.A.L., 1998. New developments in angiogenesis: a major mechanism for tumor growth and target for therapy. The Cancer Journal from Scientific American, 4, 209-17.

Joshi, M., Misra, A.N., 2001. Pulmonary disposition of budesonide from liposomal dry powder inhaler. Methods and Findings in Experimental and Clinical Pharmacology, 23, 531-536.

Jurczok , A., Fornara, P., Söling, A., 2008. Bioluminescence imaging to monitor bladder cancer cell adhesion *in vivo*: a new approach to optimize a syngeneic, orthotopic, murine bladder cancer model. BJU International, 101, 120-124.

Junyaprasert , V.B., Teeranachaideekul , V., Supaperm , T., 2008. Effect of charged and non-ionic membrane additives on physicochemical properties and stability of niosomes. AAPS Pharm.Sci.Tech., 9, 851-859.

Khandare J.N., Madhavi G. and Tamhankar B.M. ,1994.Niosomesnovel drug deliverysystem. The Eastern Pharmacist , 37, 61-64.

Kaiser, U., Hofmann , J., Schilli , M., Wegmann, B., Klotz , U., Wedel, S., Virmani, A.K., Wollmer , E., Branscheid, D., Gazdar , A.F., Havemann , K., 1996. Steroid-hormone receptors in cell lines and tumor biopsies of human lung cancer. International journal of cancer. Journal International Cancer ,67, 357-364.

Karhale Ashish, A., Chaudhari Hiralal, S., Ughade Prajkta, L., Baviskar Dheeraj, T., Jain Dinesh, K., 2012. Pulmonary drug delivery system. International Journal of Pharm.Tech. Research, 4, 293-305.

Karnofsky, D.A., 1968. Mechanism of Action of Anticancer Drugs at a Cellular Level. CA: A Cancer Journal for Clinicians CA: A Cancer Journal for Clinicians 18, 232-234.

Kaur H, D.S.A.S., 2012. Niosomes: A novel drug delivery system. Intl. J. Pharm. Sci. Rev. Res. International Journal of Pharmaceutical Sciences Review and Research, 15, 113-120.

Kawano, K., 2003. Preparation and pharmacokinetics of pirarubicin loaded dehydrationrehydration vesicles. International Journal of Pharmaceutics, 252, 73-79.

Kazi, K.M., Mandal, A.S., Biswas, N., Guha, A., Chatterjee, S., Behera, M., Kuotsu, K., 2010. Niosome: A future of targeted drug delivery systems. Journal of Advanced Pharmaceutical Technology & Research, 1, 374-380.

Kellaway, I.W.F.S.J., 1990. Liposomes as drug delivery systems to the lung. Advanced Drug Delivery Reviews , 5, 149-161.

Kerr, D.J., Rogerson, A., Morrison,G.J., Florence, A.T., Kaye, S.B., 1988. Antitumour activity and pharmacokinetics of niosome encapsulated adriamycin in monolayer, spheroid and xenograft. British Journal of Cancer, 58, 432-436.

Kerr, R., Morrison, Florence, Kaye 1988; 58: 432-36., 1988. Antitumor activity and pharmacokinetics of niosome encapsulated adriamycin in monolayer, spheroid and xenograft. Br. J. Cancer, 58, 432-436.

Kerr, J.Z., Berg, S.L., Dauser, R., Nuchtern , J., Egorin, M.J., McGuffey, L., Aleksic, A., Blaney,S., 2001, Plasma and cerebrospinal fluid pharmacokinetics of gemcitabine after intravenous administration in nonhuman primates. Cancer Chemotherapy and Pharmacology, 47, 411-414.

Keith,B., Xu, Y., Grem , J., 2003, Measurement of the anti-cancer agent gemcitabine in human plasma by high-performance liquid chromatography. Journal of Chromatography B, 785, 65-72.

Kim,K.J., Li, B., Winer,J., Armanini, M. ,Gillett, N., Phillips,H.S., Ferrara,N.,1993. Inhibition of vascular endothelial growth factor-induced angiogenesis suppresses tumour growth *in vivo*. Nature, 362, 841-844.

Kim, I., Byeon, H.J., Kim, T.H., Lee, E.S., Oh, K.T., Shin, B.S., Lee, K.C., Youn, Y.S., 2012. Doxorubicin-loaded highly porous large PLGA microparticles as a sustained- release inhalation system for the treatment of metastatic lung cancer. Biomaterials, 33, 5574-5583.

Kim, R., Emi, M., Tanabe, K., 2007. Cancer immunoediting from immune surveillance to immune escape. Immunology, 121, 1-14.

Kim, S., Shi, Y., Kim, J. Y., Park, K., Cheng, J. X., 2010, Overcoming the barriers in micellar drug delivery: loading efficiency, *in vivo* stability, and micelle-cell interaction. Expert Opinion on Drug Delivery, 7, 49-62.

Krause, K.P., Müller, R.H., 2001. Production and characterisation of highly concentrated nanosuspensions by high pressure homogenisation. International Journal of Pharmaceutics, 214, 21-24.

Kreuter, J., 2010. Colloidal drug delivery systems. Marcel Dekker, New York.,55-71,479-501.

Known, J., Lee, D.I, Park, J.M., 2009.Biopolymer-based microgels/nanogels for drug delivery application .Progress in Polymer Science, 34 , 1261-1282.

Kuo ,T., Kubota ,T. ,Watanabe, M. , Furukawa ,T. , Kase, S., Tanino, H., Saikawa ,Y., Ishibiki, K., Kitajima, M., Hoffman ,R. M., 1993, Site-specific chemosensitivity of human small-cell lung carcinoma growing orthotopically compared to subcutaneously in SCID mice: the importance of orthotopic models to obtain relevant drug evaluation data. Anticancer Research, 13,627-30.

Kubota, T., 1994, Metastatic models of human cancer xenografted in the nude mouse: the importance of orthotopic transplantation. Journal of Cellular Biochemistry ,56, 4-8.

Kumar, V., Abbas, A.K., Fausto, N., Robbins, S.L., Cotran, R.S., 2005. Robbins and Cotran pathologic basis of disease. Elsevier Saunders, Philadelphia.,15.

Lasic, D.D., 1998. Novel applications of liposomes. Trends in Biotechnology 16, 307-321.

Lavialle, F., Deshayes, S., Gonnet, F. ,2009.Nanovesicles released by Dictyostelium cells.International Journal of Pharmaceutics, 380, 206-215.

Leach, M.O., 2006. Magnetic resonance spectroscopy (MRS) in the investigation of cancer at The Royal Marsden Hospital and The Institute of Cancer Research. Physics in Medicine and Biology, 51, 61-82.

Lee, S.H., Camilli, A., 2000. Novel approaches to monitor bacterial gene expression in infected tissue and host. Current Opinion in Microbiology 3, 97-101.

Lee, K., Hong, K., Papahadjopoulos, D., 1992. Recognition of liposomes by cells: In vitro binding and endocytosis mediated by specific lipid headgroups and surface charge density. Biochimica et Biophysica Acta (BBA) - Biomembranes, 1103, 185-197.

Lee , S., Lee , K.E., Kim , J.J., Lim , S.H., 2005. The effect of cholesterol in the liposome bilayer on the stabilization of incorporated Retinol. Journal of Liposome Research ,15, 3-4.

Lefrak, E.A., Pitha, J., Rosenheim, S., Gottlieb, J.A., 1973. A clinicopathologic analysis of adriamycin cardiotoxicity. Cancer, 32, 302-314.

Letchford, K., Burt, H., 2007. A review of the formation and classification of amphiphilic block copolymer nanoparticulate structures: micelles, nanospheres, nanocapsules and polymersomes. European Journal of Pharmaceutics and Biopharmaceutics, 65, 259-269.

Lim , S.t., Forbes , B., Martin , G.P., Brown , M.B., 2001, *In vivo* and in vitro characterization of novel microparticulates based on hyaluronan and chitosan hydroglutamate. AAPS Pharm.Sci.Tech., 2,20.

Lin, N.M., Zeng, S., Ma, S.L., Fan, Y., Zhong, H.J., Fang, L., 2004. Determination of gemcitabine and its metabolite in human plasma using high-pressure liquid chromatography coupled with a diode array detector. Acta Pharmacologica Sinica, 25, 1584-1589.

Lintu, C.S., Dilip, C., Azeem,A.K, Abdul bari Mambra, Divya Raj, , LisaMaryMani, V.S., P.Vinodhini, R.,Sivapathavelan, E.,Balasubramanian, P.,Kanniyappan, 2010. Rifampicin Proniosomes- An Approach to Improve the Stability of Niosomes. Der Pharmacia Lettre, 2, 75-79.

Lipshutz, G.S., Gruber, C.A., Cao, Y., Hardy, J., Contag, C.H., Gaensler, K.M., 2001. In utero delivery of adeno-associated viral vectors: intraperitoneal gene transfer produces long-term expression. Mol. Ther., 3, 284-292.

López-Pinto, J.M., González-Rodríguez, M.L., Rabasco, A.M., 2005. Effect of cholesterol and ethanol on dermal delivery from DPPC liposomes. International Journal of Pharmaceutics 298, 1-12.

Luker, K.E., Luker, G.D., 2008. Applications of bioluminescence imaging to antiviral research and therapy: Multiple luciferase enzymes and quantitation. Antiviral Res. Antiviral Research 78, 179-187.

Ma, M., Hao, Y., Liu, N., Yin, Z., Wang, L., Liang, X., Zhang, X., 2012. A novel lipid-based nanomicelle of docetaxel: evaluation of antitumor activity and biodistribution. Int. J. Nanomed., 7, 3389-3398.

Manal, A. 2011. Thesis [Ph. D].Non-ionic surfactant vesicles as a delivery system for cisplatin. University of Strathclyde. Strathclyde Institute of Pharmacy and Biomedical Sciences,58-60.

Madlova, M., Jones, S.A., Zwerschke, I., Ma, Y., Hider, R.C., Forbes, B., 2009. Poly(vinyl alcohol) nanoparticle stability in biological media and uptake in respiratory epithelial cell layers in vitro. European Journal of Pharmaceutics and Biopharmaceutics ,72, 438-443.

Martinho, N., 2011. Recent Advances in Drug Delivery Systems. Journal of Biomaterials and Nanobiotechnology ,2, 510-526.

Martin, J.F. ,1990. Pharmaceutical manufacturing. of liposomes in "specialized drug deliverysystems manufacturing and production technology, Marc.Dekk Series, PraveenTyle, 41, 267-314.

Marty, M., Fumoleau, P., Adenis, A., Rousseau , Y., Merrouche , Y., Robinet , G., Senac, I., Puozzo, C., 2001. Oral vinorelbine pharmacokinetics and absolute bioavailability study in patients with solid tumors. Annals of Oncology ,12, 1643-1649.

Mayer, L.D., Bally, M.B, Hope, M.J. and Cultis, P.R. ,1985. Transmembrane PH gradient drug uptake process, Biochem Biophys Acta., 816, 294-302.

Madero-Visbal, R.A., Colon, J.F., Hernandez, I.C., Limaye, A., Smith, J., Lee, C.M., Arlen, P.A., Herrera, L., Baker, C.H., 2012. Bioluminescence imaging correlates with tumor progression in an orthotopic mouse model of lung cancer. Surgical Oncology 21, 23-29.

Mastsumura,Y.,2008. Polymeric Micellar DeliverySystems in Oncology. Jpn Clin Oncol , 38, 793-802.

Matsuda, A., Sasaki, T., 2004. Antitumor activity of sugar-modified cytosine nucleosides. Cancer Science 95, 105-111.

McIntosh, T.J., 1978. The effect of cholesterol on the structure of phosphatidylcholine bilayers. Biochimica et Biophysica Acta, 513, 43-58.

Mackey, J. R., Mani, R. S., Selner, M., Mowles, D., Young, J. D., Belt, J. A., Crawford, C. R., Cass, C. E., 1998, Functional nucleoside transporters are required for gemcitabine influx and manifestation of toxicity in cancer cell lines. Cancer research, 58, 4349-4357.

Manca, M., Sinico, C., Maccioni, A., Diez, O., Fadda, A., Manconi, M., 2012a, Composition Influence on Pulmonary Delivery of Rifampicin Liposomes. Pharmaceutics ,4, 590-606.

Manca, M.l., Manconi, M., Valenti , D., Lai , F., Loy, G., Matricardi , P., Fadda , A.M., 2012b, Liposomes coated with chitosan-xanthan gum (chitosomes) as potential carriers for pulmonary delivery of rifampicin. Journal of Pharmaceutical Sciences, 101, 566-575.

Menzies, D., Nair, A., Fardon, T., Barnes, M., Burns, P., Lipworth, B., 2007. An *in vivo* and in vitro comparison of inhaled steroid delivery via a novel vortex actuator and a conventional valved holding chamber. Allergy, Asthma, & Immunology, 98, 471-479.

Meroni, G., Rajabi, M., Santaniello, E., 2009, D-Luciferin, derivatives and analogues: Synthesis and *in vitro /in vivo* luciferase-catalyzed bioluminescent activity. Arkivoc,2009, 265-288.

Mc Callion, O.N.M., Patel, M.J., 1996. Viscosity effects on nebulisation of aqueous solutions. International Journal of Pharmaceutics,130, 245-249.

McCallion, O.N.M., Taylor, K.M.G., Thomas, M., Taylor, A.J., 1995. Ultrasonic Nebulisation of Fluids with Different Viscosities and Surface Tensions. Journal of Aerosol Medicine, 8, 281-284.

McDonald, E.S., Randon, K.R., Knight, A., Windebank, A.J., 2005. Cisplatin preferentially binds to DNA in dorsal root ganglion neurons in vitro and *in vivo*: a potential mechanism for neurotoxicity. Neurobiology of Disease, 18, 305-313.

Min, R., Li, T., Du, J., Zhang, Y., Guo, J., Lu, W.L., 2008. Pulmonary gemcitabine delivery for treating lung cancer: Pharmacokinetics and acute lung injury aspects in animals. Can. J. Physiol. Pharmacol. Canadian Journal of Physiology and Pharmacology, 86, 288-298.

Mitchell, J., Newman, S., Chan, H.-K., 2007. In vitro and *in vivo* aspects of cascade impactor tests and inhaler performance: A review. AAPS Pharm.Sci.Tech., 8, 237-248.

Miller, C. R., Bondurant, B., Mclean, S. D., Mcgovern, K. A., O'brien, D. F., 1998, Liposome-cell interactions in vitro: effect of liposome surface charge on the binding and endocytosis of conventional and sterically stabilized liposomes. Biochemistry, 37, 12875-12883.

Moghimi, S.M., Hunter, A.C., Murray, J.C., 2001. Long-circulating and target-specific nanoparticles: theory to practice. Pharmacological Reviews, 53, 283-318.

Moghimi, S.M., Patel, H.M., 2002. Modulation of murine liver macrophage clearance of liposomes by diethylstilbestrol. The effect of vesicle surface charge and a role for the complement receptor Mac-1 (CD11b/CD18) of newly recruited macrophages in liposome recognition. Journal of Controlled Release, 78, 55-65.

Mohamed ,A. N., Randa ,T. , El Rehem, A., Mohammed, Y. S., 2012. Formulation and evaluation of dispersed paroxetine liposomes in gel. Journal of Chemical and Pharmaceutical Research, 4, 2209-2222.

Mohan Kale, P.S., Ramandeep Singh, Geena Malhotra and Preeti Raut, 2012. Effect of size reduction techniques on doxorubicin hydrochloride loaded liposomes International Journal of Biological & Pharmaceutical Research, 3, 308-316.

Moog, R., Burger, A.M., Brandl, M., Schüler, J., Schubert, R., Unger, C., Fiebig, H.H., Massing, U., 2002. Change in pharmacokinetic and pharmacodynamic behavior of gemcitabine in human tumor xenografts upon entrapment in vesicular phospholipid gels. Cancer Chemotherapy and Pharmacology, 49, 356-366.

Moriyama, E., Niedre, M.J., Jarvi , M.T., Mocanu , J.D., Moriyama , Y., Subarsky, P.L.B., Lilge , L.D., Wilson , B.C., 2008. The influence of hypoxia on bioluminescence in luciferase-transfected gliosarcoma tumor cells in vitro. Photochemical & photobiological sciences . Journal of the European Photochemistry Association and the European Society for Photobiology, 7, 675-680.

Morrow, M., Wait, R.B., Rosenthal, R.A., Gamelli, R.L., 1987. Verapamil enhances antitumor activity without increasing myeloid toxicity. Surgery 101, 63-68.

Mugabe, C., Azghani, A.O., Omri, A., 2006. Preparation and characterization of dehydration–rehydration vesicles loaded with aminoglycoside and macrolide antibiotics. International Journal of Pharmaceutics 307, 244-250.

Mullen, A.B., Baillie, A.J., Carter, K.C., 1998. Visceral leishmaniasis in the BALB/c mouse: a comparison of the efficacy of a nonionic surfactant formulation of sodium stibogluconate with those of three proprietary formulations of amphotericin B. Antimicrobial Agents and Chemotherapy, 42, 2722-2725.

Mylonakis,N.,Athansiou,A.,Ziras,N.,Angel,J.,Rapti,A.,Lampaki,S.,Politis,N.,2010.Phase II study of liposomal cisplatin plus gemcitabine as first line treatment in inoperable (stage III B/I.V) non-small cell lung cancer. Lung Cancer,68,240-7.

Nagayasu, A., Shimooka , T., Kinouchi , Y., Uchiyama, K., Takeichi , Y., Kiwada , H., 1994. Effects of fluidity and vesicle size on antitumor activity and myelosuppressive activity of liposomes loaded with daunorubicin. Biological & Pharmaceutical Bulletin, 17, 935-939.

Nakayama, G. R., Caton, M. C., Nova, M. P., Parandoosh, Z., 1997, Assessment of the Alamar Blue assay for cellular growth and viability in vitro. Journal of Immunological Methods ,204, 205-208.

Nakamura, Y., Yamamoto, N., 2009. [Second-line treatment and targeted therapy of advanced lung cancer]. Gan to kagaku ryoho. Cancer & Chemotherapy, 36, 710-716.

Newman, S.P., Chan, H.K., 2008. In vitro/*in vivo* comparisons in pulmonary drug delivery. Journal of Aerosol Medicine and Pulmonary Drug Delivery, 21, 77-84.

Newman, S.P., Pellow, P.G., Clay, M.M., Clarke, S.W., 1985. Evaluation of jet nebulisers for use with gentamicin solution. Thorax, 40, 671-676.

Newman, S.P., Steed, K.P., Hooper, G., Jones, J.I., Upchurch, F.C., 1999. Improved targeting of beclomethasone diproprionate (250 micrograms metered dose inhaler) to the lungs of asthmatics with the Spacehaler. Respiratory Medicine 93, 424-431.

Nguyen, V.T., Morange, M., Bensaude, O., 1988. Firefly luciferase luminescence assays using scintillation counters for quantitation in transfected mammalian cells. Analytical Biochemistry 171, 404-408.

Nissim, I., Horyn, O., Daikhin, Y., Luhovyy, B., Phillips, P.C., Yudkoff, M., 2006. Ifosfamide-induced nephrotoxicity: mechanism and prevention. Cancer Research, 66, 7824-7831.

Niven, R.W., Whitcomb, K.L., Shaner, L., Ip, A.Y., Kinstler, O.B., 1995a. The pulmonary absorption of aerosolized and intratracheally instilled rhG-CSF and monoPEGylated rhG-CSF. Pharm. Res., 12, 1343-1349.

Niven, R.W., Whitcomb, K.L., Woodward, M., Liu, J., Jornacion, C., 1995b. Systemic absorption and activity of recombinant consensus interferons after intratracheal instillation and aerosol administration. Pharm. Res., 12, 1889-1895.

Niven , R.W., Schreier, H., 1990. Nebulization of liposomes. I. Effects of lipid composition. Pharm. Res., 7, 1127-1133.

Noble,C.O.,Guo,Z.,Hayes ,M.E.,Marks ,J.D.,Park, J.W.,Benz,C.C.,Kirpotin ,D.B.,Drummond ,D.C.(2009).Characterization of highly stable liposomal and immune liposomal formulations of vincristine and vinblastine.Cancer Chemother Pharmacol ,64 ,741-51.

O'Callaghan, C., Barry, P.W., 1997. The science of nebulised drug delivery. Thorax 52, 31-44.

Oh ,Y.K, Nix, D.E., Straubinger, R.M .,1995. Formulation and efficacy of liposome-encapsulated antibiotics for therapy of intracellular Mycobacterium avium infection. Antimicrob. Agents Chemother., 39,2104–2111.

Oja, C.D., Semple, S.C., Chonn, A., Cullis, P.R., 1996. Influence of dose on liposome clearance: critical role of blood proteins. Biochimica et Biophysica Acta 1281, 31-37.

Orive ,G.G., Alicia , R., Hernandez, R., M., Dominguez-Gil Alfonso , Luis, P.J., 2004, Techniques: New approaches to the delivery of biopharmaceuticals. Trends in Pharmacological Sciences ,25, 382-387.

Ost, D., Goldberg, J., Rolnitzky, L., Rom, W.N., 2008. Survival after surgery in stage IA and IB non-small cell lung cancer. American Journal of Respiratory and Critical Care Medicine, 177, 516-523.

Ozer, A.Y., Talsma, H., 1989. Preparation and stability of liposomes containing 5-fluorouracil. International Journal of Pharmaceutics, 55, 185-191.

Olson, J.A., Adler-Moore, J.P., Jensen, G.M., Schwartz, J., Dignani, M.C., Proffitt , R.T., 2008. Comparison of the physicochemical, antifungal, and toxic properties of two liposomal amphotericin B products. Antimicrobial agents and chemotherapy, 52, 259-268.

Parthasarathi ,G., Udupa N., Umadevi P. and Pillai G.K. ,1994.Niosome encapsulated of vincristine sulfate: improved anticancer activity with reduced toxicity in mice. J. Drug Target, 2,173-182.

Paolino, D., Cosco, D., Racanicchi, L., Trapasso, E., Celia, C., Iannone, M., Puxeddu, E., Costante, G., Filetti, S., Russo, D., 2010. Gemcitabine-loaded PEGylated unilamellar liposomes vs GEMZAR®: Biodistribution, pharmacokinetic features and *in vivo* antitumor activity. Journal of Controlled Release, 144, 144-150.

Paolino, D., Muzzalupo, R., Ricciardi, A., Celia , C., Picci, N., Fresta, M., 2007. In vitro and *in vivo* evaluation of Bola-surfactant containing niosomes for transdermal delivery. Biomedical Microdevices, 9, 421-433.

Park, C.W., Rhee, Y.S., Vogt, F.G., Hayes, D., Jr., Zwischenberger, J.B., DeLuca, P.P., Mansour, H.M., 2012. Advances in microscopy and complementary imaging techniques to assess the fate of drugs ex vivo in respiratory drug delivery: an invited paper. Adv. Drug. Deliv. Rev., 64, 344-356.

Parmar, J., Singh, D., Lohade, A., Hegde, D., Soni, P., Menon, M., Samad, A., 2011. Inhalational system for etoposide liposomes: Formulation development and in vitro deposition. Indian Journal of Pharmaceutical Sciences, 73, 656-662.

Parshina, N.A., Pleteneva, T.V., Baikova, V.N., Narimanov, M.N., Tyulyandin, S.A., 2008. Quantitative estimation of gemcitabine by HPLC in plasma. Pharmaceutical Chemistry Journal, 42, 288-290.

Parthasarathi, G., Udupa, N., Umadevi, P., Pillai, G.K., 1994. Niosome encapsulated of vincristine sulfate: improved anticancer activity with reduced toxicity in mice. Journal of Drug Targeting, 2, 173-182.

Patton, J.S., 1996. Mechanisms of macromolecule absorption by the lungs. Advanced Drug Delivery Reviews 19, 3-36.

Patton, J.S., Fishburn, C.S., Weers, J.G., 2004. The Lungs as a Portal of Entry for Systemic drug delivery. Proceeding- AmericanThoracic Society, 1, 338-344.

Panyam, J., Labhasetwar, V., 2003. Biodegradable nanoparticles for drug and gene delivery to cells and tissue. Advanced Drug Delivery Reviews, 55, 329-347.

Peng, X., Zhang, L., 2009. Self-assembled micelles of N-phthaloyl-carboxymethychitosan for drug delivery. Physicochemical and Engineering Aspects, 337, 21-25.

Pepe, C., Hasan, B., Winton, T.L., Seymour, L., Graham, B., Livingston, R.B., Johnson, D.H., Rigas, J.R., Ding, K., Shepherd, F.A., National Cancer Institute of, C., Intergroup Study, J.B.R., 2007. Adjuvant vinorelbine and cisplatin in elderly patients: National Cancer Institute of Canada and Intergroup Study JBR.10. Journal of Clinical Oncology ,25, 1553-1561.

Pereira, J.R., Martins, S.J., Nikaedo, S.M., Ikari, F.K., 2004. Chemotherapy with cisplatin and vinorelbine for elderly patients with locally advanced or metastatic non-small-cell lung cancer (NSCLC). BMC cancer, 4,69.

Pietzyk, B., Henschke, K., 2000. Degradation of phosphatidylcholine in liposomes containing carboplatin in dependence on composition and storage conditions. International Journal of Pharmaceutics International Journal of Pharmaceutics, 196, 215-218.

Pignon, J.P., Tribodet, H., Scagliotti, G.V., Douillard, J.Y., Shepherd, F.A., Stephens, R.J., Dunant, A., Torri, V., Rosell, R., Seymour, L., Spiro, S.G., Rolland, E., Fossati, R., Aubert, D., Ding, K., Waller, D., Le Chevalier, T., 2008. Lung adjuvant cisplatin evaluation: A pooled analysis by the LACE collaborative group.Journal of Clinical Oncology, 26, 3552-3559.

Pilcer, G., Vanderbist, F., Amighi, K., 2009. Preparation and characterization of spray-dried tobramycin powders containing nanoparticles for pulmonary delivery. International Journal of Pharmaceutics 365, 162-169.

Pitrubhakta, A.B., Shinde, A.J., Jadhav, N.R., 2012. Design, development and characterization of PEGylated liposomes of gemcitabine hydrochloride. Der Pharm. Lett. Der Pharmacia Lettre, 4, 314-329.

Poveda, A., Lopez-Pousa , A., Martin , J., del Muro , J.G., Bernabe, R., Casado , A., Balana , C., Sanmartin , O., Menendez , M.D., Escudero , P., 2005. Phase II clinical trial with pegylated liposomal doxorubicin (CAELYX /Doxil) and quality of life evaluation (EORTC QLQ-C30) in adult patients with advanced soft tissue sarcomas. A study of the Spanish Group for Research in Sarcomas (GEIS). SARCOMA -ABINGDON ,9, 127-132.

Poste, G., Doll, J., Hart, I. R., Fidler, I. J., 1980, In vitro selection of murine B16 melanoma variants with enhanced tissue-invasive properties. Cancer research 40, 1636-1644.

Potter , D., Gorschboth , C.M., Schneider , P.D., 1985, Liposome uptake by melanoma: in vitro comparison with hepatocytes. The Journal of surgical research, 39, 157-163.

Raja , R.A., Udupa, N., Uma , P., 1996, Kinetics and Tissue Distribution of Niosomal Bleomycin in Tumor Bearing Mice. Indian journal of pharmaceutical sciences. 58, 230.

Rahman, A. M., Yusuf, S. W., Ewer, M. S., 2007, Anthracycline induced cardiotoxicity and cardiac-sparing effect of liposomal formulation. Int J Nanomed, 2, 567-584.

Ramana, L., Sethuraman , S., Ranga , U., Krishnan , U.M., 2010. Development of a liposomal nanodelivery system for nevirapine. Journal of Biomedical Science, 17,57.

Rathod, S., Deshpande, S. G., 2010, Design and evaluation of liposomal formulation of pilocarpine nitrate. Indian Journal of Pharmaceutical Sciences ,72, 155-160.

Rao,R.D., Markovic,S.N., Anderson, P.M., 2003. Aerosol therapy for malignancy involving the lungs. Current Cancer Drug Targets, 3, 239-250.

Reddy, L.H., Couvreur, P., 2008. Novel approaches to deliver gemcitabine to cancers. Curr. Pharm. Des. Current Pharmaceutical Design, 14, 1124-1137.

Rejman, J., Oberle , V., Zuhorn, I.S., Hoekstra, D., 2004. Size-dependent internalization of particles via the pathways of clathrin- and caveolae-mediated endocytosis. The Biochemical Journal, 377, 159-169.

Remington, J.P., Allen, L.V., 2013. Remington : The science and practice of pharmacy. Pharmaceutical Press, London; Philadelphia.,1191-1852.

Roberts, D.L., Romay, F.J., 2005. Relationship of Stage Mensuration Data to the Performance of New and Used Cascade Impactors. Journal of Aerosol Medicine ,18, 396-413.

Ritter, J., 2008. A textbook of clinical pharmacology and therapeutics. Hodder Arnold, London.,367-396.

Rogerson, A.C.J.W.N.F.A.T., 1988. The Distribution of doxorubicin in mice following administration in niosomes. Journal of Pharmacy and Pharmacology 40, 337-42.

Rolland, E., Le Chevalier, T., Auperin, A., Burdett, S., Pignon, J.-P., 2007. Sequential radio-chemotherapy (RT-CT) versus radiotherapy alone (RT) and concomitant RT-CT versus RT alone in locally advanced non-small cell lung cancer (NSCLC): Two meta-analyses using individual patient data (IPD) from randomised clinical trials (RCTs). Journal of Thoracic Oncology, 2, 309-310.

Rubin, P.C.G., 1966. Microcirculation of tumors Part I: Anatomy, function, and necrosis. Clinical Radiology, 17, 220-229.

Ruge, C.A., Schaefer , U.F., Kirch, J., Lehr , C.M., Herrmann , J., Muller , R., Canadas, O., Echaide, M., Perez-Gil , J., Casals, C.,2012. The interplay of lung surfactant proteins and lipids assimilates the macrophage clearance of nanoparticles. PLoS ONE ,7, 40775.

Ruckmani, K., Jayakar, B., Ghosal, S.K., 2000. Nonionic surfactant vesicles (niosomes) of cytarabine hydrochloride for effective treatment of leukemias: encapsulation, storage, and in vitro release. Drug Development and Industrial Pharmacy, 26, 217-222.

Sarraf-Yazdi, S. M., Jing, D., Mark ,W., Clary, B. M., 2004, Use of *in vivo* bioluminescence imaging to predict hepatic tumor burden in mice. Journal of Surgical Research, 120, 249-255.

Sadikot, R.T., Blackwell, T.S., 2005. Bioluminescence imaging. Proceedings of the American Thoracic Society 2, 537-540.

Santos Giuberti, C., Oliveira Reis, E.C., Ribeiro Rocha, T.G., Leite, R.G., Lacerda, G.A., Oliveira, M.C.,2011. Study of the pilot production process of long-circulating and pH-sensitive liposomes containing cisplatin. Journal of Liposome Research, 21, 60-69.

Santiago , L.N., de Camargo Fenley, J., Braga, L.C., Cury , P.M., Cordeiro, J.A., 2009. The effect of different doses of cigarette smoke in a mouse lung tumor model. Int. J. Clin. Exp. Pathol. International Journal of Clinical and Experimental Pathology, 2, 176-181.

Sadler , R.C., Prime , D., Burnell , P.K., Martin, G.P., B., F., 2011. Integrated in vitro experimental modelling of inhaled drug delivery: Deposition, dissolution and absorption. Journal of Drug Delivery Science and Technology, 21, 331-338.

Schellinger, A.P., Carr, P.W., 2006. Isocratic and gradient elution chromatography: A comparison in terms of speed, retention reproducibility and quantitation. Journal of Chromatography A, 1109, 253-266.

Schreier, H., Gonzalez-Rothi, R.J., Stecenko, A.A., 1993. Pulmonary delivery of liposomes. Journal of Controlled Release, 24, 209-223.

Sengupta, S., Tyagi, P., Velpandian, T., Gupta, Y., Gupta, S., 2000. Etoposide encapsulated in positively charged liposomes: pharmacokinetic studies in mice and formulation stability studies. Pharmacological Research,42, 459-464.

Sezgin-Bayindir, Z., Yuksel, N., 2012. Investigation of formulation variables and excipient interaction on the production of niosomes. AAPS Pharm.Sci.Tech, 13, 826-835.

Senior, J., Crawley, J.C.W., Gregoriadis, G., 1985. Tissue distribution of liposomes exhibiting long half-lives in the circulation after intravenous injection. Biochimica et Biophysica Acta (BBA) - General Subjects Biochimica et Biophysica Acta (BBA) - General Subjects, 839, 1-8.

Senior, J.H., 1987. Fate and behavior of liposomes *in vivo*: a review of controlling factors. Critical reviews in therapeutic drug carrier systems 3, 123-193.

Shah, S.P., Misra, A., 2004. Liposomal amphotericin B dry powder inhaler: effect of fines on in vitro performance. Die Pharmazie, 59, 812-813.

Shepherd, F.A., Crowley, J., Van Houtte, P., Postmus, P.E., Carney, D., Chansky, K., Shaikh, Z., Goldstraw, P., International Association for the Study of Lung Cancer International Staging, C., Participating, I., 2007. The International Association for the Study of Lung Cancer lung cancer staging project: proposals regarding the clinical staging of small cell lung cancer in the forthcoming (seventh) edition of the tumor, node, metastasis classification for lung cancer. Journal of thoracic oncology , 2, 1067-1077.

Shi, B., Fang , C., Pei , Y., 2006. Stealth PEG-PHDCA niosomes: Effects of chain length of PEG and particle size on niosomes surface properties,*in vitro* drug release, phagocytic uptake,*in vivo* pharmacokinetics and antitumor activity. J. Pharm. Sci. Journal of Pharmaceutical Sciences, 95, 1873-1887.

Shipley, L.A., Brown, T.J., Cornpropst, J.D., Hamilton, M., Daniels, W.D., Culp, H.W., 1992. Metabolism and disposition of gemcitabine, and oncolytic deoxycytidine analog, in mice, rats, and dogs. Drug Metabolism and Disposition: the biological fate of chemicals, 20, 849-55

Skoog, D.A., Holler, F.J., Nieman, T.A., 1998, Principles of instrumental analysis. Saunders College Pub. ; Harcourt Brace College Publishers, Philadelphia; Orlando, Fla.,725-766.

Shubik, P., 1982. Vascularization of tumors: a review. Journal of Cancer Research and Clinical Oncology 103, 211-226.

Sinkule, J.A., 1984. Etoposide: a semisynthetic epipodophyllotoxin. Chemistry, pharmacology, pharmacokinetics, adverse effects and use as an antineoplastic agent. Pharmacotherapy, 4, 61-73

Smola, M., Vandamme, T., Sokolowski, A., 2008. Nanocarriers as pulmonary drug delivery systems to treat and to diagnose respiratory and non respiratory diseases. Int. J. Nanomed., 3, 1-19.

Smrdel, U.K.V., 2006. Erlotinib in previously treated non-small-cell lung cancer. Radiology and Oncology, 40, 39-42.

Smyth, H.D., 2003. The influence of formulation variables on the performance of alternative propellant-driven metered dose inhalers. Advanced Drug Delivery Deviews, 55, 807-828.

Snyder, L.R., Kirkland, J.J., Glajch, J.L., 1997. Practical HPLC method development. Wiley, New York.,21-41.

Soloman, R., Gabizon, A.A., 2008. Clinical pharmacology of liposomal anthracyclines: focus on pegylated liposomal doxorubicin. Clinical Lymphoma & Myeloma 8, 21-32.

Stabile, L. P., Siegfried, J. M., 2003, Sex and gender differences in lung cancer. J Gend. Specif. Med., 6, 37-48.

Stella, B., Arpicco, S., Rocco, F., Marsaud, V., Renoir, J.-M., Cattel, L., Couvreur, P., 2007. Encapsulation of gemcitabine lipophilic derivatives into polycyanoacrylate nanospheres and nanocapsules. International Journal of Pharmaceutics, 344, 71.

Stone, K.C., Mercer, R.R., Gehr, P., Stockstill, B., Crapo, J.D., 1992. Allometric relationships of cell numbers and size in the mammalian lung. American journal of Respiratory Cell and Molecular Miology, 6, 235-243.

Sottani , C., Zucchetti, M., Zaffaroni , M., Bettinelli , M., Minoia, C., 2004, Validated procedure for simultaneous trace level determination of the anti-cancer agent gemcitabine and its metabolite in human urine by high-performance liquid chromatography with tandem mass spectrometry. Rapid Communications in Mass Spectrometry : RCM, 18, 1017-1023.

Šentjurc, M., Vrhovnik, K., Kristl, J., 1999. Liposomes as a topical delivery system: the role of size on transport studied by the EPR imaging method. Journal of Controlled Release ,59, 87-97.

Sung, J.C., Pulliam, B.L., Edwards, D.A., 2007. Nanoparticles for drug delivery to the lungs. Trends in Biotechnology, 25, 563-570.

Sweetman, S.C., 2011. Martindale : the complete drug reference. Pharmaceutical Press, London; Chicago.Electronic access in Strathclyde University Library.

Sweet, D.M., Kolhatkar , R.B., Ray , A.,2009.Transepithelial transport of PEGylated anion poly (amidoamine) dendrimers. Journal of Controlled Release ,138 ,78-85.

Szoka, F.J., Milholland, D., Barza, M., 1987. Effect of lipid composition and liposome size on toxicity and in vitro fungicidal activity of liposome-intercalated amphotericin B. Antimicrobial Agents and Ahemotherapy, 31, 421-429.

Talmadge , J., Singh , R.K., Fidler, I.J., Raz, A., 2007. Murine models to evaluate novel and conventional therapeutic strategies for cancer. The American journal of pathology 170, 793-804.

Tan, Y., Yang, Z., Pan, X., Chen, M., Feng, M., Wang, L., Liu, H., Shan, Z., Wu, C., 2012. Stability and aerosolization of pressurized metered dose inhalers containing thymopentin nanoparticles produced using a bottom-up process. International Journal of Pharmaceutics, 427, 385-392.

Tang, B.C., Fu, J., Watkins, D.N., Hanes , J., 2010. Enhanced efficacy of local etoposide delivery by poly(ether-anhydride) particles against small cell lung cancer *in vivo*. Biomaterials, 31, 339-344.

Taylor, K.M.G., Taylor, G., Kellaway, I.W., Stevens, J., 1990. The stability of liposomes to nebulisation. International Journal of Pharmaceutics, 58, 57-61.

Theneshkumar, S., Lorito, G., Giordano, P., Petruccelli, J., Martini, A., Hatzopoulos, S., 2009. Effect of noise conditioning on cisplatin-induced ototoxicity: a pilot study. Med .Sci. Monit., 15, 173-177.

Tiffen, J. C., Bailey, C. G., Ng, C., Rasko, J. E., Holst, J., 2010, Luciferase expression and bioluminescence does not affect tumor cell growth *in vitro* or *in vivo*. Molecular cancer, 9,299.

Tseng,C.,Yun,W.,Yen ,K., 2009.The use of biotinylated –EGF-modified gelatin nanoparticles carrier to enhance cisplatin accumulation.Biomaterials ,30 ,3476-3485.

Tsim, S., O'Dowd, C.A., Milroy, R., Davidson, S., 2010. Staging of non-small cell lung cancer (NSCLC): A review. Respiratory Medicine, 104, 1767-1774.

Turrisi, A.T., Kim, K., Blum,R., Sause, W.T., Livingston, R.B., Komaki, R., Wagner H., Aisner, S., Johnson, D.H., 1999. Twice-daily compared with once-daily thoracic radiotherapy in limited small-cell lung cancer treated concurrently with cisplatin and etoposide. The New England journal of Medicine, 340, 265-271.

Uchegbu, I., 1998. The biodistribution of novel 200-nm palmitoyl muramic acid vesicles. International Journal of Pharmaceutics, 162, 19-27.

Uchegbu, I.F, Double, J.A. , Turton, J.A, Florence, A.T. 1995. Distribution, metabolism and tumoricidal activity of doxorubicin administered in sorbitan monostearate (Span 60) niosomes in the mouse. Pharm. Res., 12, 1019-1024.

Uchegbu, I.F., Vyas, S.P., 1998. Non-ionic surfactant based vesicles (niosomes) in drug delivery. International Journal of Pharmaceutics 172, 33-70.

Uchegbu, I.F., Double, J.A., Kelland, L.R., Turton, J.A., Florence, A.T., 1996. The activity of doxorubicin niosomes against an ovarian cancer cell lline and three *in vivo* mouse tumour models. Journal of Drug Targeting , 3, 399-409.

Udupa,U., Chandraprakash,K.S., Umadevi,P., Pillai.,G. K., 1993. Formulation and Evaluation of Methotrexate Niosomes. Drug Development and Industrial Pharmacy, 19, 1331-1342.

Ueno, H., Kiyosawa, K., Kaniwa, N., 2007. Pharmacogenomics of gemcitabine: can genetic studies lead to tailor-made therapy?. British journal of cancer, 97, 145-151.

Van ,D.A., Bouwstra ,J.A., Rensen ,A.V., Jermiasse ,E., Vringer ,T.D., Junginger ,H.E. ,1996.Preparation and characterization of non-ionic surfactant vesicles. J Colloid. Interface Sci.,178,263-3.

van Moorsel, C.J., Pinedo, H.M., Veerman, G., Bergman, A.M., Kuiper, C.M., Vermorken, J.B., van der Vijgh, W.J., Peters, G.J., 1999. Mechanisms of synergism between cisplatin and gemcitabine in ovarian and non-small-cell lung cancer cell lines. British Journal of Cancer, 80, 981-990.

Van Putte, B.P., Hendriks, J.M., Romijn, S., Pauwels, B., Vermorken, J.B., Van Schil, P.E., 2005. Combination chemotherapy with gemcitabine with isolated lung perfusion for the treatment of pulmonary metastases. The Journal of Thoracic and Cardiovascular Surgery, 130, 125-130.

Veltkamp, S.A., Pluim, D., Schellens, J.H.M., Van Tellingen, O., Beijnen, J.H., 2008. Extensive metabolism and hepatic accumulation of gemcitabine after

multiple oral and intravenous administration in mice. Drug Metabolism and Disposition, 36, 1606-1615.

Venkatesh, A., Vinay 2010. Niosomes : A Potential Drug Delivery System. Pharmbit, 22, 115.

Verma, S., Dent, S., Chow, B. J. W., Rayson, D., Safra, T., 2008, Metastatic breast cancer: The role of pegylated liposomal doxorubicin after conventional anthracyclines. Cancer Treat. Rev. Cancer Treatment Reviews, 34, 391-406.

Verma, D.D., Verma, S., Blume, G., Fahr, A., 2003. Particle size of liposomes influences dermal delivery of substances into skin. International Journal of Pharmaceutics ,258, 141-151.

Velinova, M.J., Staffhorst, R.W., Mulder, W.J., Dries, A.S., Jansen, A.J., de Kruijff, B., de Kroon, A., 2004. Preparation and stability of lipid-coated nanocapsules of cisplatin: anionic phospholipid specificity. Biochimica et Biophysica Acta (BBA) - Biomembranes ,1663, 135-142.

Vono, M., Cosco, D., Paolino, D., Celano, M., Russo, D., Fresta, M., Celia, C., 2010. In Vitro evaluation of the activity of gemcitabine-loaded pegylated unilamellar liposomes against papillary thyroid cancer cells. Open Drug Delivery Journal, 4, 55-62.

Vyas , S.P., Khar , R.K., 2003. Targeted & controlled drug delivery : novel carrier systems. CBS Publishers & Distributors, New Delhi, India., 249-276.

Watwe, R. M. and Bellare, J. R., 1995. Manufacture of liposomes - a review. Current Science, 68, 715-724.

Wang, F., Wang, Y.-C., Yan, L.F., Wang, J., 2009. Biodegradable vesicular nanocarriers based on poly(ε-caprolactone)-block-poly(ethyl ethylene phosphate) for drug delivery. Polymer, 50, 5048-5054.

Wang , L.Z., Goh, B.C., Lee , H.S., Noordhuis , P., Peters, G.J., 2003.An expedient assay for determination of gemcitabine and its metabolite in human plasma using isocratic ion-pair reversed-phase high-performance liquid chromatography.Ther. Drug. Monit.,25,552-7.

Wagner, A., Karola, V.-U., 2011.Liposome Technology for Industrial Purposes. Journal of Drug Delivery, 2011, 1-9.

Weiss, W., 1997. Cigarette smoking and lung cancer trends. A light at the end of the tunnel. Chest, 111, 1414-1416.

White, S., Bennett, D.B., Cheu, S., Conley, P.W., Guzek, D.B., Gray, S., Howard, J., Malcolmson, R., Parker, J.M., Roberts, P., Sadrzadeh, N., Schumacher, J.D., Seshadri, S., Sluggett, G.W., Stevenson, C.L., Harper, N.J., 2005.

EXUBERA®: Pharmaceutical Development of a Novel Product for Pulmonary Delivery of Insulin. Diabetes Technology & Therapeutics ,7, 896-906.

Willmann, J.K., Gambhir, S.S., van Bruggen, N., Dinkelborg, L.M., 2008. Molecular imaging in drug development. Nat. Rev. Drug Discov. Nature Reviews Drug Discovery, 7, 591-607.

Wilmann ,C., Fan ,D. ,O'brian ,C. A. ,Bucana, C. D., Fidler, I. J., 1992, Orthotopic and ectopic organ environments differentially influence the sensitivity of murine colon carcinoma cells to doxorubicin and 5-fluorouracil. International journal of Cancer, 52, 98-104.

Winton, T., Livingston, R., Johnson, D., Rigas, J., Johnston, M., Butts, C., Cormier, Y., Goss, G., Inculet, R., Vallieres, E., Fry, W., Bethune, D., Ayoub, J., Ding, K., Seymour, L., Graham, B., Tsao, M.S., Gandara, D., Kesler, K., Demmy, T., Shepherd, F., National Cancer Institute of Canada Clinical Trials, G., National Cancer Institute of the United States Intergroup, J.B.R.T.I., 2005. Vinorelbine plus cisplatin vs. observation in resected non-small-cell lung cancer. The New England Journal of Medicine, 352, 2589-2597.

Wittgen, B.P.H., Kunst, P.W.A., Perkins, W.R., Lee, J.K., Postmus, P.E., 2006. Assessing a System to Capture Stray Aerosol during Inhalation of Nebulized Liposomal Cisplatin. Journal of Aerosol Medicine, 19, 385-391.

Witschi, H., Espiritu, I., Peake, J.L., Wu, K., Maronpot, R.R., Pinkerton , K.E., 1997. The carcinogenicity of environmental tobacco smoke. Carcinogenesis, 18, 575-586.

Yamaguchi, T., Nomura, M., Matsuoka, T., Koda, S., 2009, Effects of frequency and power of ultrasound on the size reduction of liposome. Chemistry and Physics of Lipids, 160, 58-62.

Yilmaz , B., Kadioglu , Y.Y., Aksoy, Y., 2003, Simultaneous determination of gemcitabine and its metabolite in human plasma by high-performance liquid chromatography. Journal of chromatography. B, Analytical technologies in the Biomedical and Life Sciences ,791, 1-2.

Yang,Y.,Bajaj, N.,Xu, P.,Ohn ,K.,2009.Developement of highly porous large PLGA microparticles for pulmonary drug delivery.Biomaterials,30,1974-1953.

Zhou, J., Zhao, W.Y., Ma, X., Ju, R.J., Li,X.Y., Li, N., Sun, M.G., Shi, J.F., Zhang, C.X., Lu, W.L., 2013. The anticancer efficacy of paclitaxel liposomes modified with mitochondrial targeting conjugate in resistant lung cancer. Biomaterials ,34, 3626-3638.

Zabala, M., Alzuguren, P., Benavides, C., Crettaz, J., Gonzalez-Aseguinolaza, G., Ortiz De Solorzano, C., Gonzalez-Aparicio, M., Kramer, M. G., Prieto, J.,

Hernandez-Alcoceba, R., 2009, Evaluation of bioluminescent imaging for noninvasive monitoring of colorectal cancer progression in the liver and its response to immunogene therapy. Mol. Cancer, 8, 2.

Zanellato, I., Boidi, C.D., Lingua, G., Osella, D., Betta, P.G., Orecchia, S., Monti, E., 2011. In vitro anti-mesothelioma activity of cisplatin-gemcitabine combinations: Evidence for sequence-dependent effects. Cancer Chemother. Pharmacol. Cancer Chemotherapy and Pharmacology, 67, 265-273.

Zarogoulidis, P., Chatzaki, E., Porpodis, K., Domvri, K., Hohenforst-Schmidt, W., Goldberg, E.P., Karamanos, N., Zarogoulidis, K., 2012. Inhaled chemotherapy in lung cancer: future concept of nanomedicine. Int J Nanomed., 7, 1551-1572.

Zaru, M., Manca, M.L., Fadda, A.M., Antimisiaris, S.G., 2009. Chitosan-coated liposomes for delivery to lungs by nebulisation. Colloids and Surfaces B: Biointerfaces, 71, 88-95.

Zaru,M. ,Mourtas,S. , Klepetsanis,P., Fadda,M., Antimisiaris,S.G, 2007. Liposomes for drug delivery to the lungs by nebulization. European Journal of Pharmaceutics and Biopharmaceutics European Journal of Pharmaceutics and Biopharmaceutics, 67, 655-666.

.

Zeng, X.M., Martin, G.P., Marriott, C., 1995. The controlled delivery of drugs to the lung. International Journal of Pharmaceutics, 124, 149-164.

Zhang, L., Hellström, K.E., Chen, L., 1994. Luciferase activity as a marker of tumor burden and as an indicator of tumor response to antineoplastic therapy *in vivo*. Clinical & Experimental Metastasis, 12, 87-92.

Zhang, W., van Winden, E.C.A., Bouwstra, J.A., Crommelin, D.J.A., 1997a. Enhanced Permeability of Freeze-Dried Liposomal Bilayers upon Rehydration. Cryobiology, 35, 277-289.

Zhang , X., Wu , J., 2009. Establishing of the Transplanted animal models for human lung cancer. Journal of Nanjing Medical University, 23, 1-5.

Zhang, M., Quan, L., Lu , X., Bao, Y., Wu, L., Zhang, L., Wang, L., Zhang, T., 2012. Hypomethylation of fetal brain genomic DNA in neural tube defects determined by a new liquid chromatography-electrospray ionization tandem mass spectrometry (LC-MS/MS) method. Anal. Methods Analytical Methods 4, 2515-2521.

Zhang, L., Liu, L., Qian, Y. and Chen, Y. ,2008.. The effects of cryoprotectants on the freeze-drying of ibuprofen-loaded solid lipid microparticles (SLM). European Journal of Pharmaceutics and Biopharmaceutics, 69,2, 750-759.

Zauner, W., Farrow, N., Haines, M.R., 2001. *In vitro* uptake of polystyrene microspheres: effect of particle size, cell line and cell density. Journal of Controlled Release, 71, 39-51.

Zinn ,K., Chaudhuri ,T. R., Szafran, A. A., O'quinn ,D., Weaver ,C., Dugger, K. Lamar, D. ,Kesterson, R. A. ,Wang, X., Frank ,S. J., 2008, Noninvasive bioluminescence imaging in small animals. ILAR Journal / National Research Council, Institute of Laboratory Animal Resources ,49, 103-115.

Zhou, Q., Liu, L., Zhang, D., Fan, X., 2012b. Analysis of gemcitabine liposome injection by HPLC with evaporative light scattering detection. Journal of Liposome Research ,22, 263-269.

Zhu, S., Lansakara, P.D.S.P., Li, X., Cui, Z., 2012. Lysosomal delivery of a lipophilic gemcitabine prodrug using novel acid-sensitive micelles improved its antitumor activity. Bioconjugate Chem. Bioconjugate Chemistry, 23, 966-980.

Yamamoto, N., Tsurutani, J., Yoshimura, N., Asai, G., Moriyama, A., Nakagawa, K., Kudoh, S., Takada, M., Minato ,Y., Fukuoka, M., 2006. Phase II study of weekly paclitaxel for relapsed and refractory small cell lung cancer. Anticancer Research, 26,777-81

Yoo, J.-W., Doshi, N., Mitragotri, S., 2011. Adaptive micro and nanoparticles: Temporal control over carrier properties to facilitate drug delivery. Advanced Drug Delivery Reviews, 63, 1247-1256.

Yu, L., Hales, C.A., 2011. Long-term exposure to hypoxia inhibits tumor progression of lung cancer in rats and mice. BMC cancer ,11,331.

Yoo, J.-W., Doshi, N., Mitragotri, S., 2011. Adaptive micro and nanoparticles: Temporal control over carrier properties to facilitate drug delivery. Advanced Drug Delivery Reviews ,63, 1247-1256.

Xu, Q., Zhang, Y., Trissel, L.A., 1999. Physical and chemical stability of gemcitabine hydrochloride solutions. Journal of the American Pharmaceutical Association (Washington,D.C. : 1996) ,39, 509-13